

Journal of Print and Media Technology Research

Scientific contributions

The consequences of choosing
and specifying brand colors
directly from a screen – and the need
for brand color management

Michael Abildgaard Pedersen

85

Accuracy of spot color reproduction in a 7-color,
expanded gamut, flexographic printing system

Reem El Asaleh, Martin Habekost and Abhay Sharma

99

A new approach to fuzzy logic analysis
of Indian currency recognition

Sonia Sarkar and Arun Kiran Pal

119

A comparison of current solutions
for creating web animations on Apple hardware

Jaka Mušič and Helena Gabrijelčič Tomc

129

ISSN 2414-6250



9 772414 625001

Editor-in-Chief

Gorazd Golob (Ljubljana)

Published by **iarigai**
www.iarigai.org

The International Association of Research
Organizations for the Information, Media
and Graphic Arts Industries

Journal of Print and Media Technology Research

A PEER-REVIEWED QUARTERLY

PUBLISHED BY

The International Association of Research Organizations
for the Information, Media and Graphic Arts Industries
Magdalenenstrasse 2, D-64288 Darmstadt, Germany
<http://www.iarigai.org>
journal@iarigai.org

EDITORIAL BOARD

EDITOR-IN-CHIEF

Gorazd Golob (Ljubljana, Slovenia)

EDITORS

Anne Blayo (Grenoble, France)
Timothy C. Claypole (Swansea, UK)
Edgar Dörsam (Darmstadt, Germany)
Nils Enlund (Helsinki, Finland)
Patrick Arthur C. Gane (Helsinki, Finland)
Mladen Lovreček (Zagreb, Croatia)
Scott Williams (Rochester, USA)

ASSOCIATE EDITOR

Markéta Držková (Pardubice, Czech Republic)

SCIENTIFIC ADVISORY BOARD

Ian Baitz (Toronto, Canada)
Irena Bates (Zagreb, Croatia)
Davide Deganello (Swansea, UK)
Jay Amrish Desai (Nagpur, India)
Elena Fedorovskaya (Rochester, USA)
Diana Gregor Svetec (Ljubljana, Slovenia)
Jon Yngve Hardeberg (Gjøvik, Norway)
Gunter Hübner (Stuttgart, Germany)
Dejana Javoršek (Ljubljana, Slovenia)
Igor Karlovits (Ljubljana, Slovenia)
Helmut Kipphan (Schwetzingen, Germany)
Yuri Kuznetsov (St. Petersburg, Russian Federation)
Magnus Lestelius (Karlstad, Sweden)
Igor Majnarić (Zagreb, Croatia)
Thomas Mejtoft (Umeå, Sweden)
Erzsébet Novotny (Budapest, Hungary)
Alexandra Pekarovicova (Michigan, USA)
Anastasios Politis (Athens, Greece)
Cathy Ridgway (Egerkingen, Switzerland)
Wolfgang Schmidt (Munich, Germany)
Tomáš Syrový (Pardubice, Czech Republic)
Li Yang (Stockholm, Sweden)
Werner Zapka (Stockholm, Sweden)

A mission statement

To meet the need for a high quality scientific publishing platform in its field, the International Association of Research Organizations for the Information, Media and Graphic Arts Industries is publishing a quarterly peer-reviewed research journal.

The journal is fostering multidisciplinary research and scholarly discussion on scientific and technical issues in the field of graphic arts and media communication, thereby advancing scientific research, knowledge creation, and industry development. Its aim is to be the leading international scientific journal in the field, offering publishing opportunities and serving as a forum for knowledge exchange between all those interested in contributing to or learning from research in this field.

By regularly publishing peer-reviewed, high quality research articles, position papers, surveys, and case studies as well as review articles and topical communications, the journal is promoting original research, international collaboration, and the exchange of ideas and know-how. It also provides a multidisciplinary discussion on research issues within the field and on the effects of new scientific and technical developments on society, industry, and the individual. Thus, it intends to serve the entire research community as well as the global graphic arts and media industry.

The journal is covering fundamental and applied aspects of at least, but not limited to, the following topics:

Printing technology and related processes

- ⊕ Conventional and special printing
- ⊕ Packaging
- ⊕ Fuel cells and other printed functionality
- ⊕ Printing on biomaterials
- ⊕ Textile and fabric printing
- ⊕ Printed decorations
- ⊕ Materials science
- ⊕ Process control

Premedia technology and processes

- ⊕ Colour reproduction and colour management
- ⊕ Image and reproduction quality
- ⊕ Image carriers (physical and virtual)
- ⊕ Workflow and management

Emerging media and future trends

- ⊕ Media industry developments
- ⊕ Developing media communications value systems
- ⊕ Online and mobile media development
- ⊕ Cross-media publishing

Social impact

- ⊕ Media in a sustainable society
- ⊕ Environmental issues and sustainability
- ⊕ Consumer perception and media use
- ⊕ Social trends and their impact on media

Submissions to the Journal

Submissions are invited at any time and, if meeting the criteria for publication, will be rapidly submitted to peer-review and carefully evaluated, selected and edited. Once accepted and edited, the papers will be published as soon as possible.

✉ Contact the Editorial office: journal@iarigai.org

Journal of Print and Media Technology Research

2-2022

June 2022



The information published in this journal is obtained from sources believed to be reliable and the sole responsibility on the contents of the published papers lies with their authors. The publishers can accept no legal liability for the contents of the papers, nor for any information contained therein, nor for conclusions drawn by any party from it.

Journal of Print and Media Technology Research is listed in:

Emerging Sources Citation Index

Scopus

DOAJ – Directory of Open Access Journals

Index Copernicus International

NSD – Norwegian Register for Scientific Journals, Series and Publishers

Contents

A letter from the Editor <i>Gorazd Golob</i>	83
Scientific contributions	
The consequences of choosing and specifying brand colors directly from a screen – and the need for brand color management <i>Michael Abildgaard Pedersen</i>	85
Accuracy of spot color reproduction in a 7-color, expanded gamut, flexographic printing system <i>Reem El Asaleh, Martin Habekost and Abhay Sharma</i>	99
A new approach to fuzzy logic analysis of Indian currency recognition <i>Sonia Sarkar and Arun Kiran Pal</i>	119
A comparison of current solutions for creating web animations on Apple hardware <i>Jaka Mušič and Helena Gabrijelčič Tomc</i>	129
<hr/>	
Topicalities <i>Edited by Markéta Držková</i>	
News & more	143
Bookshelf	145
Events	151



A letter from the Editor

Gorazd Golob

Editor-in-Chief

E-mail: gorazd.golob@jpmtr.org

journal@iarigai.org

The four research papers contained in the present issue are covering different research fields within the scope of the Journal. The first two deal with color reproduction. One is addressing the problem of a proper definition of CIELAB values of spot colors in the design and pre-press part of the graphic arts production process. The second one is dedicated to the accuracy of color reproduction in 7-colour flexographic printing used as an alternative to the traditional application of specific spot colors.

The use of the fuzzy logic based method in the recognition of counterfeiting and worn Indian currencies, using their characteristics expressed as 3D graphs, is presented in the third research paper.

The last paper is based on a study of the suitability of different methods for the animation of graphic objects included in a website, on different Apple and Nokia hardware, equipped with different operating systems and browsers.

All four papers are bringing the first, promising results of the conducted research. I hope that in further publications of the research results in the mentioned fields, we can also expect more in-depth presentations of the theoretical foundations, a broader presentation of the results, and finally elaborated methods that would also allow for use in everyday research practice and modern technologies.

In the Topicalities, edited by Markéta Držková (marketa.drzkova@jpmtr.org) an overview of the recently ending series of Horizon 2020 is shown in News & more section, as well as some achievements in additive manufacturing and publications released by Intergraf in the past year. In the Bookshelf an overview of books on different fields within the scope of the Journal is given, including history, communication technology, materials, and printed electronics.

Also, the presentations of academic dissertations are included in the Bookshelf. Vladimir Cviljušac defended his thesis on printed computer-generated holograms at the University of Zagreb, Croatia. The thesis on the development of a robotic cell for printing of electronic circuits on free-form substrates was defended by Gioia Furia at Grenoble INP, France. The third presented thesis, dealing with ink-jet printing of metal halide perovskites-based solar cells was defended by Edgar Ricardo Nandayapa Bermudez at the Humboldt-Universität zu Berlin, Germany.

In the Events section, an overview of conferences and symposia is given, together with the information on some postponed events. The pandemic is still bringing uncertainty to the organizers and visitors, so some events are organized in hybrid or even online form. The combined [iarigai](#) and IC conferences in September will take place in Greenville, South Carolina, USA, and it is planned to be an in person event.

In the recent period, the status of the Journal was slightly improved. The Journal is listed in Scopus, and due to some registered citations, the SCImago Journal Rank (SJR) is calculated. Also at Clarivate (Web of Science), the Journal is indexed in ESCI, and a new Journal Citation Indicator (JCI) is calculated. The calculated indices are very low, however, the trend is positive and this can be a reason for a growing interest in publication in the Journal in the last year. Unfortunately, a number of manuscripts were rejected due to being out of scope, and returned to the author(s) with some advice for improvements and revisions, however, some were accepted for reviewing and finally also for publication. I really hope the trend will continue and the content, level, and structure of the received manuscripts will be appropriate for publication. We all need a quality journal dedicated to our research fields, available and open to authors and readers.

Ljubljana, June 2022

JPMTR-2208
DOI 10.14622/JPMTR-2208
UDC 774.8:004.353|62.5

Research paper | 160
Received: 2022-04-26
Accepted: 2022-05-27

The consequences of choosing and specifying brand colors directly from a screen – and the need for brand color management

Michael Abildgaard Pedersen

The Danish School of Media and Journalism (DMJX),
Department of Media Production and Management,
72 Emdrupvej, 2400 Copenhagen NV, Denmark

map@dmjx.dk

Abstract

This paper examines some of the implications of choosing brand colors directly from a software program, based on what the designer sees on the screen. The reason is that more and more graphic arts designers tend to choose colors directly from the screen and to a lesser extent from a physical color catalog such as the Pantone fans. Therefore, designers do not really know what color they have chosen until it is available in the final printed form and this can bring unpleasant surprises. The starting point for this study was the digital solutions from Adobe CC and the web service Pantone Connect. The focal point was sRGB, as Pantone recommends, which also is the standard for internet and mobile devices. Initially, the problem with using a small color space as sRGB to select and define brand colors was investigated. Examples of Pantone colors outside sRGB gamut but still available for the designer to choose without any warnings, have been sought. For example, if the designer chooses Pantone Green C as a brand color, the result would be a color difference of 10.5 ΔE_{00} . The CIELAB values for a color defined in sRGB were compared to the CIELAB reference values for the same color as it will appear as a printed spot color. This gives a color difference ΔE_{00} between how the color appears on the screen versus the physical color as it appears on a print, printed as 1-color solid spot color. Pantone Connect's feature for converting colors from sRGB to Pantone Solid spot color is also investigated. As an example, entering sRGB values for cyan (0/255/255) resulted in a proposal for Pantone 311 C as Best Match, giving a color difference of 17 ΔE_{00} between the reference values for Cyan and the reference values for the proposed Pantone 311 C. In addition, the feature to extract color code values from an uploaded photo was examined. An iPhone screenshot image of Pantone 1505 C (orange) was uploaded to Pantone Connect, which interpreted the color as being Pantone 1585 C giving a color difference of 6.3 ΔE_{00} . The overall conclusion is that it is very uncertain and unpredictable to choose colors directly from a screen. The color differences between the color as it appears on the screen and the color as it appears on the final print can be very large and thus be the cause of the customer's dissatisfaction, even if the customer is partly responsible. As a consequence of the lack of management and control in this area, brand color management is introduced as a new technical concept. It is an extension of traditional color management, so it also includes color selection, color specification, color description and an extended form of color control.

Keywords: sRGB, spot colors, Pantone Connect, color difference, color reproduction

1. Introduction and background

Traditional color management is concentrated on the four Cs: Consistency, Calibration, Characterization, and Conversion (Adams, Sharma and Suffoletto, 2006). These are primarily processes that take place inside a printing company. However, many other important color management processes before and after these four Cs are not included in traditional color management.

While all processes after the four Cs, including the color reproduction (printing) and color control, are richly covered by international process standards, like ISO 12647-1:2013, other parts of ISO 12647, and ISO 17972-4:2018 (International Organization for Standardization, 2013; 2018), and guidelines and specifications from industry organizations, e.g. Fogra, bvdM, GATF, GRACoL and Idealliance, it seems that there are virtually no technical guidelines for processes

before the four Cs in traditional color management. Namely Color Choice, Color Specification, and Color Description. These are processes typically performed by the brand owner and the designer.

Textbooks for designers are mainly focused on the creative process of choosing colors/hues including which colors fit well together, how to make different color themes, and what the different colors symbolize, e.g. Eiseman (2000), Drew and Meyer (2006). It has not yet been possible to find any textbook aimed at designers that focuses on technical color specification, definition and reproducibility. Although Finkle (2019) on his web blog warns against choosing brand colors that are out of gamut. In addition, none of the well-known textbooks for the printing industry includes these design subjects (Green, 1999; Berns, 2000; Kipphan, 2001; Adams, Sharma and Suffoletto, 2006); some textbooks, however, have brief remarks regarding Pantone colors that cannot be reproduced in CMYK. Fogra (2009) addresses that color matching at the beginning of the production process is not yet defined by a particular standard. Fred Bunting (1998) argues that RGB values that produce the exact color you want on one device will look quite different on another device. However, this argument is just used for implementing color management.

Thus, there seems to be a lack of technical knowledge in this particular area; to select and specify brand colors that can be reproduced across platforms and especially choosing colors from a software program that displays colors in sRGB. Thus, this area does not appear to be subject to the same controlled conditions as all subsequent processes in e.g. print production or media production across media platforms. There is a need to include these first processes into the traditional color management processes, which this study will suggest.

In this first color choice step, the designer and brand owner must decide which color to choose. Initially which hue (red, violet, purple, blue, green, yellow, orange, brown, black, white, or metallic). If designers have the perception that they can choose freely from every conceivable color, the foundation is laid for a difficult production and a dissatisfied brand owner. At this first point, designers want a color that expresses a certain feeling or a certain set of emotional values that a specific company (the designer's customer) possesses.

Therefore, color reproducibility is typically secondary or absent to the designer's mind at this stage. The fact, that the chosen color later must be reproducible in print (on paper, plastic, metal, or other substrates), on screens (computer screen, smartphone screen, tablet, TV, etc.), and perhaps even as wall paint, painted chairs and tables – yes, in every conceivable physical and vir-

tual situation – is rarely included in the designer's considerations at this point (Pedersen, 2016). A completely new study (Chung and Liu, 2022) states that brand color reproduction and its conformity assessment require aims and tolerances and designers should specify these.

This color choosing process can be done in several ways. Either from a physical sample or object (e.g. a previous print, a fruit or something else), from a physical color catalog (like a Pantone fan) or from a software program (viewed through a computer screen).

Often, the designer chooses colors based on personal preferences and personal taste. In many cases, they choose colors that are bright and chromatically saturated. However, most of these brand colors cannot be reproduced in printing technologies using the process colors CMYK (Pedersen, 2016; 2018). In addition, many of these colors cannot even be displayed on RGB screens, which a "Gamut Warning" attempts to warn the designer about in Adobe CC. However, these warnings are often ignored, as designers do not know what the warning refers to.

Thus, the problem is passed on to the next link in the value chain, the print providers that now face an unsolvable problem. How to reproduce an irreproducible color. Already here, the future dissatisfaction of the brand owner and designer is founded. Neither the brand owner, nor the designer will ever get to see color they thought they had chosen. Therefore, this color selection process is crucial for all subsequent processes. It becomes central how designers choose the brand color for a brand.

However, over the last decade, we have seen more and more designers and design agencies opting out of investing in physical Pantone color guide decks. Either to save money or because they think a digital solution is easier, or both. Since Pantone has developed into a fashion company, about 200 new colors are released every year, including "The color of the year". That is why professional designers need to invest in at least six physical Pantone fans (Pantone, 2014; 2019) every year: Formula Guide (Coated & Uncoated), Color Bridge Guide (Coated & Uncoated), and CMYK (Coated & Uncoated). However, for a one-man business, 700 to 800 euros is a lot of money to spend each year for a new set of Pantone fans.

In March 2022, an apparent dispute between Adobe and Pantone resulted in that Pantone Color Libraries no longer will be part of the Adobe CC software package. Instead, designers now have to buy a subscription to Pantone Connect that can act as a plug-in for Adobe CC (Pantone, 2022). Thus, designers must subscribe to both Adobe CC and Pantone Connect.

It can thus be expected that even more designers and brand owners in the future will choose their colors directly from their software application. None of the 75 Graphic Design students at the Danish School of Media and Journalism (DMJX) University College has a set of Pantone fans; they choose colors directly from the screen, and this will increase the risk of an inappropriate color choice.

As previous studies have shown, designers and brand owners tend to choose brand colors that cannot be reproduced satisfactorily in CMYK (Pedersen, 2016; 2018). It is also a well-known fact that computer screens do not always display colors correctly, so what will happen if colors increasingly are selected directly from what is seen on a screen?

Unfortunately, the designers do not get much help. They are even directly misled. In the same way that Pantone has always specified CMYK values for those Pantone colors that cannot be reproduced satisfactorily in CMYK (Pedersen, 2016), for years Pantone has also specified sRGB values for all their Pantone colors, even for those colors that cannot be displayed through sRGB. Pantone even recommends that the designer starts by entering sRGB values when working with a Pantone color (Figure 1).

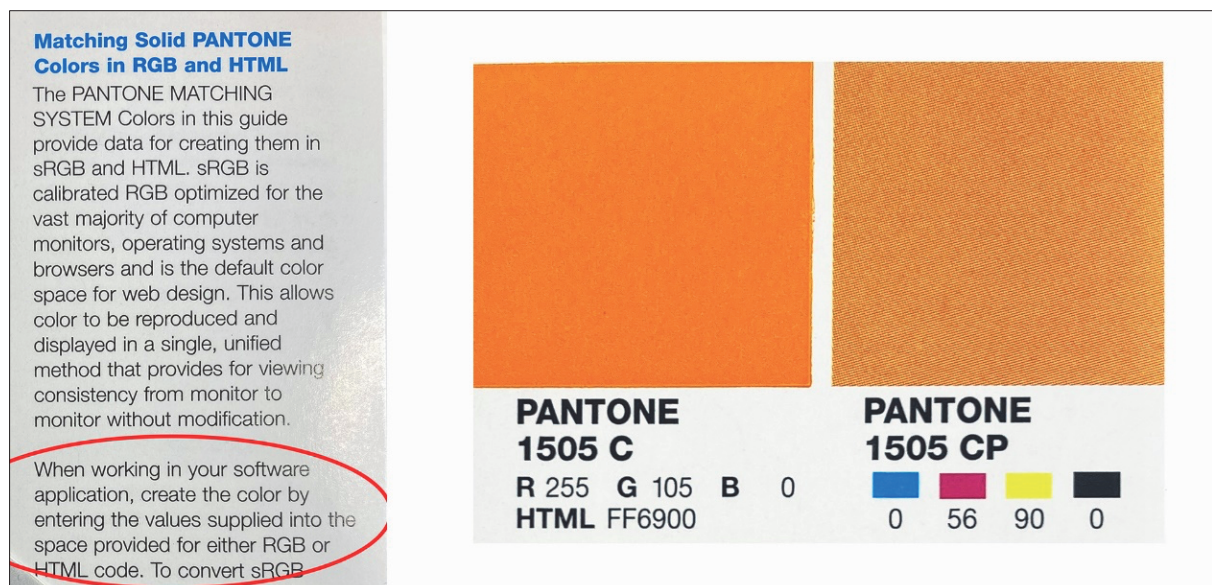
Even though sRGB is the standard for web colors and mobile devices (Stokes, et al., 1996; International Electrotechnical Commission, 1999; 2003), AdobeRGB color space is the default in Adobe CC applications, like InDesign and Photoshop. Moreover, the graphics arts

industry recommends eciRGB (ECI, 2022; Kleeberg, et al., 2018) since this color space is larger than sRGB and AdobeRGB. Besides, both sRGB and AdobeRGB have a white point D65 which is different from the recommended D50 and therefore eciRGB ensures a more uniform color conversion to CMYK and spot colors in print production (Kleeberg, et al., 2018).

There is only one case where sRGB seems to be the sensible choice, namely when the artwork only needs to be published and displayed through the Internet and mobile devices. If a designer does artwork for both print and web, it could be obvious to recommend working in sRGB, as this will ensure that colors appear uniform across platforms and media although it will be a compromise that excludes many colors. All colors outside the sRGB gamut will be changed and thus be “wrong”.

However, if the designers enter the specified sRGB values for e.g. Pantone 1505 C, they will have specified the color incorrectly from the start, without being aware of it. And if the color subsequently is printed as “correct” spot color, there will be a large color difference between the color they have seen on the screen and the color they see as the printed spot color.

This study will examine the consequence of choosing colors from sRGB as Pantone recommends. For example, what will happen if Pantone’s sRGB values for Pantone 1505 C is entered into an Adobe CC application, meaning what color difference will there be between the sRGB version and the reference spot color Pantone 1505 C?



a)

b)

Figure 1: Pantone’s recommendation to start with sRGB (a) and the recommended sRGB values for PMS 1505 C, from the Pantone Color Bridge fan (b) (Pantone, 2014)

When Pantone specifies both CIELAB values and sRGB values for a spot color, does that mean that the CIELAB values for these sRGB values are equal to the CIELAB values for the reference spot color?

How large color differences ΔE_{00} can be expected for spot colors outside the sRGB gamut?

2. Methods

First, a CIE a^*b^* diagram was drawn where the three RGB color spaces sRGB, AdobeRGB and eciRGB were

plotted. This diagram was used to search for areas outside of sRGB where spot colors are likely to have a large color difference. CIELAB values for this gamut mapping were found via Adobe CC, Color Picker, where RGB values were entered, e.g. red: 255 0 0, after which CIELAB values for this were read out (Table 1).

Then, Pantone's web service Pantone Connect was used to search for specific Pantone spot colors in this out-of-gamut area. The reference values (CIELAB and sRGB) were extracted and used in the CIE a^*b^* diagram to plot the Pantone colors (Figure 2) and calculate the color differences.

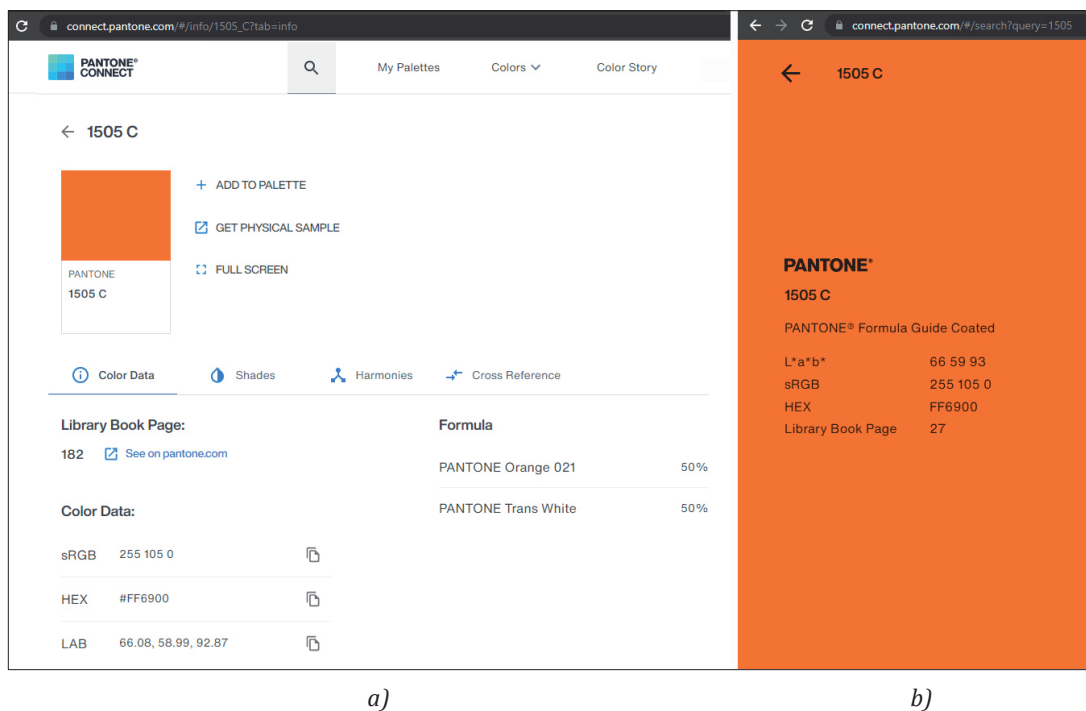


Figure 2: The split image shows the Pantone Connect (Pantone, 2022) search results for Pantone 1505 C: (a) Color Data mode, and (b) full screen mode; the latter method is used when the designers know what Pantone color they want

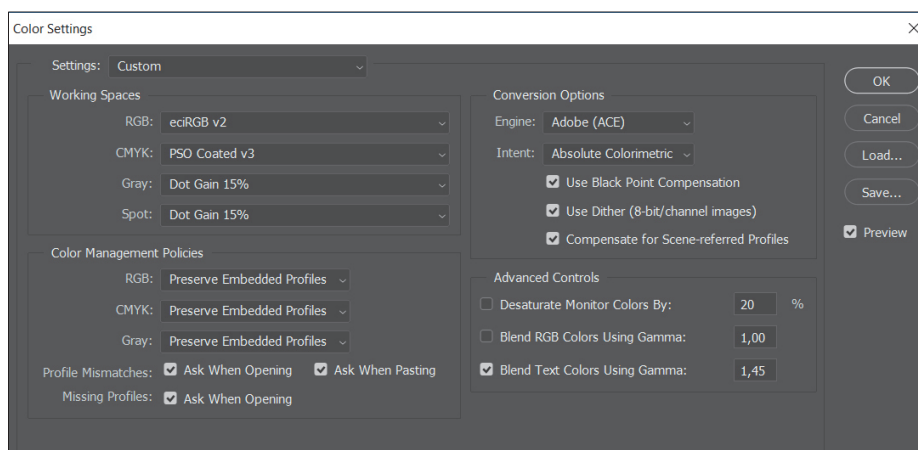


Figure 3: Adobe CC set up: open Color Settings > Working Spaces > Select the appropriate RGB (sRGB, AdobeRGB or eciRGB), and set Rendering Intent to Absolute Colorimetric

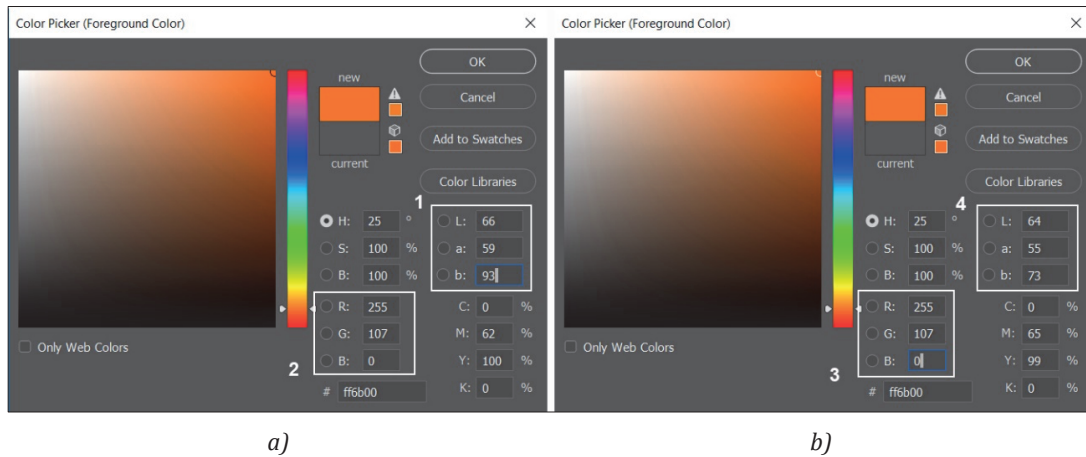


Figure 4: Split image shows the process (a) from CIELAB to sRGB: (1) open Color Picker > enter Pantone’s reference values (CIELAB) for Pantone color, (2) the corresponding sRGB values for these CIELAB values are shown > Cancel, and (b) from sRGB to CIELAB: (3) open Color Picker > the found sRGB values are entered, (4) the corresponding CIELAB values for these sRGB values are shown

The CIELAB values for the reference sRGB values were found via the Adobe CC application Photoshop, Color settings according to Figure 3, and process according to Figure 4. CIELAB values for a reference color and for the sRGB version of this reference color were imported into Excel, where the color difference ΔE_{00} was calculated. This color difference value expresses the difference between the optimally printed spot color and the color that a calibrated and profiled screen will display. Thus, the results of this study presuppose that the screens are calibrated, profiled, and otherwise comply with the requirements for viewing conditions, as described in ISO 3664:2009 (International Organization for Standardization, 2009). Otherwise, the results will be even more unpredictable.

3. Results

3.1 Colorimetric reference values for mapping RGB gamuts and Pantone spot colors

In Table 1, CIELAB values for three RGB gamuts are shown. These values are used to plot the gamut edge in a CIE $a^* b^*$ diagram, in Figure 5.

By an immediate assessment of the values in Table 1, it appears that sRGB is the smallest color space while eciRGB is the largest. This also appears to be the case in Figure 5.

The 33 spot colors shown in Figure 5 are all colors that are either on the edge or outside the sRGB gamut. The individual color differences as determined by the process described in section 2 are shown in Table 2, which also shows color difference values for AdobeRGB and eciRGB. Although it appears that Pantone 320 is inside the AdobeRGB gamut, the values in Table 2 show that the color is outside. The reason is that Figure 5 is a 2D representation of a 3D color space and thus the illustration is not quite reliable (Lindbloom, 2007). Although Fogra recommends a maximum color difference of $2.5 \Delta E_{00}$ for spot colors (Bertholdt, 2010), the difference of a maximum of $3.0 \Delta E_{00}$ (Pedersen, 2016) is used in this study, as colors are compared across print and screen media.

If the designers select a color by entering the specified sRGB values, they will get a result depending on what Color Settings they have (sRGB, AdobeRGB, or eciRGB) in Adobe CC application. For example, if the designer

Table 1: CIELAB values for gamut mapping RGB in a CIE $a^* b^*$ diagram, shown in Figure 5

	sRGB			AdobeRGB			eciRGB_V2		
	L^*	a^*	b^*	L^*	a^*	b^*	L^*	a^*	b^*
Red (R)	54	81	70	63	90	78	63	96	109
Green (G)	88	-79	81	83	-128	87	82	-128	82
Blue (B)	30	68	-112	30	69	-114	33	47	-109
Cyan (G+B)	91	-51	-15	86	-83	-22	86	-96	-26
Magenta (R+B)	60	94	-60	68	101	-51	69	99	-47
Yellow (R+G)	98	-16	93	98	-16	104	97	-11	108

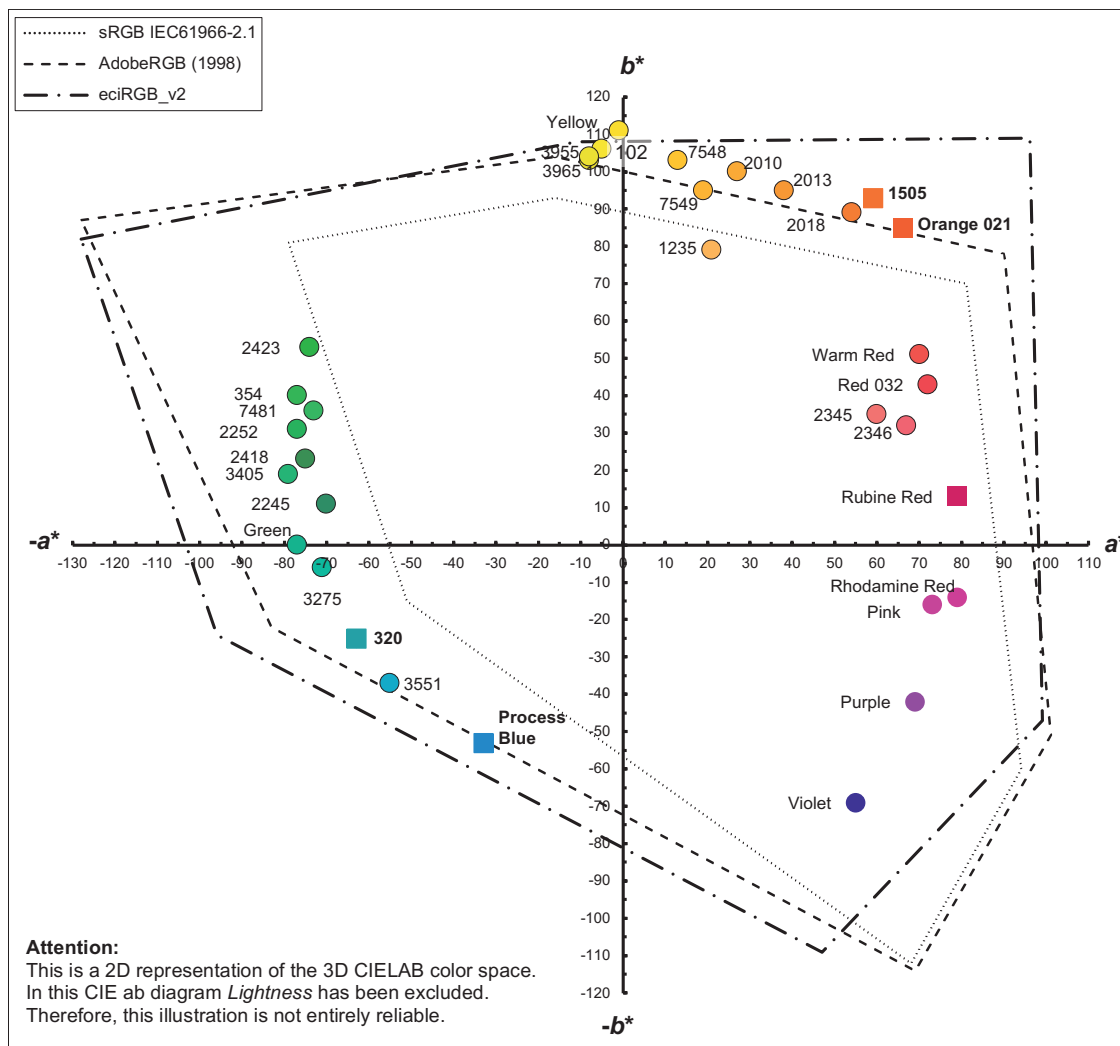


Figure 5: CIE $a^* b^*$ diagram showing 3 RGB gamuts and 33 Pantone Solid Coated spot colors, the five squares are colors that are outside both sRGB and AdobeRGB and with ΔE_{00} beyond 3, according to Table 2

enters the sRGB values for Pantone 1505 C the resulting CIELAB values are 64/56/73 if Color Settings is set to sRGB, and 66/59/79 if AdobeRGB is applied. Entering the sRGB values will give an ΔE_{00} of 5.9 if Color Settings is set to sRGB, and an ΔE_{00} of 4.5 if Color Settings is set to AdobeRGB.

Even if the designer defines the color as 1505 C and enters the correct CIELAB reference values for this color, the screen will still display the sRGB version or the AdobeRGB version or another RGB version of this color and the difference will be surprisingly large when compared to the printed spot color version of 1505 C.

3.2 Entering sRGB values in an AdobeRGB working space

So far, these studies have been exclusively about the cases where the designer has deliberately set their

Color Settings as recommended when entering the reference sRGB values. However, many designers have set up AdobeRGB as their default color space. If the designer is not aware of this problem or does not know anything about the different RGB color spaces, the designer will probably enter Pantone’s recommended sRGB values into the AdobeRGB working space. The result of this approach is given in Table 3.

3.3 Extracting sRGB and CIELAB values from a photo

Pantone Connect also offers an option to extract color code values from a photo that needs to be uploaded. However, if the photo is in sRGB, because the designer has used their mobile device to take the photo, the colors are not captured correctly, and the screen does not show the correct color. Thus, the result is not necessarily valid.

Table 2: 33 spot color reference CIELAB and their equivalents determined from sRGB reference values in three RGB gamuts, and the resulting color differences, the color differences ΔE_{00} beyond 3 are marked in red

Pantone solid coated spot color	Pantone connect reference			sRGB					AdobeRGB				eciRGB_V2			
	L^*	a^*	b^*	L^*	a^*	b^*	ΔE_{ab}^*	ΔE_{00}	L^*	a^*	b^*	ΔE_{00}	L^*	a^*	b^*	ΔE_{00}
Process Blue	48	-33	-53	52	-11	-45	23.7	11.0	49	-23	-51	4.2	48	-31	-52	0.7
2418	45	-75	23	49	-45	29	30.9	10.7	45	-71	24	1.2	45	-75	23	0.0
Green	58	-77	0	62	-46	9	32.5	10.5	59	-72	1	1.5	58	-77	0	0.0
320	53	-62	-25	58	-33	-16	30.8	10.4	54	-51	-23	3.3	53	-59	-25	0.9
2245	45	-70	11	49	-42	17	28.9	10.3	45	-65	12	1.4	45	-70	11	0.0
3551	58	-55	-37	62	-28	-28	28.7	9.8	59	-46	-35	2.9	58	-55	-37	0.0
3405	59	-79	19	63	-52	26	28.2	9.4	59	-79	19	0.0	59	-79	19	0.0
3275	61	-71	-6	65	-45	2	27.5	8.9	61	-70	-6	0.2	61	-71	-6	0.0
2252	57	-77	31	60	-54	37	24.0	8.0	57	-77	31	0.0	57	-77	31	0.0
354	60	-77	40	63	-57	45	20.8	6.9	60	-70	40	1.8	60	-77	40	0.0
1505	66	59	93	64	56	73	20.3	5.9	66	59	79	4.5	66	59	93	0.0
2423	58	-74	53	61	-58	57	16.8	5.8	58	-74	53	0.0	58	-74	53	0.0
7481	63	-73	36	65	-58	41	15.9	5.5	63	-73	36	0.0	63	-73	36	0.0
Orange 021	61	66	85	60	65	71	14.1	4.7	61	66	75	3.4	61	66	85	0.0
1235	81	21	79	80	20	62	17.1	4.6	81	21	79	0.0	81	21	79	0.0
Yellow	89	-1	111	89	0	87	24.0	4.4	89	0	97	2.5	89	0	102	1.6
2010	79	27	100	77	24	80	20.3	4.3	79	27	89	2.5	79	27	97	0.7
2018	68	54	89	66	51	74	15.4	4.3	68	54	80	2.9	68	54	86	0.9
2013	75	38	95	73	34	77	18.5	4.2	75	38	86	2.4	75	38	95	0.0
7548	84	13	103	83	11	84	19.1	3.7	84	14	93	2.2	84	13	99	0.8
3955	88	-8	104	88	-8	86	18.0	3.5	88	-8	95	1.7	88	-8	100	0.7
3965	87	-8	103	87	-7	85	18.0	3.4	87	-7	94	1.7	87	-8	99	0.7
102	90	-5	106	90	-4	88	18.0	3.4	90	-4	97	1.6	90	-5	102	0.7
7549	80	19	95	79	19	81	14.0	3.3	80	19	89	1.3	80	19	95	0.0
2346	64	67	32	62	65	28	4.9	2.4	64	67	32	0.0	64	67	32	0.0
2345	67	60	35	65	57	31	5.4	2.3	67	60	35	0.0	67	60	35	0.0
Rhodamine Red	52	79	-14	50	79	-17	3.6	2.3	52	79	-14	0.0	52	79	-14	0.0
Rubine Red	44	79	13	45	71	13	8.1	2.1	46	72	16	3.0	45	74	15	1.9
Warm Red	59	70	51	57	69	49	3.0	1.9	59	70	51	0.0	59	70	51	0.0
Purple	48	69	-42	47	68	-44	2.4	1.3	48	69	-42	0.0	48	69	-42	0.0
Pink	51	73	-16	50	72	-18	2.4	1.3	51	73	-16	0.0	51	73	-16	0.0
Red 032	55	72	43	54	70	41	3.0	1.2	75	72	43	0.0	55	72	43	0.0
Violet	19	55	-69	21	50	-67	1.0	2.1	20	50	-67	1.8	23	41	-62	5.4

Figure 6 shows an example of how it works. Via Pantone's Connect app for iPhone, the Pantone 1505 C is displayed in full screen mode. A screenshot of this is taken, and uploaded to the web service Pantone Connect. The web service estimates the color to be Pantone 1585 C.

However, there is a color difference of 6.3 ΔE_{00} between these two colors. Since Pantone 1505 C cannot be displayed satisfactorily on a screen with sRGB (cf. Table 2 and 3), the uploaded photo is not a representation of Pantone 1505 C but the closest, however unknown color, within the sRGB gamut. This unknown color captured in the photo was thus interpreted as being Pantone 1585 C.

3.4 Choosing the most saturated colors in sRGB via Pantone Connect

The previous examples raise the question of how saturated colors can actually become if designers are working in sRGB. The primary colors red, green and blue, as well as the secondary colors cyan, magenta and yellow should be the most chromatic colors in sRGB. The values for these colors are shown in Tables 1 and 4, and they are used to draw the gamut edge in Figure 5.

In Table 1, the sRGB values for the primary and secondary colors are entered into Adobe CC, Color Picker, after which the CIELAB values for these sRGB values are read. The same sRGB values are entered into

Table 3: The reference CIELAB values for 33 spot colors and their equivalents determined from sRGB reference values when sRGB values are entered in an Adobe RGB color working space, the color differences ΔE_{00} beyond 3 are marked in red

Pantone solid coated spot color	Spot color reference			Pantone sRGB reference				Color difference	
	L^*	a^*	b^*	L^*	a^*	b^*	ΔE_{00}	ΔE_{00}	
Process Blue	48	-33	-53	52	-11	-45	11.0	4.1	
2418	45	-75	23	49	-45	29	10.7	3.3	
Green	58	-77	0	62	-46	9	10.5	2.6	
320	53	-62	-25	58	-33	-16	10.4	3.6	
2245	45	-70	11	49	-42	17	10.3	3.0	
3551	58	-55	-37	62	-28	-28	9.8	2.7	
3405	59	-79	19	63	-52	26	9.4	2.2	
3275	61	-71	-6	65	-45	2	8.9	2.2	
2252	57	-77	31	60	-54	37	8.0	2.5	
354	60	-77	40	63	-57	45	6.9	3.5	
1505	66	59	93	64	56	73	5.9	6.9	
2423	58	-74	53	61	-58	57	5.8	4.4	
7481	63	-73	36	65	-58	41	5.5	4.5	
Orange 021	61	66	85	60	65	71	4.7	7.0	
1235	81	21	79	80	20	62	4.6	2.9	
Yellow	89	-1	111	89	0	87	4.4	3.2	
2010	79	27	100	77	24	80	4.3	4.6	
2018	68	54	89	66	51	74	4.3	5.3	
2013	75	38	95	73	34	77	4.2	4.7	
7548	84	13	103	83	11	84	3.7	3.8	
3955	88	-8	104	88	-8	86	3.5	1.8	
3965	87	-8	103	87	-7	85	3.4	2.1	
102	90	-5	106	90	-4	88	3.4	2.5	
7549	80	19	95	79	19	81	3.3	4.8	
2346	64	67	32	62	65	28	2.4	4.0	
2345	67	60	35	65	57	31	2.3	3.8	
Rhodamine Red	52	79	-14	50	79	-17	2.3	6.4	
Rubine Red	44	79	13	45	71	13	2.1	9.2	
Warm Red	59	70	51	57	69	49	1.9	5.0	
Purple	48	69	-42	47	68	-44	1.3	4.9	
Pink	51	73	-16	50	72	-18	1.3	5.8	
Red 032	55	72	43	54	70	41	1.2	6.1	
Violet	69	24	-29	69	23	-29	0.8	2.9	

Table 4: Corresponding CIELAB values for the sRGB values and their comparison with the CIELAB values for reference spot color and Pantone Connet's suggestion for nearest PMS color, with color differences

Reference spot color	Reference						Nearest PMS color				
	R	G	B	L^*	a^*	b^*	L^*	a^*	b^*	ΔE_{00}	
Yellow	255	255	0	98	-16	93	3945 C	90	-9	92	6.0
Orange	255	127	0	68	46	75	151 C	70	47	79	1.9
Red	255	0	0	54	81	70	2347 C	49	75	67	5.2
Magenta	255	0	255	60	94	-60	2385 C	54	69	-29	10.5
Purple	210	30	210	51	78	-51	Purple C	48	69	-42	4.1
Violet	70	0	150	21	50	-65	Violet C	19	55	-69	2.0
Blue	0	0	255	30	68	-112	2736 C	23	36	-73	9.6
Cyan	0	255	255	91	-51	-15	311 C	71	-35	-27	17.0
Green	0	255	0	88	-79	81	2271 C	65	-68	51	18.0

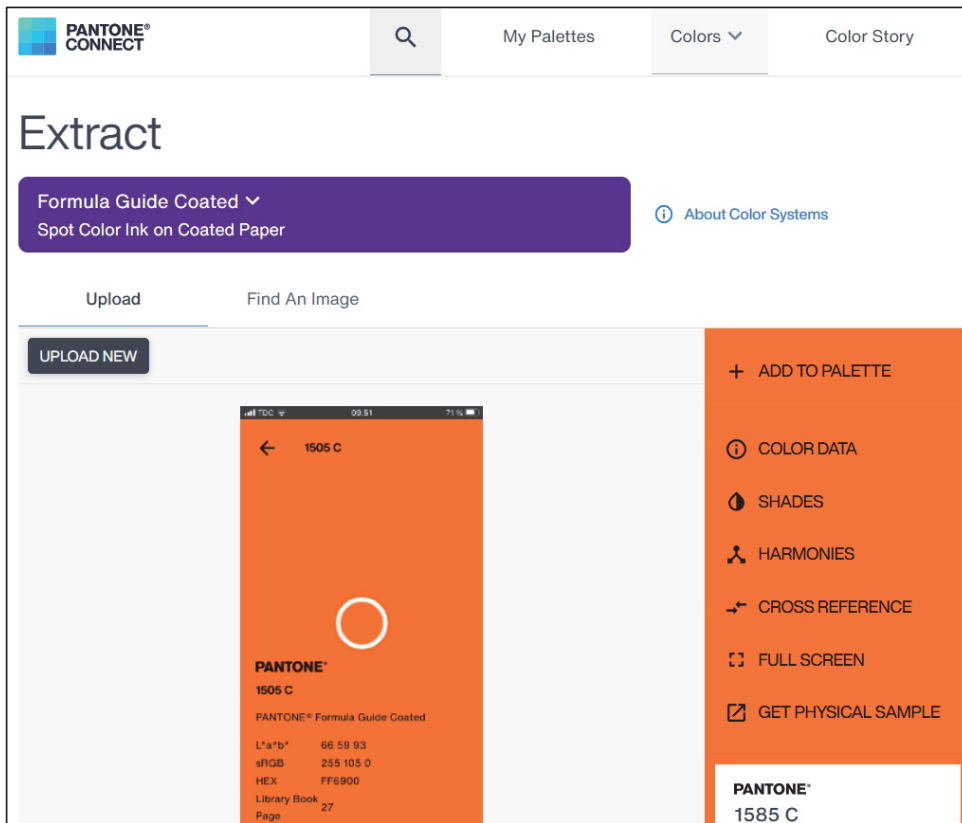


Figure 6: Uploading a photo of Pantone 1505 C, which is interpreted as being Pantone 1585 C by Pantone Connect

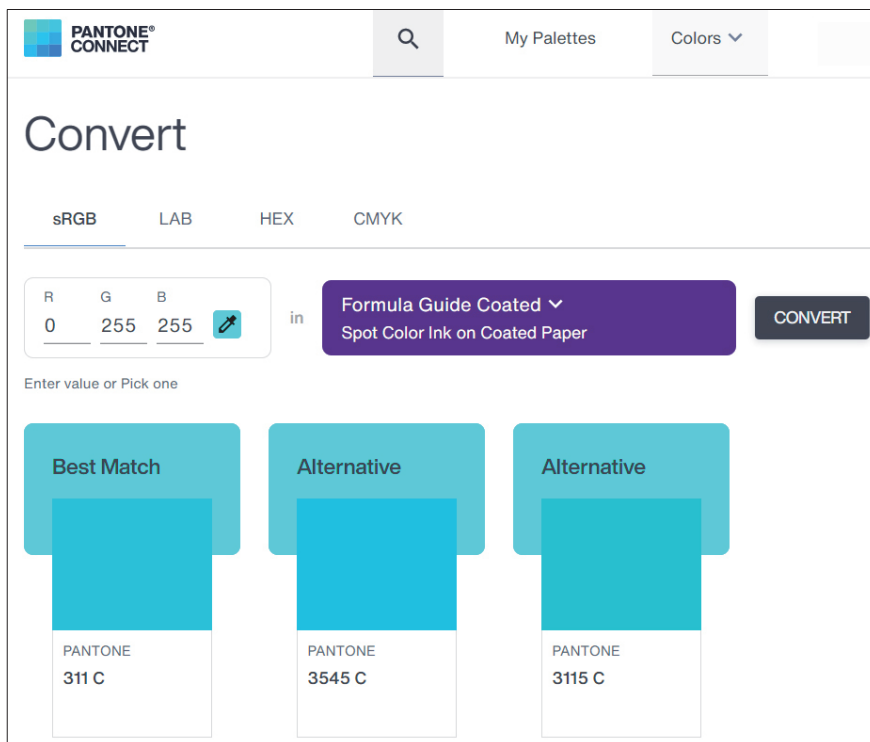


Figure 7: The sRGB values for Cyan (0/255/255) are entered, after which Pantone 311 C is suggested by Pantone Connect

Pantone Connect, Convert, after which this web service suggests the nearest Pantone color (Figure 7). The CIELAB values for the proposed Pantone spot color is compared to the CIELAB values for the sRGB colors, after which a color difference is calculated. In Table 4 the six colors from Table 1 are complemented by three more colors: orange, purple and violet.

In the example from Figure 7, Pantone Connect will suggest Pantone 311 C if the designers enter sRGB values for Cyan. This will give a color difference of 17 ΔE_{00} as shown in Table 4. However, that information does not appear in Pantone Connect. Thus, it is associated with great uncertainty to convert colors from sRGB to Pantone Solid spot colors by using the Pantone Connect web application.

3.5 The need for brand color management

As can be seen from the examples from this study, the processes of color selection, color specification and color description are not subject to the same controlled conditions as all subsequent color management and production processes.

In Brand Color Management, which hereby is introduced as a new concept, the four traditional Cs of color management are expanded to nine Cs, thus including the entire color selection process also including the decision on which acceptable color differences the brand owner will be willing to accept – or have to accept, as described in previous studies (Pedersen, 2016; 2018). Thereby, all the process, from the initial color choice to the final consequences of this color choice is covered. The nine Cs of brand color management from color selection to the final control of the reproduced color are illustrated in Figure 8, with each step of brand color management briefly explained in the following sections.

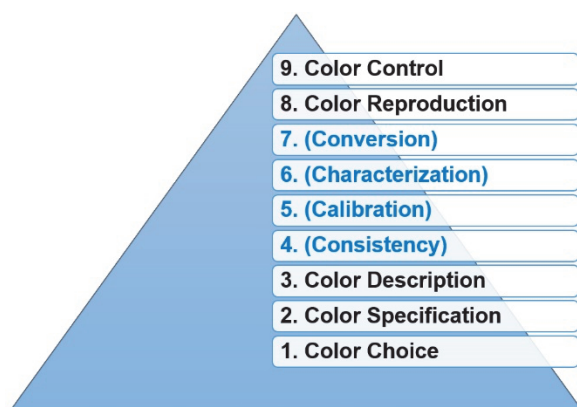


Figure 8: The nine Cs of brand color management, the terms in parentheses are the traditional four Cs in color management

3.5.1 Color choice

In this first step, designers and brand owners are focused on finding a color/hue that represents the company or the upcoming campaign as described in the Introduction. Thus, the first considerations are focused on, whether it should be a red, violet, purple, blue, green, yellow, orange, brown, black, white, or metallic color, including the degree of blackness, tints and brightness. Once the hue is selected (e.g. orange), the next step begins.

3.5.2 Color specification

In this second step, the chosen color must be specified in more detail (which orange?). The goal is to identify and name the color (e.g. Pantone 1505 C) as described in sections 3.2, 3.3 and 3.4. This step should also include examinations of whether the chosen color can be reproduced satisfactorily across technologies, including different printing methods, substrates, and color system, like CMYK (coated and uncoated), RGB (sRGB), RAL, NCS, Munsell, and possibly other relevant systems. Already in this second step, it is necessary to decide how large a color difference (ΔE_{00}) the brand owner is willing to accept.

The answer to this question can often be found by calculating the color difference between coated and uncoated (PMS 1505 C vs 1505 U) and between spot color and process color (Pantone 1505 C vs 1505 CP and 1505 U vs 1505 UP). This specific part is described in previous studies (Pedersen, 2016; 2018). Thus, this color specification step is also the step that should consider the present study's discussions regarding the choosing of colors from screen (e.g. Pantone 1505 C vs the sRGB version of this color).

3.5.3 Color description

In the third step, there is a need for technical descriptions of the color in a brand manual. However, at this point, it is possible that the designers and brand owners have had to choose a different color due to the expected color differences that would have been unacceptably large if the first choice of color were reproduced. Eventually, the chosen brand color must be described technically for the various reproduction technologies, described in section 3.5.2. This information should be present in the corporate brand manual, visual identity guide or design guide, as described in an earlier work (Pedersen, 2016).

The intention of this step is to ensure that various industries (e.g. the printing industry, the online/web industry, paint, etc.) is able to reproduce the brand color in their different technologies.

3.5.4 The four Cs of traditional color management

The steps four to seven are the four steps comprising the well-known Cs of traditional Color Management: Consistency, Calibration, Characterization and Conversion (as mentioned above and described in e.g. Adams, Sharma and Suffoletto, 2006). Thus, there is no need for further descriptions in this study.

3.5.5 Color reproduction

This eighth step in brand color management is the actual reproduction of the chosen brand color. This step includes prepress, where the digital file is prepared for the selected printing method, including the use of relevant ICC profile and proofing. Moreover, it includes the actual print production, including setup and proof check.

This area is richly described in various process standards (e.g. series of ISO 12647) and in guidelines from industry organizations such as bvdn and Idealliance. Thus, there also is no need for further descriptions in this study.

3.5.6 Color control

In this ninth and final step of brand color management, the reproduced color is measured, controlled and it is checked, whether the color difference lies within the tolerances described in the brand manual. Although this step is also part of the eighth step, this color control step is so central that it should receive special attention. If the press setup process is focused on making the print look like a contract proof or to comply to a process standard, there is a risk that focus will be removed from how the printed brand color looks like.

If the chosen brand color is printed as a halftone combination of the four CMYK process colors, measurements should also be made inside the printed image on the place where the brand color is printed as described in a previous study (Pedersen, 2018). The measurements should reveal, whether there is an incorrect tone value increase, gray balance, or color conversion (color management).

This way, it gives a real color difference value of the printed version of the brand color compared to the reference for this brand color. Apart from that, measurement of colors and measurement conditions are already described in various process standards such as series of ISO 12647 and ISO 13655:2009 (International Organization for Standardization, 2013; 2009) and if the first eight steps are performed as recommended, there is no need for further elaboration of this last step.

4. Discussion

As stated in the introduction, the purpose of this study was to find out how large color differences designers are risking when choosing a brand color directly from a software program via a computer screen. This study shows examples of color differences of up to 11 ΔE_{00} when the designer enters sRGB values for a Pantone color (Process Blue, Table 2) and up to 18 ΔE_{00} if the designer enters sRGB values into Pantone Connect, convert and applies the proposed Best Match (Pantone 2271 C, Table 4). Even in cases where the designer enters a Pantone color's sRGB values into a larger color space such as AdobeRGB, it will result in unpredictable large color differences of 9.2 ΔE_{00} (Rubine Red C, Table 3). Finally, the example in section 3.3 shows that the ability to extract color code values from an uploaded photo is unpredictable and risky. The example results in a color difference of 6.3 ΔE_{00} .

The basic risk of choosing colors from screen is that the screen and sRGB cannot display the color; that the designers' software states they have chosen. Thus, when the designers choose the most clear and chromatic saturated green color (RGB 0/255/0) they are told that they have chosen Pantone 2271 C. If this subsequently is described in a brand manual and a printing company thus prints Pantone 2271 C as a spot color, there will be an unsatisfactory, large color difference between the screen version and the print version of 18 ΔE_{00} (see Table 4).

Naturally, these results are not unambiguous and accurate for what will happen every time designers choose colors from screen. The goal has been to find the large color differences and thus the high risks. For many Pantone colors that are not bright and chromatically saturated there might be no significant color differences. At the same time, the risk and the mentioned color differences will only apply when the designer's artwork is used across print and digital media. When the artwork is only to be used on the internet and displayed via screens, this discussion might not be relevant. Even though, it is difficult to imagine that a brand color will only be displayed on a screen and never on a physical media.

It is unfortunate that Pantone recommends designers to start by entering sRGB values when working with a color. Especially when there are no longer any warnings that the selected color is out of gamut. Likewise, it is unfortunate that the many options in Pantone Connect do not include gamut warnings and color difference information. Finally, it is misleading when Pantone both specifies CIELAB values for the spot color next to the sRGB values, without any warning that this spot color is out of sRGB gamut. As the color data infor-

mation now appears, Pantone sets the sRGB values to be equal to the CIELAB values. It may be advisable to bring an out of gamut warning.

4.1 Practical implications

The results can initially be used to draw attention to the risk of choosing colors directly from screen. Especially when choosing bright and chromatically saturated brand colors that might be reproduced across media platforms. Unlike the Pantone Color Manager software and Adobe CC's previous Color Picker tools, Pantone Connect does not display color warnings for colors outside of gamut. Therefore, the designers themselves must be aware of the risk and this study's method can be used to investigate whether a given color is outside gamut. Thus, the method must already be used in the first three steps of brand color management, namely when choosing, specifying and describing a new brand color. Introducing a brand color management model also draws attention to the responsibilities of designers and brand owners. It shows an overview of the entire process from color choice to color measurement

control of the reproduced color, and it shows the need for communication between designers, brand owners and print providers.

5. Conclusions

The conclusion is that it is associated with high risk when choosing colors directly from a software program via a computer screen. The result is unpredictable and there is a risk of passing on incorrect information to the next link in the value chain, especially if the chosen color is a very bright and chromatic saturated color.

Designers and brand owners therefore have to use physical color swatches when choosing a brand color. For example, if they choose the virtual version of Pantone 1505 C from the screen, they must check how this color really looks like in a Pantone fan deck.

The new model for brand color management can help to focus on especially the first three steps: color selection, color specification and color description.

References

- Adams, R.M., Sharma, A. and Sufioletto, J.J., 2008. *Color management handbook: a practical guide*. Pittsburgh, PA: PIA/GATF Press.
- Bertholdt, U., 2010. *Fundamentals for the standardization of spot colours in offset printing: Fogra research report no. 32.158*. Munich, Germany: Fogra.
- Berns, R.S., 2000. *Billmeyer and Saltzman's principles of color technology*. 3rd ed. New York, NY: John Wiley & Sons.
- Bunting, F., 1998. *The COLOR SHOP color primer: an introduction to the history of color, color theory, and color measurement*. Light Source Computer Images, Inc., an X-Rite Company.
- Chung, R.Y. and Liu, Y., 2022. Acceptability-based brand color tolerance, a case study. *Journal of Imaging Science and Technology*, 66(3), pp. 030509-1–030509-7. <https://doi.org/10.2352/J.ImagingSci.Technol.2022.66.3.030509>.
- Drew, J. and Meyer, S., 2006. *Color management for logos – a comprehensive guide for graphic designers*. Brighton, UK: RotoVision.
- ECI, 2022. *Colour standards: Working colour spaces*. [online] Available at: <<http://www.eci.org/doku.php?id=en:colourstandards:workingcolorspaces>> [Accessed 9 April 2022].
- Eiseman, L., 2000. *Pantone guide to communicating with color*. Cincinnati, OH: How Books.
- Finkle, C., 2019. *Choosing colors for a brand*. Brand Marketing Blog (blog) Available at: <<https://brandmarketingblog.com/articles/branding-how-to/colors/>> [Accessed 24 May 2022].
- Fogra, 2009. *Fogra softproof handbook*. München, Germany: Fogra.
- Green, P., 1999. *Understanding digital color*. 2nd ed. Pittsburgh, PA: Graphic Arts Technical Foundation.
- International Electrotechnical Commission, 1999. *IEC 61966-2-1:1999 Multimedia systems and equipment – Colour measurement and management – Part 2-1: Colour management – Default RGB colour space – sRGB*. Geneva, Switzerland: IEC.
- International Electrotechnical Commission, 2003. *IEC 61966-2-1:1999/AMD1:2003 Amendment 1 – Multimedia systems and equipment – Colour measurement and management – Part 2-1: Colour management – Default RGB colour space – sRGB*. Geneva, Switzerland: IEC.
- International Organization for Standardization, 2009. *ISO 3664:2009 Graphic technology and photography – Viewing conditions*. Geneva, Switzerland: ISO.
- International Organization for Standardization, 2004. *ISO 12647-1:2013 Graphic technology – Process control for the production of half-tone colour separations, proof and production prints – Part 1: Parameters and measurement methods*. Geneva, Switzerland: ISO.

- International Organization for Standardization, 2009. *ISO 13655:2009 Graphic technology – Spectral measurement and colorimetric computation for graphic arts images*. Geneva, Switzerland: ISO.
- Kipphan, H. ed., 2001. *Handbook of print media: technologies and production methods*. Berlin, Heidelberg: Springer.
- Kleeberg, D., Süßl, F., von Oeynhausen, R., Hoffstadt, H., Seitz, J., Hansen, M., Hebes, T., Drümmer, O., Willfahrt, R., Wipperfürth, F. and Tatzauer, W., 2018. *MediaStandard print 2018: technical guidelines for data, proof and production run printing*. Berlin, Germany: bvdn.
- Lindbloom, B.J., 2007. *Using the chromaticity diagram for color gamut evaluation*. (online) Available at: <<http://www.brucelindbloom.com/ChromaticityGamuts.html>> [Accessed 25 May 2022].
- Pantone, 2014. *Pantone Color Bridge Coated*. New Jersey, NJ: Pantone LLC.
- Pantone, 2019. *Pantone Formula Guide Solid Coated: ink colors and formulas for packaging, print and graphics*. New Jersey, NJ: Pantone LLC.
- Pantone, 2022. *Pantone Connect*. [web-application] Pantone. Available at: <<https://connect.pantone.com>> [Accessed May 2022].
- Pedersen, M.A., 2016. Why most brand manuals fail when it comes to defining brand colors; and how to determine acceptable color deviations for specific brand color. In: P. Gane, ed. *Advances in Printing and Media Technology: Proceedings of the 43rd International Research Conference of iarigai*. Toronto, Canada, August 2016. Darmstadt, Germany: iarigai, pp. 91–100.
- Pedersen, M.A., 2018. Reality check: what to expect when buying different print products for a campaign – brand color reproduction across print substrates and technologies. In: P. Gane, ed. *Advances in Printing and Media Technology, Proceedings of the 45th International Research Conference of iarigai*. Warsaw, Poland, October 2018. Darmstadt, Germany: iarigai, pp. 27–35.
- Stokes, M., Anderson, M., Chandrasekar, S. and Motta, R., 1996. *A standard default color space for the internet – sRGB, Version 1.10*. [online] W3C. Available at: <<https://www.w3.org/Graphics/Color/sRGB.html>> [Accessed 22 May 2022].



JPMTR-2119
DOI 10.14622/JPMTR-2119
UDC 655.1:774.8

Research paper | 161
Received: 2021-12-21
Accepted: 2022-04-05

Accuracy of spot color reproduction in a 7-color, expanded gamut, flexographic printing system

Reem El Asaleh, Martin Habekost and Abhay Sharma

School of Graphic Communications Management,
Toronto Metropolitan University,
Toronto, ON, Canada

reem.elasaleh@ryerson.ca
mhabekos@ryerson.ca
sharma@ryerson.ca

Abstract

Expanded gamut printing involves expanding the number of process colors (cyan, magenta, yellow and black) by orange, green and violet colors to reproduce many spot colors with the new fixed ink set (CMYKOGV). This study focuses on evaluating flexographic expanded gamut printing on a narrow web flexographic label press located at Toronto Metropolitan University. Esko Equinox and GMG OpenColor expanded gamut software solutions were used, where each system was tested with its own proprietary characterization test chart. The Idealliance Expanded Color Gamut (ECG) test target was also used in this study. A verification test chart was created, with selected Pantone spot colors. The test chart was then processed using the characterization data from the proprietary and nonproprietary characterization press runs. The builds of the selected Pantone colors were analyzed and CIEDE2000 color difference was calculated. Both software solutions did better in regards to color accuracy with their proprietary characterization targets than using the data gathered from the Idealliance ECG small chart.

Keywords: extended color gamut, flexographic printing, Pantone spot colors, test chart, print contrast

1. Introduction

Flexography printing has been dominating the packaging industry for a decade due to its economical and fast process, ability to print on a wide variety of substrate materials such as corrugated cardboards, label stock, and metallic film, with minimal breakdowns and low maintenance cost.

Traditionally in flexography, printing a package with additional spot colors means setting four-color process units along with an additional one to three units dedicated for spot colors. This usually results in a loss in make-ready for changing the plates and loading spot color onto the press for the next run. This is time-consuming as additional time would be wasted just to make sure the spot colors are correct. This is also material intensive as any leftover ink needs to be stored for possible reuse in the future.

As flexography continues to develop methods and approaches to improve its productivity and quality, the challenge to overcome issues related to reducing cost, decrease make-ready time, and consistent reproducing

spot colors becomes the new reality for many companies. Implementing expanded gamut technology would help to resolve such challenges.

Expanded gamut printing involves adding three colors, orange, green, and violet (OGV) to the conventional process colors cyan, magenta, yellow, and black (CMYK) to expand the gamut of a printing press. Thus, achieving more spot colors reproduction using the combination of these process colors set without the need of having the actual spot color in the printing unit. And therefore, improving production efficiency with less ink and material used, less make-up ready time on the press, and more press capacity while achieving up to 90 % of the Pantone Plus book (Ellis, 2017).

1.1 Historic developments of expanded gamut printing

The concept of expanded gamut printing has been around in the last century with different implementations and approaches until what we know today (Balasubramanian, 1999; Van De Capelle, 2006; Simoni, Butler and Deighton, 2017). The history of this technol-

ogy has been discussed and covered in several publications – by John Seymour in two articles (2018a, 2018b), Habekost and Grusecki (2019) and El Asaleh, Habekost and Biga (2020).

In the early 1990's the High-Fidelity (HiFi) color printing technology was introduced by Mills Davis and Dan Carli. Similar to expanded gamut, HiFi color printing employs adding other inks to the standard CMYK process colors for wider colors reproduction on the press. Some common HiFi Color systems are Pantone Hexachrome (CMYKOG), Küppers (CMYKRGB), DuPont's HyperColor, and ColorBlind MaxCYM (CMYKCMY). This concept was widely used in offset printing (Hutcheson, 1999).

Expanded gamut as it is understood today goes beyond CMYK printing by adding OGV colors. The benefits of expanded gamut printing have been nicely summed up by Baldwin (2016). The benefits are as follows:

- Ink savings (only seven colors are needed, no spot colors)
- Reduced press characterizations
- Reduced wash-ups
- Ganging jobs
- Material savings (inks and substrates)

At the 2019 TAGA conference, Hargrove (2019) demonstrated with data from a print company that printed the same job(s) conventionally and later with expanded gamut technology that there was a cost reduction of \$845 from the original cost of \$2285 to \$1440. The company needed half the make-ready time and half the press time. There were fewer wash-ups, less ink waste and the job had less of an environmental impact.

While most approaches were mainly focused on publication and commercial offset printing, other research focused on testing different approaches to implement expanded gamut printing in flexography. For instance, in the study by O'Hara, Congdon and Lindsay (2019) the research team reduced the chroma of OGV colors from 100 % to 80 % in 10 % increments.

The main points from the study were:

- The greatest chroma of the OGV colors does not mean the largest gamut volume.
- The greatest chroma does not mean the most Pantone colors. Low chroma inks can often make more Pantone colors.
- The greatest gamut volume does not mean the most Pantone colors.
- The ink film thickness appears to influence the gamut size beyond its influence on the chroma of solids.

A review of the latest technological and fundamental evaluations in multicolor printing was demonstrated in the paper of Politis, et al. (2015). The study also summarized research results from two latest studies in expanded gamut printing with silk-screen and flexographic printing. The study tested several color separation and screening techniques and it was concluded that the quality of expanded gamut would be achieved and standardized with a fixed set of six or seven colors.

The Flexo Quality Consortium group researched to test the concept of expanded gamut technology in flexography printing (Rich, 2012). The study concluded that this concept has promising benefits and results especially if there are 10 or more stations available to handle CMYKOGV inks with the addition of white ink, metallic inks, and clear coating. Moreover, it was concluded that using the CMYKOGV ink set would increase gamut across various tested substrates used in their study.

Since expanded gamut printing is a hot topic in the industry at the moment many premedia software solutions are available to implement seven color printing. All these software solutions require that characterization charts need to be printed on the press together with the inks and substrate that will be used for expanded gamut printing, so the software knows what the gamut of the process is. The number of test patches on these characterization charts is also a topic of discussion. For instance, Hoffstadt (2019) gave a presentation at the 2019 TAGA conference on the ideal number of test patches for expanded gamut printing. The study suggested that the ideal number of test patches should be between 1000 and 5000 patches.

In the summer of 2019 Sharma (2019) conducted an evaluation of spot color reproduction in multicolor printing. Several software vendors participated in the study. A test chart was created and processed through various software solutions. The aim of this study was not to determine which solution was the best, but how each software handled expanded gamut printing. One of the tests conducted in this study looked also at how a spot color was built using three, four or more colors. The study output the test charts on an Epson P9000 inkjet proofer and also on an HP Indigo 7900. There was no output of the test chart on a flexographic or offset press which is commonly used in the production of packaging using spot colors (Sharma and Seymour, 2020). In Europe, Fogra has also been active in the evaluation of expanded gamut solutions. In the research project on multiprimary printing in 2019 and at Color Management Symposium in February 2020 solutions for expanded gamut were shown (Li, 2021; Wessendorf, 2020). Participants in the Fogra study also processed a test chart and the color accuracy of the rendered Pantone colors was analysed.

Idealliance (n.d.) has also been quite active over the past few years and formed a committee to create a seven-color characterization target similar to the IT8.7/4 target used for four-color print characterization. This test target is available for free to anyone interested in expanded gamut printing. This project has a small 400 patch target and a large four-page target with 4340 patches (35 × 31 patches on 4 pages).

Idealliance has created a task force that is part of the Print Properties Committee to come up with a standardized test chart that can be used by anyone with any color management software that can handle expanded gamut printing. In fall 2019 Idealliance (n.d.) released their test charts for expanded gamut printing. Version 1 of their test charts included a small test chart with 400 test patches and a large test chart with 4340 test patches. Idealliance encourages the industry to test these charts and upload their measurement data to their website so the Print Properties Committee can evaluate the effectiveness of their two test charts.

The authors of the present paper have conducted earlier studies with expanded gamut printing in digital printing, inkjet printing and offset printing at the School of Graphic Communications Management and the results of these studies were presented at the 2019 and 2020 TAGA conferences (Habekost and Grusecki, 2019; El Asaleh, Habekost and Biga, 2020) and published in *Color Research and Application* (Sharma and Seymour, 2020). In response to interest from the community, we now evaluate flexographic printing.

2. Methods

The premise of this study was to get a better understanding of characterizing a press for expanded gamut printing with seven-color CMYKOGV process. The color press has only these seven process colors and is able to run even jobs with a number of spot colors on them.

Since printing with an expanded gamut is still relatively new there is no standardized test chart available like the IT8.7/4 for four-color offset printing except the above-mentioned test charts created recently by Idealliance. A number of premedia color management software vendors offer a solution for expanded gamut printing and use their own proprietary test chart that works with their software, but not with the software from another company.

2.1 Study parameters

In this study, the software solutions for expanded gamut printing from GMG Color and Esko were used. GMG's solution is called OpenColor. Esko's expanded

color gamut technology is branded "Equinox" in which color measurements and transforms are made and stored in Curve Pilot and Color Pilot. In the current implementation, information from these two products was applied to PDF files via an Automation Engine workflow.

The School of Graphic Communications Management is in possession of a four-color narrow web 7" flexographic label press. In the summer of 2019, this press was extended by three additional print units and allows now to use the expanded gamut print process. Due to the limitations of the press, the Idealliance Small Chart (ISC chart) with 400 test patches was used in this study. The study consists of four main parts:

1. Optimization
 - a. Determine the optimum combination of anilox rollers and ink viscosity for this study.
2. Curve Calibration
 - a. Determine the curves for the seven process colors for optimum press performance.
3. Characterization
 - a. Using the proprietary test charts from Esko and GMG and also ISC test charts
 - b. Select up to 50 in-gamut Pantone colors for conversion to expanded gamut printing
 - c. Create custom test charts for these 50 test colors
 - d. Process this test chart with the color data from Esko, GMG and the ISC
 - e. The data from the ISC chart will be processed with both software applications
 - f. Create four PDF files of the 50 test colors that have been built with the data from the three characterization runs (see d.).
4. Verification run
 - a. Print the four PDF files on one press sheet and measure the color data from them and compare for color accuracy with standard color values from Pantone for these colors.

2.2 Equipment used (software and hardware)

For this study a number of software and hardware was used, therefore the list is quite long.

Software:

- Esko Color Pilot v18.1.0
- Esko Curve Pilot v18.1.0
- Esko Automation Engine v18.1.0
- GMG OpenColor v2.4.1
- MS-Excel v16.45 for Mac

Hardware:

- Comco Cadet 700 – 7” narrow-web label press
- Inks: water-based flexographic inks from Siegwerk
- Anilox rollers with 1.8–2.5 billion cubic microns (BCM) volume and 800–1000 lpi line count
- Media: Label Supply Extragloss LTR ‘Low Tack Removable’ 40#
- Plates: water-washable plates from Toyobo with a thickness of 0.067 inches were made to FIRST 6.0 specifications (Flexographic Technical Association, 2017)
- Micrometer: Mitutoyo Absolute digital micrometer
- Flexo plate analyzer: Betaflex system
- Flexo plate imager: Esko CDI Spark 2530
- Anderson & Vreeland Orbital X plate processor with CL-50 Whirl-A-Way AV Polymer Removal System
- Measurement instruments (spectrophotometers):
 - X-Rite eXact S/N 28618
 - X-Rite iPro2 S/N 1 104 522
 - Techkon SpectroDens S/N B312506

Measurement conditions: M1, D50 for all measurement instruments, status T. The pressroom had a relative humidity between 50 % and 55 % and the temperature was kept between 20 °C and 22 °C.

2.3 Press runs

It was mentioned earlier that this study needed four main press runs. These press runs were:

- Optimization run
- Curve calibration run
- Characterization run
- Verification run.

All press runs took place in the press lab of the School of Graphic Communications Management.

2.3.1 Optimization press run

This press run was designed to determine the best combination of ink viscosity and anilox rollers for each of the seven process colors. Two factors were taken into consideration for this evaluation. One was the printed color density that was achievable and the other one was which anilox volume can be used without causing dot bridging or other print defects. Another factor was also the available anilox rollers in the press lab. The dynamic ink viscosity was determined from measurements of efflux time with a Zahn cup #2. The optimum dynamic ink viscosities are listed in Table 1.

Table 1: Optimum ink viscosities for this study measured with a Zahn-Cup #2, converted to dynamic viscosity

Color	Viscosity (mPa·s)
Yellow	105
Magenta	90
Cyan	144
Orange	105
Green	105
Violet	90
Black	90

The press form used for this part of the study is a pre-made file that was supplied by Esko. An extended version of the actual calibration file that was used is shown in Figure 1.

2.3.2 Curve calibration press run

After the determination of the best combination of anilox rollers and ink viscosity for the seven process colors, a curve calibration run was required. This press run determines the plate curves for each color. Some colors might need cut-back curves, while others might require so-called bump curves.

The test chart used for this press run can be seen in Figure 2.

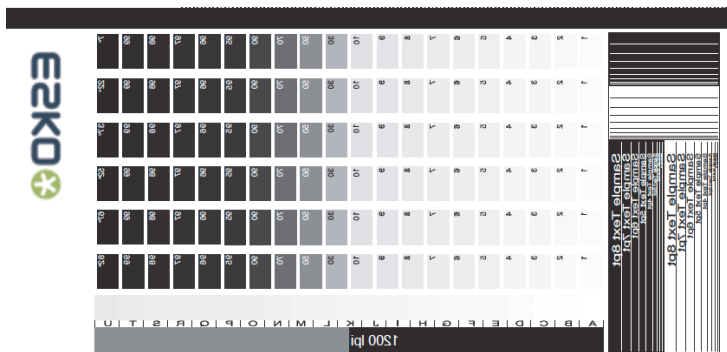


Figure 1: An extended version of the press form that was provided by Esko and used in the optimization run to determine the best combination of ink viscosity and anilox rollers for each of seven process colors

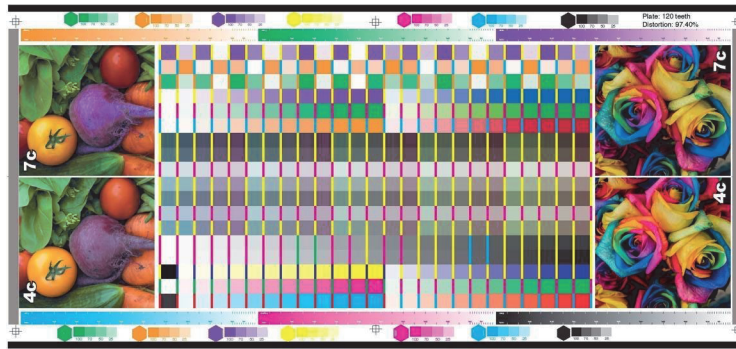


Figure 2: Test chart used for the determination of the tone value curves for all seven colors

The press run was conducted with the ink viscosities determined during the optimization run. Through the combination of ink viscosity and anilox roller used for each color, the target printed color densities were determined. For orange, green and violet the printed color density was measured using the Spot Color Tone Value (SCTV) mode on an X-Rite eXact according to ISO 20654 (International Organization for Standardization, 2017). Since the press used in this study is a manual press with no automatic doctor blade pressure settings and automatic setting of the ink fountain roller it took a couple of attempts to find the ideal settings. Once these settings were learned the following target printed color densities were established.

Table 2: Target printed color densities for all future press runs in this study

Color	Target printed color density
Yellow	0.75
Magenta	0.95
Cyan	1.31
Orange ($\lambda = 450 \text{ nm}$)	1.17
Green ($\lambda = 630 \text{ nm}$)	1.63
Violet ($\lambda = 550 \text{ nm}$)	1.56
Black	1.24

Adjustment curves for all seven colors were determined using Color Pilot from Esko. It was also ensured that only opposing colors were placed on the same screen angle to avoid any moiré.

Three different characterization charts were used to evaluate the color behavior of the same printing process:

- Esko Equinox 4x4 EDK chart with 3872 patches
- GMG OpenColor characterization chart with 700 patches
- ISC chart with 400 patches.

It is relevant to examine the color gamut that each of the three different characterization charts deter-

mines from the printing process. It is important that a characterization chart samples the color response of the system, not under sampling the color space with sparse data from which to create a color model, nor oversampling the color space wasting color patches that add no further information, all the while reaching the extremes of the gamut limits. In fact, the choice of the correct number of patches has been tested and evaluated ad infinitum in conventional literature (Deshpande, Green and Pointer, 2015).

At the 2019 Annual Technical Conference of TAGA Hoffstadt (2019) gave a presentation on the ideal number of test patches for expanded gamut printing. If the same 9-step resolution from CMYK would be applied to CMYKOGV about 5 million test patches would be needed and "...even with only 4 steps per ink, we have $4^7 = 16384$ patches at a rather poor grid resolution..." (Hoffstadt, 2019). Then the question was what can be done to reduce the number of test patches to a number between 1000 and 5000. At the time the number of patches used by GMG OpenColor was 4200 (35 x 30 patches on 4 pages). At the same conference, a presentation by Braun and Alejandro (2019) showed that not much more accuracy is gained by test charts with many test patches. The number of test patches needed depends on the number of colorants used in the print process. For example, the number of test patches needed for GRACoL 2006 to achieve a 95th percentile of CIEDE2000 color differences of less than 1.0 is 150 (Figure 3).

For a seven-color print process, the optimum number of test patches to achieve a 95th percentile of a CIEDE2000 of 1.0 is around 3000 (Figure 4).

The paper by Braun and Alejandro (2019) provides a formula (Equation [1]) that can be used to calculate the number of test patches that are needed to achieve a certain ΔE , for a specified printing system.

$$e = \frac{k}{n^g} \quad [1]$$

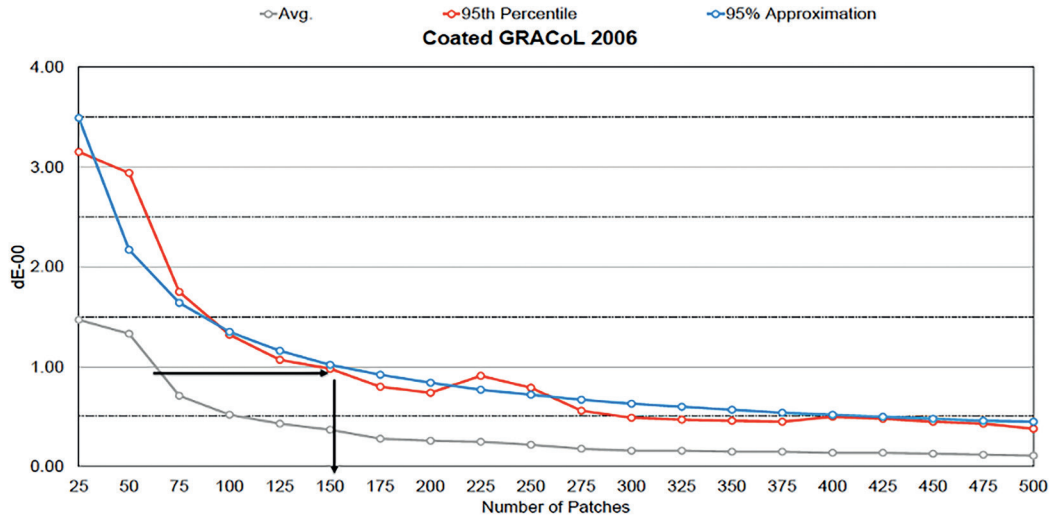


Figure 3: Number of test patches needed to achieve a 95th percentile of the test patches to have a CIEDE2000 of 1.0 according to Braun and Alejandro (2019)

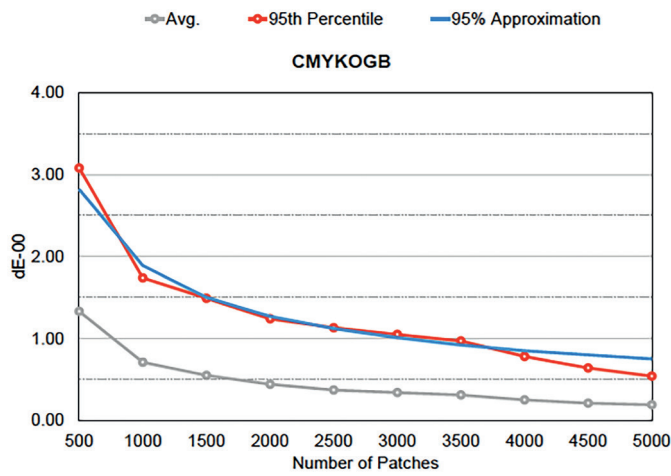


Figure 4: Number of test patches needed to achieve a 95th percentile of the test patches to have a CIEDE2000 of 1.0 according to Braun and Alejandro (2019)

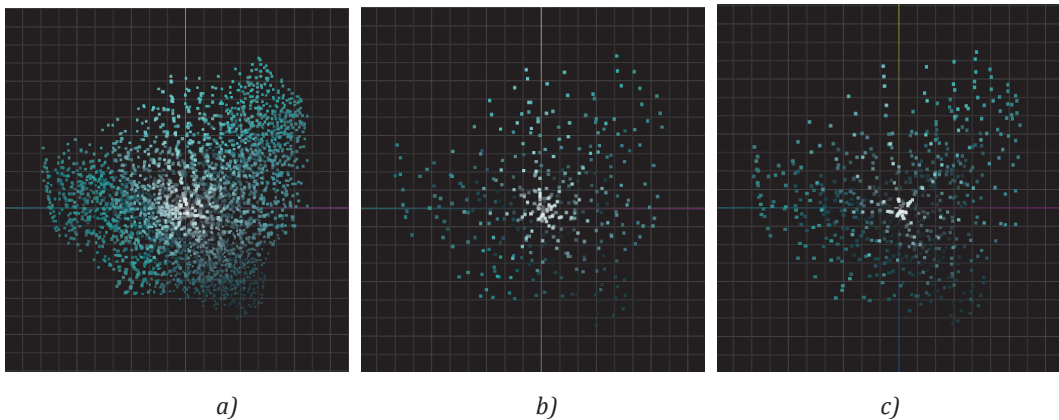


Figure 5: Presentation of Esko EDK (a), GMG (b), and ISC (c) color gamuts; from the L*a*b* values in 2-dimensional color gamut presentation we see that the EDK (a) solution has many more patches while the ISC (c) appears to be missing data from some areas of the color space

where the symbol e represents the ΔE value that one wants to achieve. Braun and Alejandro (2019) also provide numbers for k and g . For a seven-color system the factor $k = 100.00$ and the exponent $g = 0.57$. Solving the equation for n for a ΔE of 1 results in the number of patches needed to achieve a ΔE of 1 as 3227. A closer look at Figure 4 shows that the curve of the 95th percentile intersects with a y -axis value of 1 around this number of patches.

2.3.3 Characterization press runs

After the successful creation of the plate curves for the output of plates for any future press runs in this study the plates for the characterization press runs were made. The ink viscosities for the characterization press runs were kept within a variance of $\pm 5\%$ from the target ink viscosity values listed in Table 1.

The test chart for the Esko characterization press run consists of all seven colors, but not all seven colors are printed at once. The press run is split up into four different runs:

- CMYK
- OMYK (Orange)
- CGYK (Green)
- CMVK (Violet)

The Esko EDK four test charts can be seen in Figure 6.

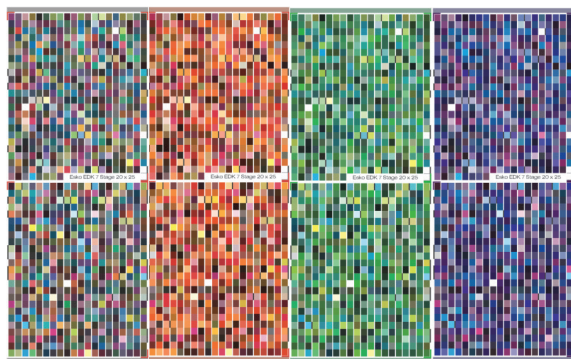


Figure 6: Esko EDK test charts with a total of 3872 patches; the four charts have been used to sequentially explore different parts of color space

The test charts were read into the Color Pilot software so the Pantone Plus Solid Coated v3 M1 color library can be built using the seven process colors.

The next characterization press run took place on day two of the experiment. On this day two characterization press runs took place. The first press run of that day was used to print the proprietary test chart from GMG and the second press run was used to print the ISC chart.

An image of the GMG test chart can be seen in Figure 7. The chart is an exact fit for our printing plate and measurable with our measuring instrument (i110 table) without further cutting. The test chart has a total area coverage limit of 300%.

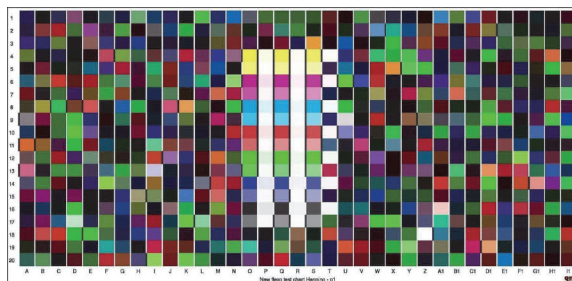


Figure 7: GMG test chart with 700 patches; the number of patches is user-defined for our printing process and it covers the whole gamut in a single chart

After the press run the test chart was measured with the i1Pro2 listed above and imported into GMG's OpenColor software to build the Pantone Plus Solid Coated color library using the seven process colors.

The last test chart that needed to be printed was the ISC chart (Figure 8). This chart was measured in the expanded gamut software solutions from Esko and GMG; again, so the Pantone Plus Solid Coated color library can be built using the seven process colors.

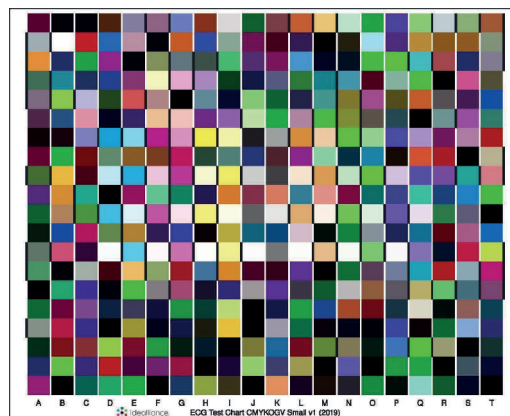


Figure 8: Idealliance Small Chart with 400 patches; it is an exact fit for the printing plate and measurable in our measuring instrument without further cutting

From Figures 6 to 8 it can be seen that the size of the test chart varies greatly. The Esko test charts have a total of 3872 patches, the GMG test chart has 700 patches and the ISC chart contains 400 patches.

One of the questions is, "Do more test patches result in a more accurate prediction of the color builds of the Pantone?"

It needs to be said also, that the data from the characterization test charts were read in with the same measurement instrument using the respective measurement tools from either Esko and GMG and test measurements from each test chart were sent to their respective vendor. The only measurement data that was sent to both vendors was the data from the ISC chart.

2.3.4 Verification runs

Using the Check Gamut tool in Esko’s Color Pilot, we were able to check how each ink in the Pantone Plus Solid Coated ink book will be reproduced with the percentage of each output ink. Also, the tool would show how close the converted color would be to the original via CIEDE2000 information. The conversion was conducted using the Equinox profile and color strategy information that was generated using Esko’s characterization data.

Out of the tested Pantone Plus Solid Coated book with 2139 colors, 1037 Pantone colors were selected with a CIEDE2000 of less than one. This represents 48.5 % of the Pantone Plus Solid Coated colors. These colors would be considered “in-gamut” colors. We then extracted 27 colors from that list that will be used in the verification target. The selected colors were closely distributed in lightness, hue and chroma. In Figure 9 the selected colors and their respective hue values are shown.

In addition, the verification target included CMYKOGV solids, black tint (0 %, 25 %, 50 %, 70 % and 100 %),

and three additional tint ramps for spot colors that were chosen to be close to the OGV colors of the printing process as follows:

- PANTONE 151 C: 25 %, 50 %, 70 %, 100 % (orange)
- PANTONE Green C: 25 %, 50 %, 70 %, 100 % (green)
- PANTONE 2091 C: 25 %, 50 %, 70 %, 100 % (violet)

The final verification target with all the selected patches plus the tint ramps of the three Pantone colors P151 C, Green C and P2091 C is shown in Figure 10.



Figure 10: Custom test chart for the verification press runs showing the selected 27 test Pantone patches with tint ramps for black and three Pantone colors P151 C, Green C and P2091 C

For the verification test run to take place, the small custom test chart needed to be placed onto the plate template that was used during this study. The custom test chart was placed four times onto the plate template.

Two of the custom test charts had been processed by Esko using the data from the EDK test chart (Figure 6) and ISC chart (Figure 8) and the other two test charts

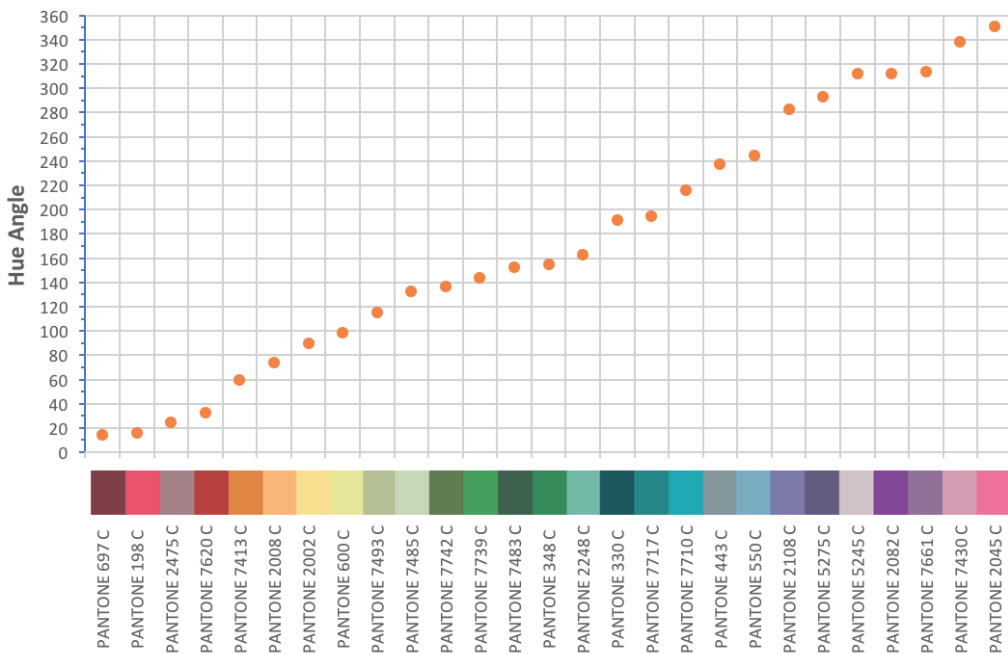


Figure 9: Hue angle distribution for the 27 selected verification Pantone targets; the selected colors cover the whole gamut and are closely distributed in lightness, hue and chroma

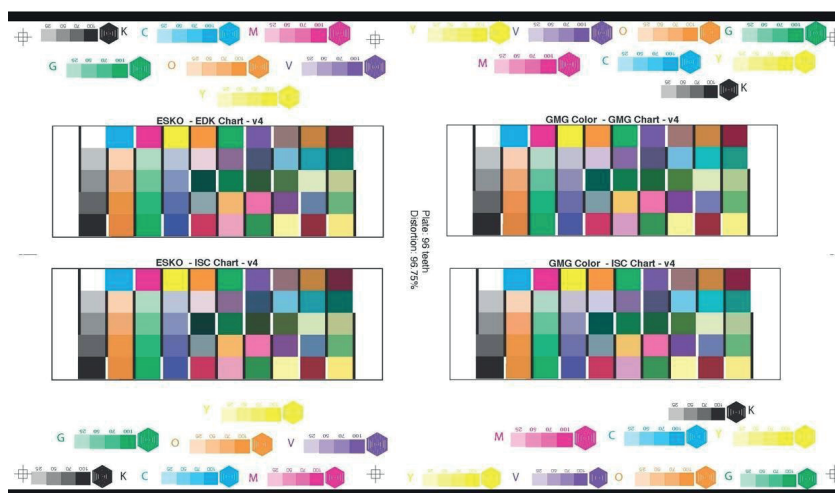


Figure 11: Layout of the test chart used in the verification run; the left charts were processed with Esko software using data from Esko property target (top left) and ISC target (bottom left). The right charts were processed with GMG software using data from GMG property target (top right) and ISC target (bottom right)

were processed by GMG using the data from their characterization test chart (Figure 7) and the ISC chart (Figure 8). The verification press run took place two months after the characterization run. The layout of the test charts can be seen in Figure 11.

From Figure 11 it can be seen that the test charts have been labelled clearly to indicate which software was used to process the custom test chart shown in Figure 10.

2.4 Press variation

After having looked at the accuracy of the color reproduction of the selected in-gamut test colors and seeing that test color builds done by Esko resulted in higher CIEDE2000 values compared to the Pantone Plus Solid Coated reference values than the color builds done by GMG raised the question about variations between the various characterization press runs.

A good tool to look at press variation is to examine the tone value curves from the various characterization runs. Measurements of the characterization and verification runs (Esko verification run, GMG verification run) were done in December 2020.

The following charts were measured with a Techkon SpectroDens listed in the chapter 2.2:

- Esko EDK target with the following sub-targets:
 - CMYK
 - OMYK (orange)
 - CGYK (green)
 - CMVK (violet)
- GMG characterization target
- ISC chart

All data were measured with a Techkon SpectroDens in M1 mode, status T. The following parameters were measured:

- Printed color density
- $L^*a^*b^*$ values
- Tint densities of the 70 %, 50 %, and 25 % patches
- Tint value measurements were performed using the SCTV function for all colors

The purpose of these measurements was to determine if there were differences between the press runs of the various targets. The results are split between the gear and drive side of the press. Besides generating the tone value curves for each of the runs, the color difference for the seven colors between characterization run(s) and verification run was also determined and expressed in CIEDE2000 values. Another quality measure for press runs is the calculation of print contrast.

2.5 Print contrast

According to Breede (1999), Handbook of Graphic Arts Equations, “Print contrast measures the ratio of a shadow area density to solid ink density.” A high print contrast ratio can be used as a measure for superior print quality. In offset printing, the 75 % tint patch is used to determine the print contrast, but in flexography, the 70 % tint patch is being used for this determination. For the determination in our study, the print contrast on the CMYK colors was only used and calculated using the following formula (Breede, 1999):

$$\text{Print contrast} = \frac{(\text{Solid ink density} - \text{density of 75 \% tint})}{(\text{Solid ink density})} \quad [2]$$

3. Results and discussions

3.1 Color differences of the tested Pantone colors

Figure 12 shows the average CIEDE2000 between the expected $L^*a^*b^*$ values of 27 in-gamut spot colors based on the Pantone Plus Solid Coated library and the printed and measured $L^*a^*b^*$ values for that spot colors. Figure 12 shows two columns with results for the Esko solution when using the proprietary Esko Equinox 4×4 EDK characterization chart (Esko-EDK) and the results when Esko created a color characterization with the non-proprietary, ISC chart (Esko-ISC).

In general, we see that many colors can be reproduced to < 2 CIEDE2000 (a typical tolerance in package printing), and we see that Equinox generally produces lower ΔE (better results) when using the 4×4 EDK chart (3872 patches) compared to the ISC chart (400 patches). Lower CIEDE2000 reflects better matching, thus, overall Esko achieved better matching when using its proprietary data over non-proprietary Idealliance data.

In the same way, Figure 13 presents results for GMG Color, showing data for OpenColor when using the proprietary OpenColor characterization chart (GMG-GMG) and the results when OpenColor used the non-proprietary, ISC chart (GMG-ISC).

In general, we again see that many colors can be reproduced to < 2 CIEDE2000, and that OpenColor produces much lower CIEDE2000 when using the OpenColor chart (700 patches) compared to the ISC

chart (400 patches). As in the case of Esko, overall GMG achieved better matching when using its proprietary data over non-proprietary Idealliance data.

Table 3: The CIEDE2000 statistics for the 27 spot colors for the Esko Equinox solutions with the 4×4 EDK chart is compared to the same solution when using the ISC chart

Color differences	Esko-EDK	Esko-ISC
Minimal	0.82	0.99
Standard	1.29	1.92
Average	2.45	3.49
95 th percentile	4.77	6.15
Maximal	5.08	9.93

Table 4: The CIEDE2000 statistics for the 27 spot colors for the GMG OpenColor solutions with OpenColor characterization chart is compared to the same solution when using the ISC chart

Color differences	GMG-GMG	GMG-ISC
Minimal	0.69	0.96
Standard	0.75	1.15
Average	1.55	2.94
95 th percentile	3.22	4.58
Maximal	3.87	5.49

The average CIEDE2000 values over the 27 in-gamut spot colors are shown in Tables 3 and 4, for Esko Equinox and GMG OpenColor, respectively. We see that both vendors have a lower average CIEDE2000 when using their own proprietary characterization chart compared to the generic ISC chart.

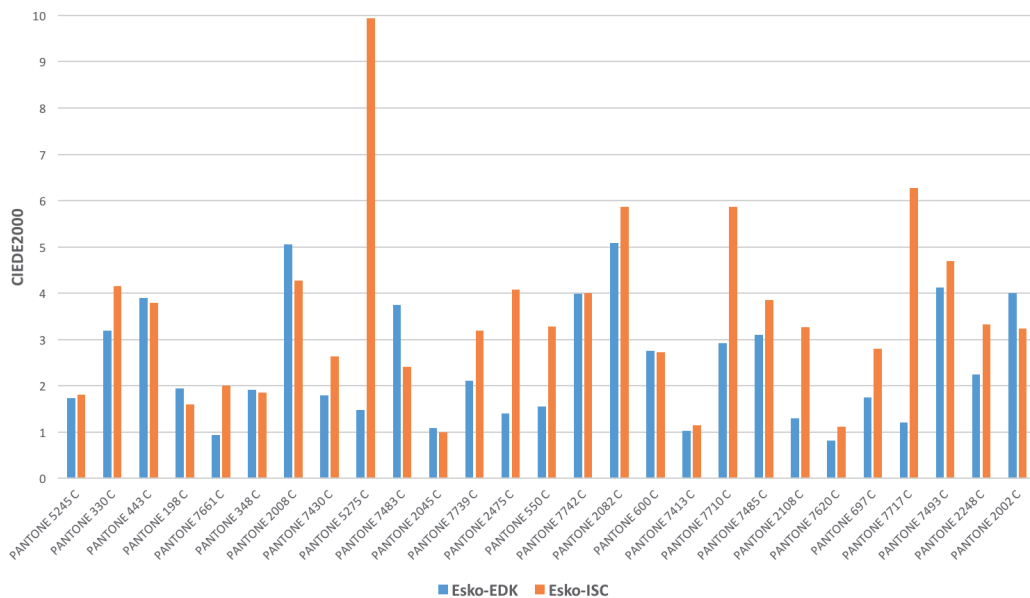


Figure 12: Average CIEDE2000 values between the Pantone Plus Solid Coated $L^*a^*b^*$ library values and the printed and measured values for Esko when using the 4×4 EDK chart (marked blue) and the ISC chart (orange)

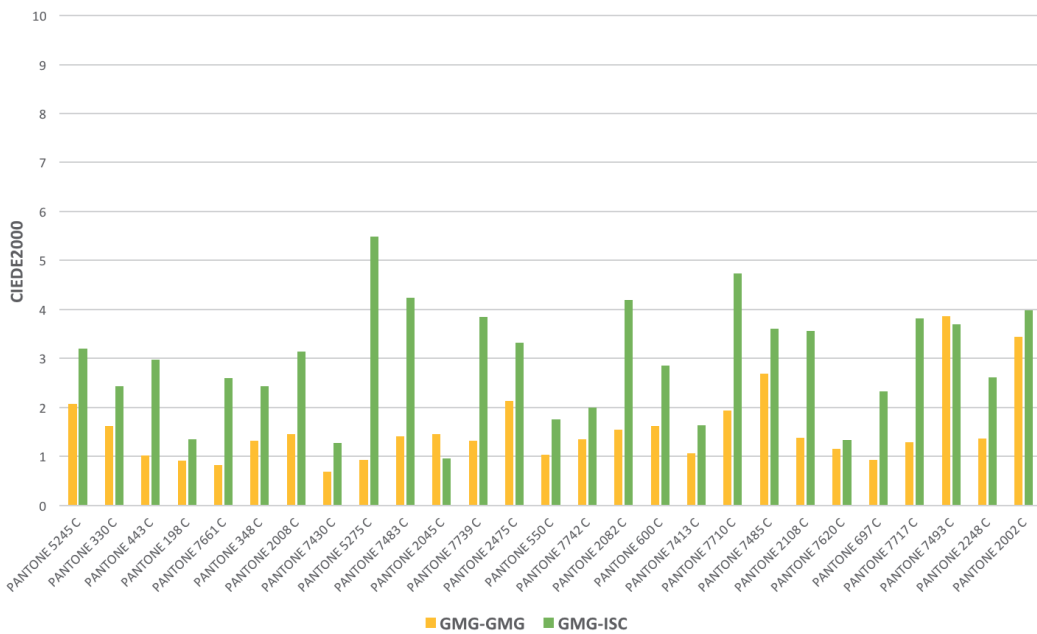


Figure 13: Average CIEDE2000 values between the Pantone Plus Solid Coated L*a*b* library values and the printed and measured values for GMG Color when using the OpenColor chart (marked yellow) and the ISC chart (green)

The separation build for the spot colors was analyzed between the vendor solutions. In particular different spot color builds were analyzed in terms of CMYKOGV inking values.

using violet while GMG favored a CMYK-only build. In analyses of the separations, in general, we saw that GMG frequently favored a CMYK-only build.

As it is shown in Figure 14, Pantone 2108 C was reproduced with similar CIEDE2000 accuracy by both vendors, however, analysis of the inking showed Esko

Pantone 443 C was reproduced inaccurately by Esko, but accurately by GMG OpenColor. The human observer is very sensitive to this mid-tone, neutral color ($L^*a^*b^* = \{64, -4, -6\}$) and a small shift in printed color

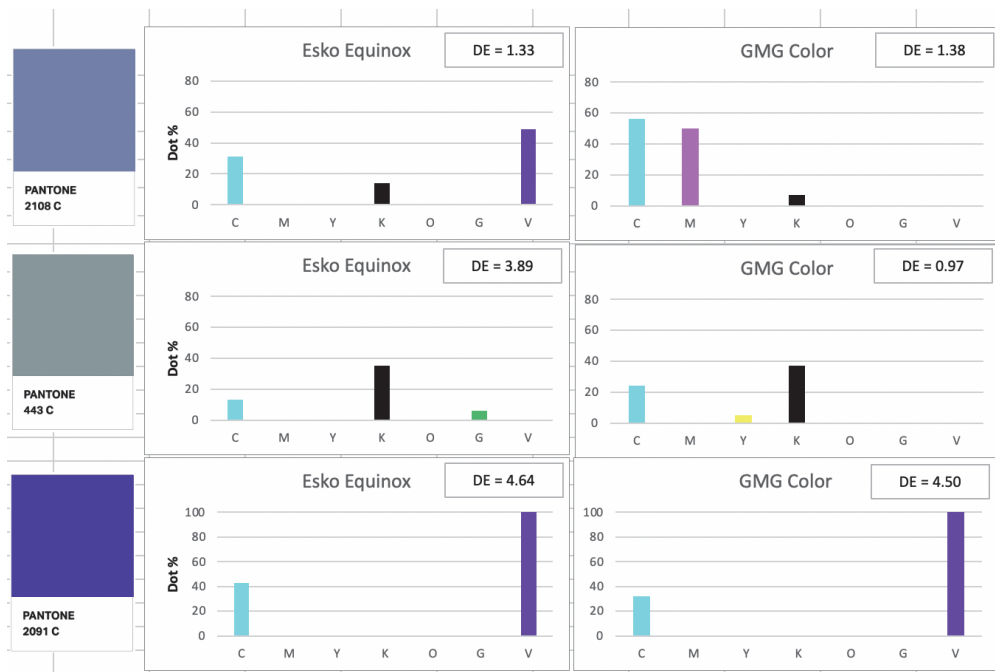


Figure 14: The separation build for three different spot colors was analyzed between the vendor solutions

can create a large CIEDE2000. Pantone 2091 C used a similar separation in both vendors’ software, and was out of gamut and was subsequently reproduced with a high CIEDE2000 by both solutions. Pantone 2091 C was not part of the testing set of 27 spot colors, instead, it represented a spot color very close to the violet ink used on press and was used to “tempt” the vendor solutions to use an expanded gamut colorant in the separation, and indeed OpenColor was forced to use a non-CMYK colorant – violet.

3.2 Results from the color gamut and test charts patches number

In the analysis of the $L^*a^*b^*$ two-dimensional projection of the characterization measurements, Figure 5, we see that the Esko EDK solution has many more patches and therefore a much denser color cloud. A large number of patches appear to needlessly oversample the color space as it does not lead to lower ΔE in the analysis. Furthermore, the larger number of patches requires four press runs on a narrow web flexo press as used in this project and also by a typical packaging customer. A large number of patches could be useful in a very “noisy”, unstable printing process, as the large number of patches can provide a smoothing function and the solution is expected to be very robust in the presence of press variations. The fact that four press runs are used to create this single dataset is somewhat self-defeating as each press run necessarily introduces its own variations. See the section 3.7 on press variation.

At the other extreme, the ISC chart has so few patches (or patches with poorly chosen inking values) that some areas of the color space remain unsampled, thus a color algorithm receives no colorimetric information from these colors with which to develop a color model

and lookup table, supporting the findings where both vendor solutions created the least accurate separations when using the ISC chart characterization data.

3.3 Printed color densities

The average printed color densities for all the press runs were compared to determine if there was considerable variation for these values. The results of these measurements can be seen in Figure 15, where you can see the average printed color densities for all seven process colors. The ink densities that stand out the most are the densities for orange, green and violet in the verification run that are a little bit higher than the average printed color densities printed in the previous runs, and the density for cyan in the GMG characterization run.

From Figure 15 one can conclude that there were some printed color density variations. Overall, these variations were only somewhat significant for the OGV inks in the verification press run. Since these values do not show a great difference, it is important to also examine the tone value curves of all the press runs conducted in this study.

3.4 Spot color tone value curves

A point of interest is the tone value curves since tint values of CMYKOGV are used to build the Pantone colors. Differences between the characterization runs and the verification run in the tone value curves are a possible source of error. The tone value curves were measured with the Techkon SpectroDens in SCTV mode. Typical examples of the curves are shown in Figures 16 and 17 and detailed curves from all the runs can be found in the Appendix.

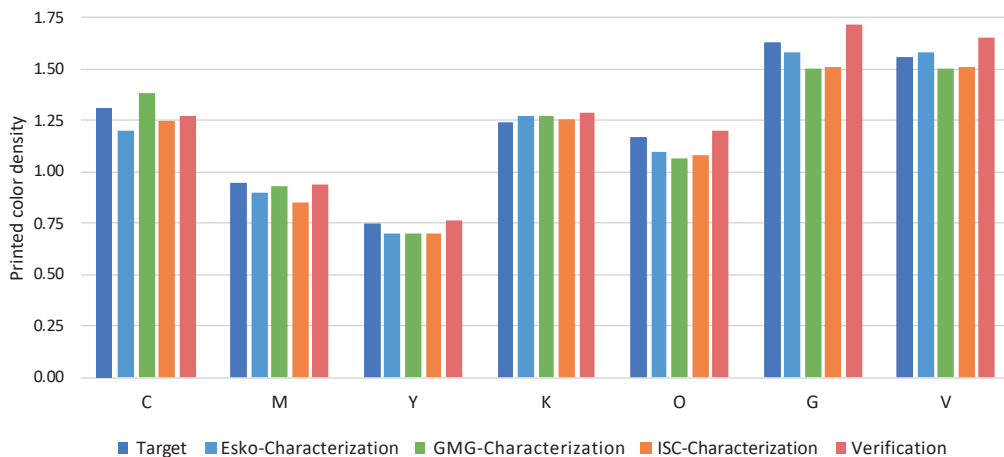


Figure 15: Average printed color densities for the seven process colors for all press runs; while print ink densities variation exists in all seven colors, OGV colors score higher ink densities in the verification run compared to other runs

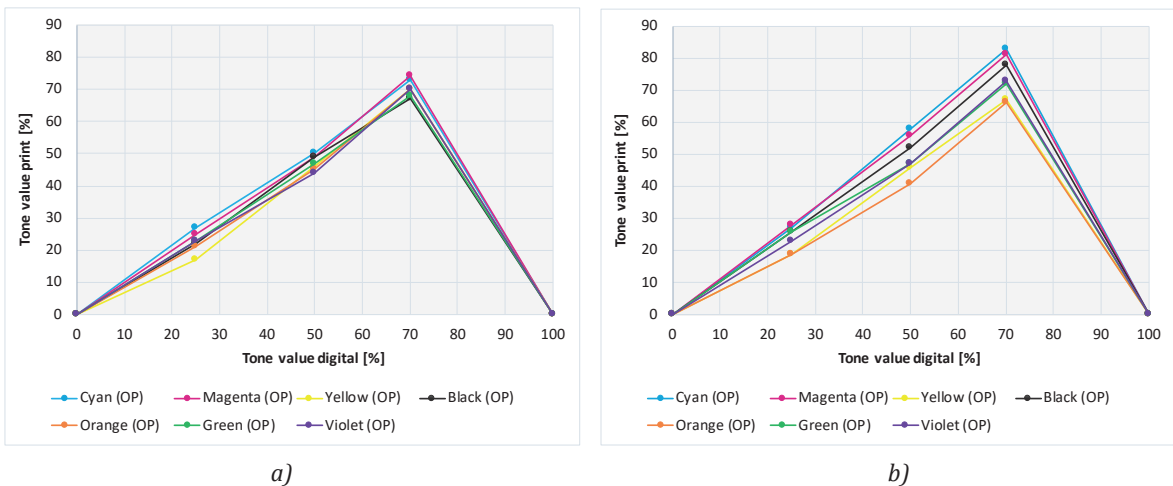


Figure 16: The SCTV tone value curves from the Esko verification run for the gear (a) and operator (b) side; variation in tonal values is noticeable between the two sides

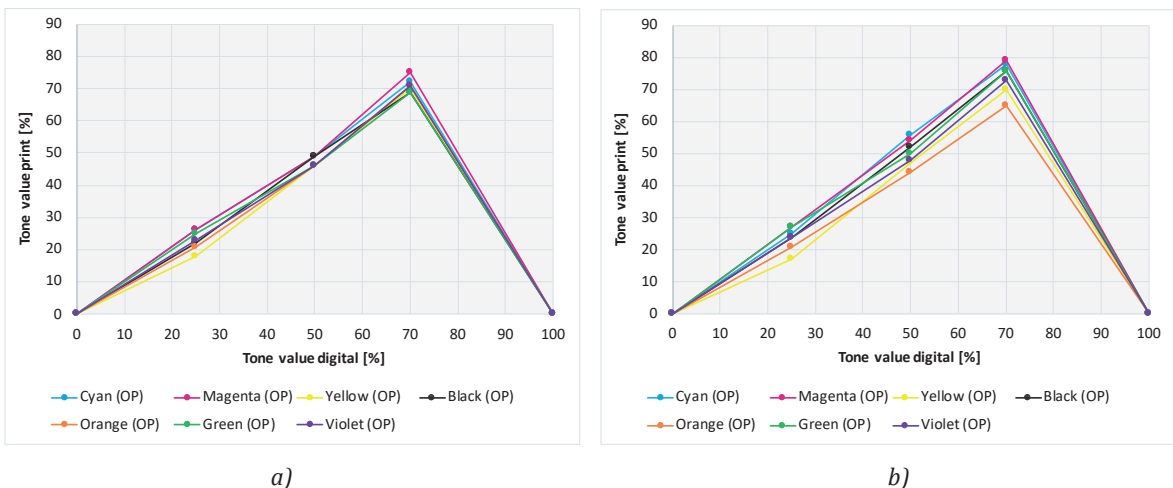


Figure 17: The SCTV tone value curves from the GMG verification run for the gear (a) and operator (b) side; variation in tonal values is noticeable between the two sides

From Figures 16 and 17 it can be seen that there is a difference in the SCTV curves between the gear and the operator side. Most likely this is due to the purely mechanical and analog setting of the printing plate against the anilox roller, but the behavior is consistent between the different press runs. The curves are different from the traditional dot gain curves as they used spectral reflectance values to calculate tonal value. There is more spread in tonal values on the operator side than on the gear side. On some occasions, some colors scored more or less tonal values from one side to another which reflects press variation across a different side of the press.

3.5 Color differences between the runs

For the determination of the color differences between the characterization and verification runs the $L^*a^*b^*$ values of the 100 % solids of the seven process colors

CMYKOGV were averaged from the measured press sheets and the CIEDE2000 was calculated. The results are shown in Figures 18 and 19. While overall variations between press runs are small, the color differences between the press runs are noticeable in cyan, black and violet colors.

The biggest color differences were determined for cyan and black colors between the Esko EDK characterization run and the verification run. Surprisingly the color differences between the ISC characterization run and the Esko verification run for ISC are in general smaller. The largest color differences were determined for cyan, black and violet colors with a maximum value of CIEDE2000 of 2.91 for cyan, followed by 2.61 for black and 2.07 for violet. The average CIEDE2000 between the Esko characterization runs and the verification run was 1.67. For the color differences between the ISC characterization run and verification run the

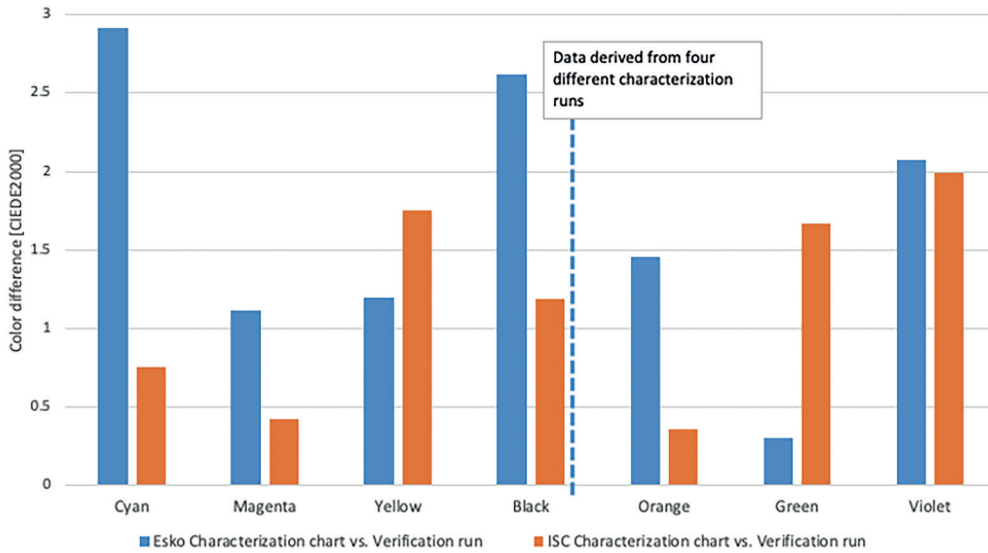


Figure 18: CIEDE2000 values between the Esko characterization and verification run and the ISC characterization run and the Esko verification run; a lower CIEDE2000 is better

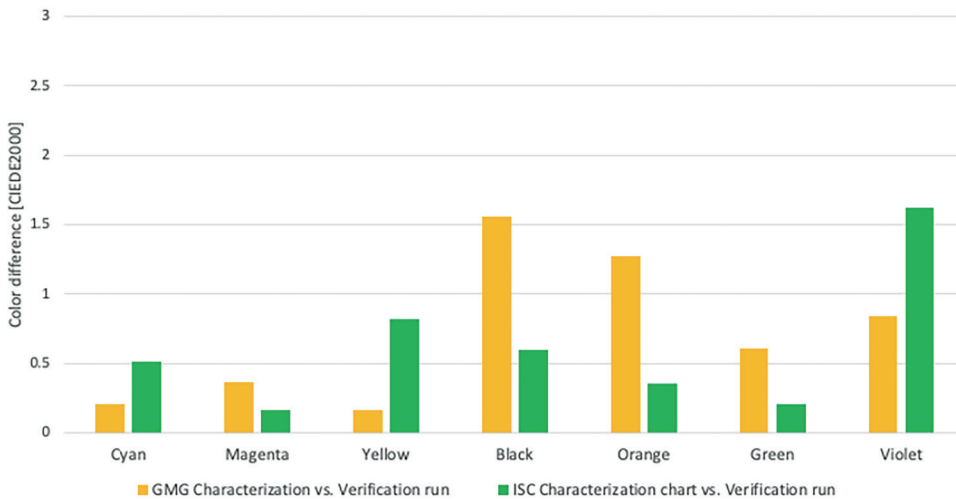


Figure 19: CIEDE2000 values between the GMG characterization and verification run and the ISC run and the GMG verification run; a lower CIEDE2000 is better

largest differences were determined for violet, yellow and green. The maximum value of 1.99 was determined for violet, followed by 1.75 for yellow and 1.67 for green color. The average CIEDE2000 between the ISC characterization run and the Esko verification run was 1.16.

The same evaluation was done for the press runs associated with the GMG characterization and verification run. Figure 19 paints a slightly different picture. While overall variations between press runs are small, the color difference between the press runs are noticeable in black, orange and violet colors. The largest color differences between the characterization and the verification run have CIEDE2000 values of 1.56 for black, followed by 1.27 for orange and 0.84 for violet. The average

color difference was 0.72. The largest color differences between the ISC characterization run and GMG verification run for ISC were determined for violet, yellow, and black colors. The maximum value of 1.62 was determined for violet, followed by 0.82 for yellow and 0.6 for black. The average CIEDE2000 between the ISC characterization run and the GMG verification run was 0.61.

3.6 Print contrast results

Figure 20 shows the print contrast for all the print runs. Aside from the outlier values in cyan in GMG runs, yellow in ISC run, the remaining runs have close print contrast values. Noticeable variation still occurs between Esko EDK and verifications runs.

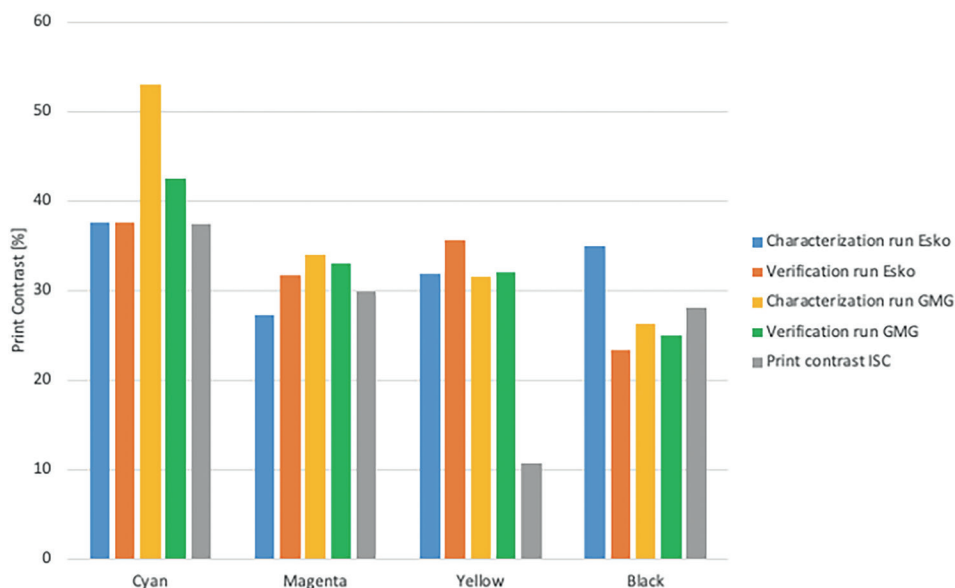


Figure 20: Print contrast percentage values for all print runs; a higher print contrast percentage is more desirable

3.7 Variations between print runs

Overall, it can be said that there was some variation between the characterization and the verification press runs. The biggest variations were found in the four Esko EDK runs and the verification run. The variations between the four characterization press runs for the EDK target were expected, because there were basically four different press runs. Print units were manually taken of impression and put on impression. Even though great care was taken to minimize printing pressure variations due to the fully manual nature of the press used in this study these variations manifested themselves in the variations of the tone value curves and also in the color differences between the characterization runs and the verification runs. The color differences were larger for the press runs conducted for the Esko workflow solution than for the press runs conducted for the GMG workflow solution.

4. Conclusions

One of the main outcomes of this study was that it is possible to print Pantone spot colors using expanded gamut print technology on a more than 20-year-old narrow-web printing press. Another outcome was that it is possible to get quite accurate color build results using 700 test patches to create the characterization of the press. The biggest variations were found in the four Esko EDK runs, and the verification run. The variations between the four characterization press runs for the EDK target were expected, because there were basically four different press runs. It is also important to correctly record all press run parameters so they can be recreated

at future press runs. The process comprising an optimization run to determine the best combination of anilox roller and ink viscosity, a curve calibration run to determine the tone value curves for each of the seven process colors, a characterization run to map the color gamut of the printing press, and inks used on press and verification run to validate all the previous steps results in quite an accurate color build of the tested Pantone colors.

In label and package printing, the typical color difference tolerance for reproducing spot colors is <2 CIEDE2000. In this study, many colors were reproduced to that tolerance as we see, in essence, the average CIEDE2000 that was achieved when reproducing the 27 tested spot colors was 2.45 when using Esko Equinox solutions with Esko EDK chart compared to 3.49 when using the same solution with Idealliance Small Chart. In addition, we achieved an average of CIEDE2000 of 1.55 with GMG Open Color solutions with OpenColor characterization target compared to 2.94 when using the same solution with Idealliance Small Chart.

Color management software plays a significant role in achieving accurate color metrics at different stages of this process. In expanded gamut technology, the software must come with the best ink separation build algorithm to modulate a 7-color printing system using the provided gamut generated from printed characterization charts. In addition, this study demonstrates the correlation between the number of patches and the effective sampling of color responses of the printing system. While a large number of patches would better suit a very noisy, unstable printing process, it does not result in lower ΔE . Lower number of patches, on the other hand, would result in missing color sampling

information and thus less accurate separation which was the case with Idealliance Small Chart. Both color management software used in this study showed better results with their own target compared to generic Idealliance Small Chart.

A future project emanating from this study can be to optimize the ink set and even the substrate used on the press to achieve a wider gamut, so more of the Pantone colors can be reproduced using expanded gamut technology.

Acknowledgments

We would like to thank the following individuals and companies for their support of this project:

- Julian Fernandez, Esko
- Mark Samworth, Esko
- Birgit Plautz, GMG Americas
- Charlotte Curphey, GCM student
- GCM technicians Khaled Ahmed and Darsan Sivanantharajah

Author Abhay Sharma is pleased to acknowledge funding support from Toronto Metropolitan University in the form of a Seed Grant from The Creative School.

References

- Balasubramanian, R., Xerox Corporation, 1999. *System for printing color images with extra colorants in addition to primary colorants*. U.S. Pat. 5,870,530.
- Baldwin, C., 2016. Expanded gamut printing 101. *Labels and labeling*, [online] Available at: <<http://www.labelsandlabeling.com/sites/labelsandlabeling/files/magazine/labels-vol38-issue2-2016/html5forpc.html?page=50>> [accessed 25 January 2020].
- Braun, T. and Alejandro, J., 2019. Optimal test charts. In: *Proceedings of the 71st Annual Technical Conference*. Minneapolis, MN, 17–20 March 2019. Warrendale, PA: TAGA, pp. 89–96.
- Breede, M.H., 1999. *Handbook of graphic art equations*. Pittsburgh, PA: GATF Press, p. 87.
- Deshpande, K., Green, P. and Pointer, M.R., 2015. Gamut evaluation of an n -colour printing process with the minimum number of measurements. *Color Research and Application*, 40(4), pp. 408–415. <https://doi.org/10.1002/col.21909>.
- El Asaleh, R., Habekost, M. and Biga, E., 2020. Brand color reproduction using expanded gamut technology with offset printing. In: *Proceedings of the 72nd Annual Technical Conference*. Wexford, PA, 15–18 March 2020, Warrendale, PA: Taga, pp. 14–37.
- Ellis, R., 2017. *The printer's guide to expanded gamut*. [pdf] Techkon. Available at: <<https://www.techkonusa.com/wp-content/uploads/2017/02/Techkon-Expanded-Gamut-Whitepaper-Final.pdf>> [accessed January 2020].
- Flexographic Technical Association, 2017. *Flexographic Image Reproduction Specifications & Tolerances – FIRST 6.0*. Bohemia, NY: FTA.
- Habekost, M. and Grusecki, I., 2019. Color accuracy of corporate colors in expanded gamut reproduction. In: *Proceedings of the 71st Annual Technical Conference*. Minneapolis, MN, 17–20 March 2019. Warrendale, PA: TAGA, pp. 97–108.
- Hargrove, K., 2019. Expanding your printer's reach: the rise of expanded gamut. In: *Proceedings of the 71st Annual Technical Conference*. Minneapolis, MN, 17–20 March 2019. Warrendale, PA: TAGA, p. 198.
- Hoffstadt, H., 2019. Characterization of multicolor printing: challenges and solutions. In: *Proceedings of the 71st Annual Technical Conference*. Minneapolis, MN, 17–20 March 2019. Warrendale, PA: TAGA, pp. 222–236.
- Hutcheson, D., 1999. *HiFi color growing slowly*. [pdf] GATFWorld (reprint). Available at: <http://www.hutchcolor.com/PDF/HiFiupdate98_2000_04.pdf> [Accessed January 2021].
- Idealliance, n.d. *Extended Color Gamut (ECG) project: global expanded color gamut (ECG) characterization target*. [online] Available at: <<https://idealliance.org/specifications/expanded-color-gamut-ecg-project/>> [Accessed January 2020].
- International Organization for Standardization, 2017. *ISO 20654:2017 Graphic technology – Measurement and calculation of spot colour tone value*. Geneva: ISO.
- Li, Y., 2021. *Professional colour communication in multiprimary printing (Fogra 13.003)*. [online] Available at: <<https://fogra.org/en/research/prepress-technology/multiprimary-printing-13003>> [Accessed January 2022].
- O'Hara, L., Congdon, B. and Lindsay, K., 2019. Optimizing chroma and lightness of OGV inks for expanded color gamut. In: *Proceedings of the 71st Annual Technical Conference*. Minneapolis, MN, 17–20 March 2019. Warrendale, PA: TAGA, pp. 237–245.

- Politis, A., Tsigonias, A., Tsigonias, M., Gamprellis, G., Tsimis, D. and Trochoutsos, C., 2015. Extended gamut printing: a review on developments and trends. In: *Proceedings of the 1st International Printing Technologies Symposium – PrintInstanbul 2015*. Istanbul 8–10 October 2015. Istanbul, Turkey: Marmara University.
- Rich, D., 2012. *Expanded color gamut primaries: the FQC EG project*. [online] Available at: <<https://www.flexography.org/industry-news/expanded-color-gamut-primaries-fqc-eg-project/>> [Accessed January 2022].
- Seymour, J., 2018a. *Expanded gamut – when an idea's time has come*. [online] Available at: <<http://johnthematguy.blogspot.com/2018/04/expanded-gamut-when-ideas-time-has-come.html>> [Accessed 15 September, 2018].
- Seymour, J., 2018b. *The heyday of expanded gamut printing patents*. [online] Available at: <<https://www.flexoglobal.com/blog-articles/2018/seymour-05-the-heyday-of-expanded-gamut-printing-patents.html>> [Accessed 21 January, 2019].
- Sharma, A., 2019. *Ryerson University Expanded Gamut Study 2019*. [pdf] Ryerson University. Available at: <<https://colorkarma.com/wp-content/uploads/2021/09/ExpandedGamutStudy2019.pdf>> [Accessed August 2019].
- Sharma, A. and Seymour, J., 2020. Evaluation of expanded gamut software solutions for spot color reproduction. *Color Research and Application*, 45(2), pp. 315–324. <https://doi.org/10.1002/col.22471>.
- Simoni, M., Butler, G., and Deighton, R., Sun Chemical Corporation, 2017 *Expanded color gamut*. U.S. Pat. 9,649,868 B2.
- Van De Capelle, J.-P., Agfa-Gevaert N.V., 2006. *Method and a device for determining multi-ink color separations*. U.S. Pat. 7,123,380 B2.
- Wessendorf, A., 2020. Die digitale Transformation wird niemals abgeschlossen werden. Flexo+Tief Druck, [online] 21 January. Available at: <<https://www.flexotiefdruck.de/menschen-maerkte/die-digitale-transformation-wird-niemals-abgeschlossen-werden/>> [Accessed January 2022].

Appendix

Detailed SCTV curves from the Esko characterization press runs

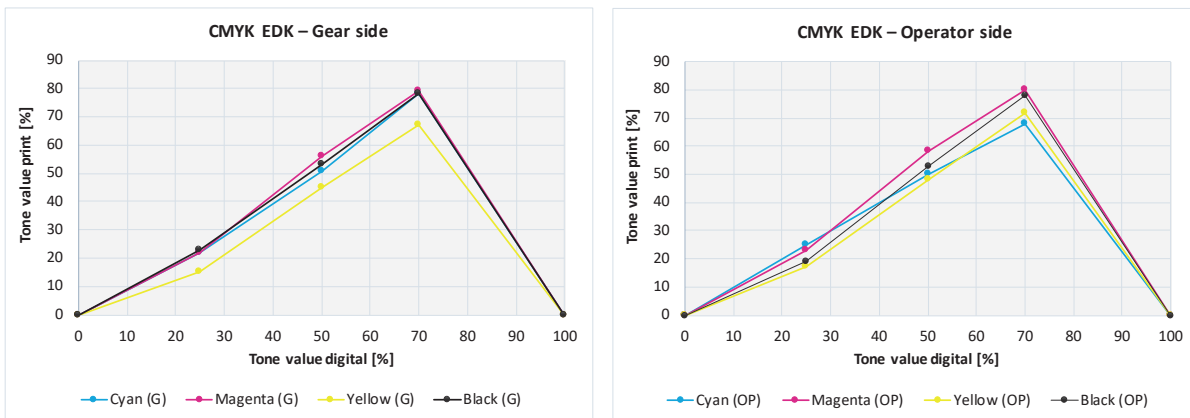


Figure A1: CMYK EDK tone value curves

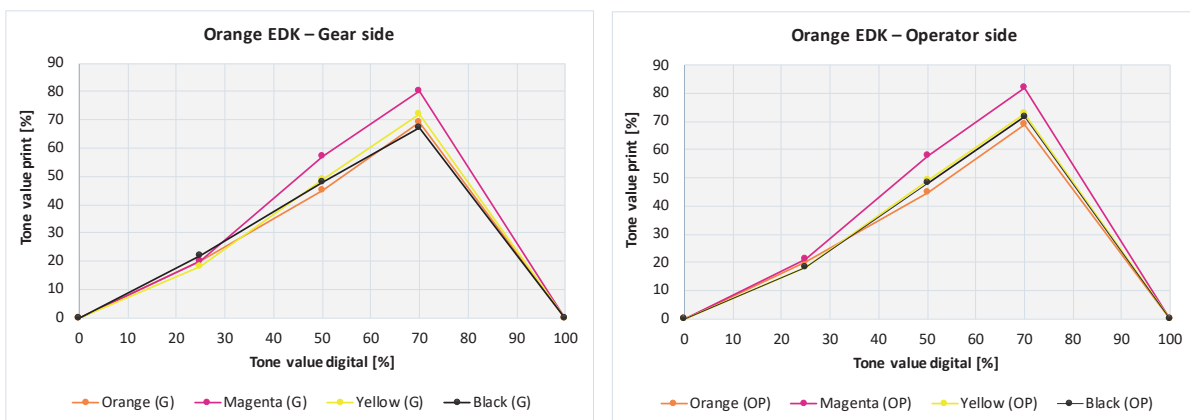


Figure A2: OMYK (Orange) EDK target tone value curves

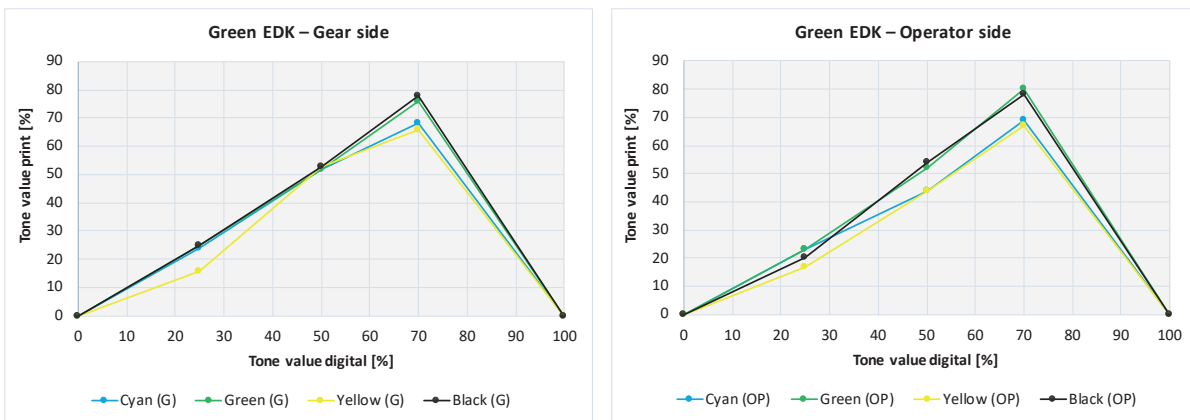


Figure A3: CGYK (Green) EDK target tone value curves

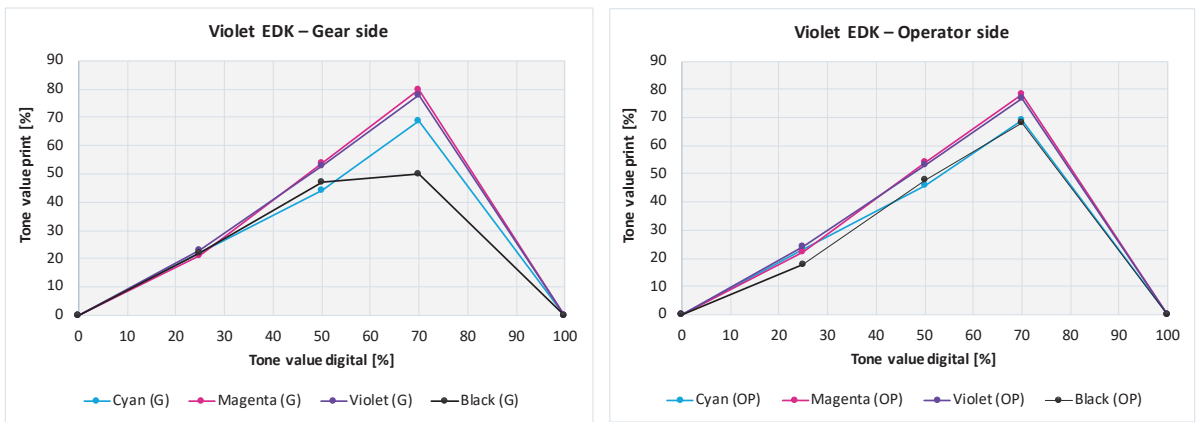


Figure A4: CMVK (Violet) EDK target tone value curves

Detailed SCTV curves from the GMG characterization press run

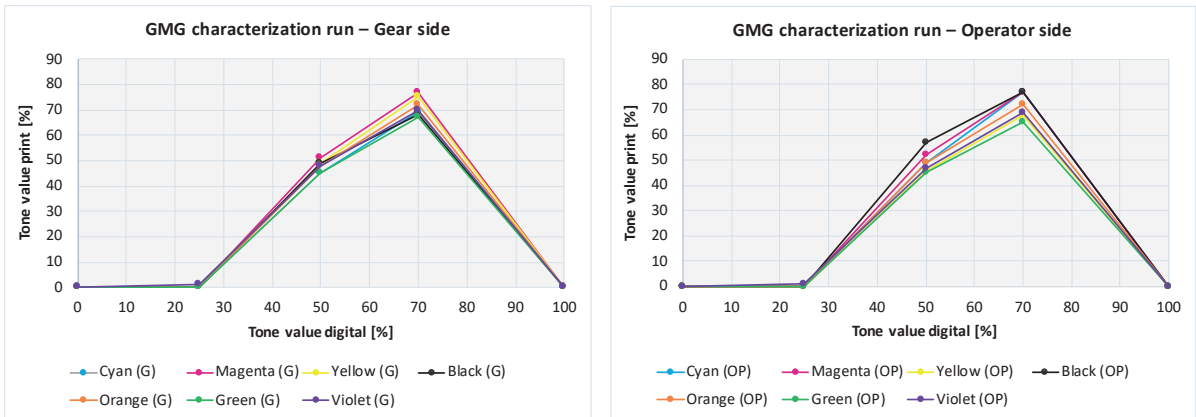


Figure A5: Tone value curves for the GMG characterization run

Detailed curves from the ISC chart characterization run

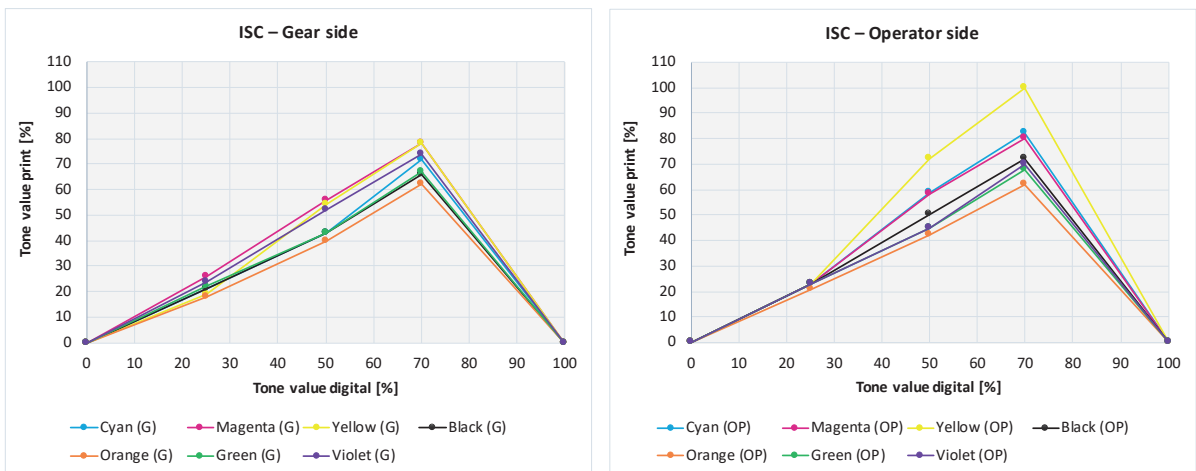


Figure A6: Tone value curves for the ISC characterization run

A detailed list of the selected Pantone patches for the verification target



Figure A7: Verification target

#	ColorName	%	
A1	Black	0	
A2	Black	25	
A3	Black	50	
A4	Black	75	
A5	Black	100	
B1	Cyan	100	
B2	PANTONE 151 C	25	
B3	PANTONE 151 C	50	
B4	PANTONE 151 C	75	
B5	PANTONE 151 C	100	
C1	Magenta	100	
C2	PANTONE Green C	25	
C3	PANTONE Green C	50	
C4	PANTONE Green C	75	
C5	PANTONE Green C	100	
D1	Yellow	100	
D2	PANTONE 2091 C	25	
D3	PANTONE 2091 C	50	
D4	PANTONE 2091 C	75	
D5	PANTONE 2091 C	100	
E1	Orange	100	
E2	PANTONE 5245 C	100	
E3	PANTONE 330 C	100	
E4	PANTONE 443 C	100	
E5	PANTONE 198 C	100	
F1	Green	100	
F2	PANTONE 7661 C	100	
F3	PANTONE 348 C	100	
F4	PANTONE 2008 C	100	
F5	PANTONE 7430 C	100	
G1	Violet	100	
G2	PANTONE 5275 C	100	
G3	PANTONE 7483 C	100	
G4	PANTONE 2045 C	100	
G5	PANTONE 7739 C	100	
H1	PANTONE 2475 C	100	
H2	PANTONE 550 C	100	
H3	PANTONE 7742 C	100	
H4	PANTONE 2082 C	100	
H5	PANTONE 600 C	100	
I1	PANTONE 7413 C	100	
I2	PANTONE 7710 C	100	
I3	PANTONE 7485 C	100	
I4	PANTONE 2108 C	100	
I5	PANTONE 7620 C	100	
J1	PANTONE 697 C	100	
J2	PANTONE 7717 C	100	
J3	PANTONE 7493 C	100	
J4	PANTONE 2248 C	100	
J5	PANTONE 2002 C	100	

Figure A8: Description of color patches of the verification target

JPMTR-2207
DOI 10.14622/JPMTR-2207
UDC 336.74(540)168.3

Research paper | 162
Received: 2022-04-25
Accepted: 2022-05-28

A new approach to fuzzy logic analysis of Indian currency recognition

Sonia Sarkar and Arun Kiran Pal

Department of Printing Engineering, Jadavpur University,
Salt Lake Campus, Block-LB, Plot-8, Sector-III, Salt Lake,
Kolkata-700106, India

sonia140897@gmail.com
arunkiranpal@gmail.com

Abstract

In the modern society the advancement and development in the field of scanning and printing technology is rapidly increasing day by day. This gives rise to the generation of counterfeit currency notes in the economy. The goal of this present investigation is to limit the circulation of fake currency notes using logic that can be also referred as fuzzy logic. This paper deals with the utility of fuzzy logic in the domain of Indian currency notes. An integrated banknote detection system implementing a fuzzy-based security features classifier has been developed. The important security features that have been considered are on the basis of the Indian denominations used as well as present in foreign currency notes. The rules that have been developed are formulated upon logic, observation, people's feedback and experiences while dealing with currency notes. With the help of the Surface Viewer several output surfaces have been generated upon varying the security features with each other. This gives an evaluation approach to the existing security features for controlling banknote forgery.

Keywords: security features, fuzzy inference system, membership functions, IF-THEN rules, Surface Viewer

1. Introduction

For any country worldwide money is an economic unit that functions as a generally accepted medium of exchange for transactional purposes in an economy. Counterfeit currency refers to a currency that closely resembles the original currency of a country, but that is produced without the legal approval of the government, which creates a negative impact on the overall economy. The expansion of latest banking services necessitates the requirement for automatic currency recognition and authentication system; hence it is the need of the hour to design a system that is helpful in recognition of paper currency notes correctly. Therefore, in this work, a system of logic has been incorporated for addressing banking crises or as an alternate to verify the resolvability of banks while minimizing the impact on the important economy. An integrated system for a quantitative approach has been made for the evaluation of security features present in the Indian banknotes. This framework is based on the fuzzy logic architecture that explains with a flow diagram to describe the methodology. Seven important security features have been considered which

are already present in the denominations used in this study as well as present in foreign currency notes.

Among all the security features present in the currency notes, seven security features are applied to the inference system to get the desired output based on a decision-making process. The condition of a security feature is classified in terms of its linguistic variables as 'poor', 'fair' or 'excellent' using a 3-point Likert scale. The output gives the result based upon the conditions of the security features. According to people's feedback and experiences on banknotes, analysis has been done in order to formulate human thinking by using fuzzy IF-THEN rules. The rules determine the actual process in the system and consequently give an evaluation based on that. The evaluated results at the output determine whether a currency note is genuine, worn, or counterfeit considering the condition of its security features that are present at the input. The 3D graphs are generated based on the rules and their characteristics show the curve of a genuine, worn, or counterfeit currency by considering variations of the security features. Seven security features considered in the present study are watermark, security thread,

hologram, intaglio printing, latent image, micro-lettering and see-through register. The security features of Indian currency notes are explained in detail by various researchers (Ali, Gogoi and Mukherjee, 2014; Mann, Shukla and Gupta, 2015).

In the field of fuzzy logic in banking and financial applications Seung Yong Kwon with his colleagues (Kwon, et al., 2016) proposed a fuzzy-based classifier based on heuristic design of fuzzy rules and membership functions that could determine the fitness of banknotes through an objective, systematic method rather than subjective judgment. Mohammad Saber Iraj and Saeid Anjakani Moghadam (Iraj and Moghadam, 2016) also presented an approach known as Adaptive Neuro Fuzzy System (ANFIS) method based on wavelet features with vision sensing, which indicated better and more accurate results. Nagy Ramadan Darwish and Ashraf M. El Nour (Darwish and El Nour, 2018) aimed to propose an intelligent fuzzy-based framework for evaluating the most important security features of Egyptian banknotes. Their proposed framework depended on the Likert scales and the utilization of fuzzy logic for classification of banknotes that were genuine or counterfeit. Rodel Emille T. Bae with other researchers (Bae, et al., 2019) presented a study that had been divided into two parts: a template matching technique for feature extraction and comparison of accuracy between fuzzy logic algorithms and K-Channel Nearest Neighbour (KNN) based on the information they gathered. Revati and Somashekhar Dhanyal (Revati and Dhanyal, 2019) proposed a work that was to provide an easy and efficient system for the detection of fake and original notes based on the input image features. In this work they used a feature based Fuzzy classifier along with some digital image processing methods to extract the features of currency images for recognition as well as for verification. Marc Sanchez-Roger and colleagues (Sanchez-Roger, Oliver-Alfonso and Sanchís-Pedregosa, 2019) attempted a study to critically examine fuzzy logic as an effective, useful method to be applied to financial research and, particularly, to the management of banking crises by using artificial intelligence techniques. In the present investigation a new methodology has been developed on the basis of the operation of fuzzy logic for the recognition of Indian currency notes by obtaining several output surfaces of the seven security features considered.

2. Proposed methodology

The proposed methodology depends upon the operation of fuzzy logic for the categorization of Indian currency notes as counterfeit, worn and genuine. The first step deals with using the triangular membership function where the inputs are fuzzified to acquire fuzzy sets.

Conversion of crisp values into linguistic variables is performed in the second step. The transformation of the values of each crisp input into the grades of its membership function is done for linguistic terms of fuzzy sets. Later in the testing phase to fuzzify the security features these membership functions are considered. The third step is known as fuzzy inference system that is used in a fuzzy rule to decide outcome of the rule based upon the given input rule information. Fuzzy rules signify experience, survey, feedback or modelling knowledge. In the rule consequence, to calculate the outcome for the output variables fuzzy inference is needed when particular information is assigned to the input variables.

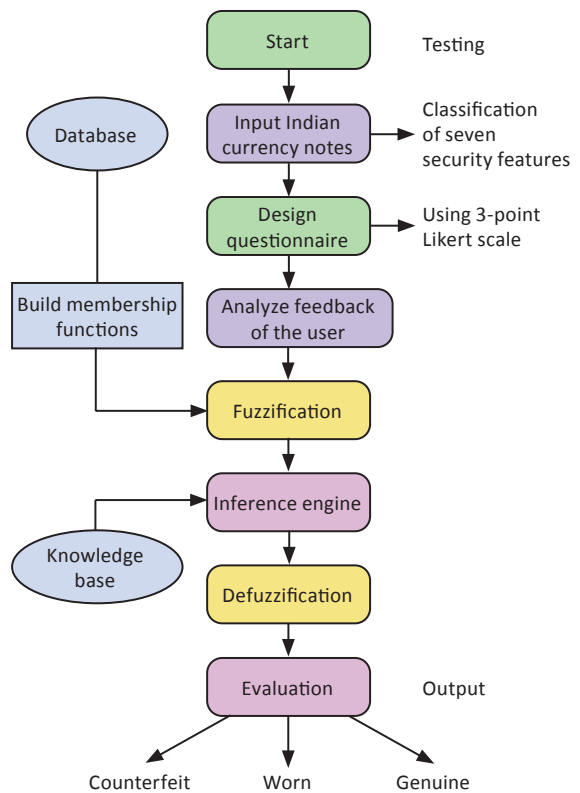


Figure 1: Framework of the proposed methodology

The proposed framework takes into account the Mamdani fuzzy rules (Mamdani and Assilian, 1975). Three fuzzy variables, namely ‘poor’, ‘fair’ and ‘excellent’, are used to describe the feature variations at the input side and ‘counterfeit’, ‘worn’ and ‘genuine’ are the variations present at the output. Since the fuzzy inference system processes all of the cases in a parallel approach therefore it makes the decision more logical and reasonable. The outputs of fuzzy values are defuzzified in order to generate a crisp value for the given variables. To choose a single output based on the suggested fuzzy sets there are numerous defuzzification methods provided. But from them the most frequently

used defuzzification strategies are: the maximizing decision, the mean of maximum method and the centres of gravity method.

In the present investigation, the defuzzification strategy used is known as the centre of gravity method. After the evaluation phase specific graphs are generated in the Surface Wiewer, which depicts the output according to the given input. The flowchart in Figure 1 represents the proposed framework.

3. Fuzzy inference system

A fuzzy inference system is the fundamental unit of a fuzzy logic system. It is a type of computer prototype which is supported by fuzzy set theory, fuzzy IF-THEN rules, and fuzzy reasoning (Chen and Pham, 2000). Different functional blocks constitute its structure. Fuzzy set theory is used by a fuzzy inference system to map inputs to its outputs. It is generally based upon a nonlinear mapping that derives its output from a group of fuzzy IF-THEN rules. The range and domain of non-linear mapping can be fuzzy points or sets that are multidimensional in nature (Tsatiris and Kitikidou, 2018). It takes into account novel methods to solve day to day problems.

The characteristics of a fuzzy inference system consist of conversion of fuzzy variable into a crisp variable using a defuzzification unit that accompanies the system. Regardless of the input which can be in the form of fuzzy or crisp, the result from a fuzzy inference system is always a fuzzy set. When the system is used as a controller it is essential to have a fuzzy output.

The essential structure of a fuzzy inference system consists of three entities such as a database or dictionary that contains the participation functions, which are applied in the fuzzy rules. Rule base accommodates all the required fuzzy rules. A reasoning mechanism is performed made upon the guiding principle and the facts given to understand a reasonable conclusion or outcome.

All the necessary information regarding a fuzzy inference system is displayed by the MATLAB applicaton Fuzzy Logic Designer. It comprises the information about the most recent operation that is displayed at the bottom by the status line. The name of an input or output variable, its type, and its default range is presented by the Current Variable area. And to let the user modify the different fuzzy inference functions, dropdown lists are present. At the MATLAB prompt the command “Fuzzy” needs to be typed to open the Fuzzy Logic Designer. The fuzzy inference system consists of the names of the variables at the input side as well

as at the output side. The input variables are always present at the left-hand side whereas the output variables are present at the right-hand side. In the present study, Mamdani-type inference has been used. A seven-input, one-output system has been constructed here. The seven inputs are watermark, security thread, hologram, intaglio printing, latent image, micro-lettering and see-through register. As soon as the new names of the input and output variables are assigned the diagram becomes updated to reflect the changes as shown in Figure 2. There is now a new variable in the workspace called Currency that contains all the information about this system.

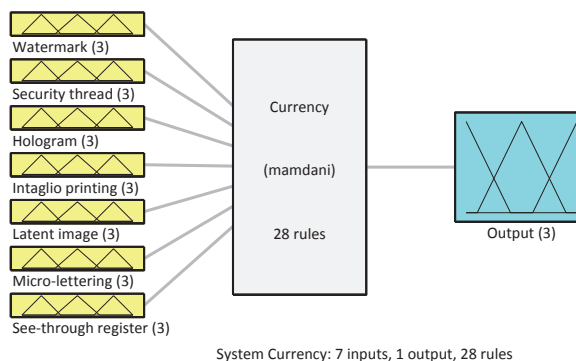


Figure 2: Mapping of all the security features to the output

3.1 Triangular membership function

Membership functions illustrate fuzziness that is all the information that is present within a fuzzy set whether the elements are continuous or discrete in those fuzzy sets (Sivanandam, Sumathi and Deepa, 2007). To solve practical problems, membership functions can be expressed as a technique that focuses upon experience rather than knowledge. It is always represented in graphical forms. Triangular membership function explains how each point in the input space is mapped to its membership value in the range of 0 and 1. The membership function editor lets the user edit as well as display all the membership functions which are connected with all the variables present at the input and output for the entire fuzzy inference system.

The different linguistic variables ‘poor’, ‘fair’ and ‘excellent’ and their associated membership functions at the input for security feature ‘watermark’ are shown in Figure 3. Each of the remaining security features ‘security thread’, ‘hologram’, ‘intaglio printing’, ‘latent image’, ‘micro-lettering’ and ‘see-through register’ are having the same membership functions. The separate three triangles denote that each of the security features may have varying conditions hence separate categories known as ‘poor’ ‘fair’ and ‘excellent’ are chosen under the corresponding security features.

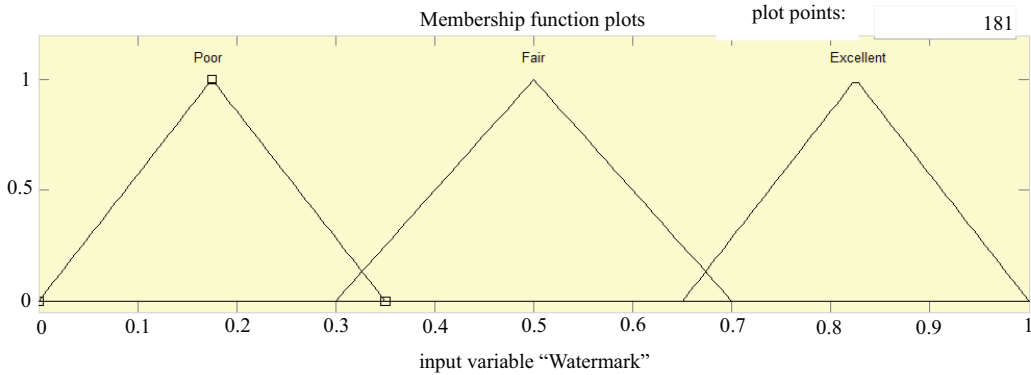


Figure 3: Triangular membership functions for input variable 'Watermark'

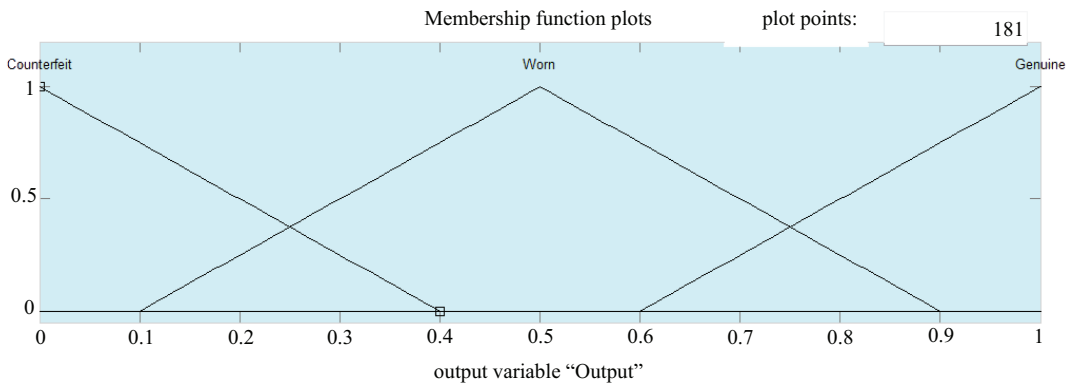


Figure 4: Triangular membership functions for variable 'Output'

The different linguistic variables 'counterfeit', 'worn' and 'genuine' and their associated membership functions at the output are shown in Figure 4. The shape of the membership function is such that the currency notes in our day to day lives are mostly worn since it gets circulated from one hand to another. Hence the two categories 'counterfeit' and 'genuine' take a certain part under the triangular curve 'worn'. This in turn states that a currency note can be worn as well as counterfeit and also a genuine currency note can be worn.

3.2 Fuzzy IF-THEN rules

The graphical Rule Editor interface helps the user to develop fuzzy IF-THEN rules. The Rule Editor takes into consideration the number of input and output variables as well as their corresponding membership functions that are already defined in the Fuzzy Logic Designer. The construction of the rule statements takes place automatically by using the Rule Editor.

The first 16 rules are based upon the experiences of the experts of the departments of forgery and counterfeiting (Darwish and El Nour, 2018). These sixteen rules altogether also deal with the feedback of the public about banknotes. It has been observed that these rules contain three sets of repetitive conditions. Therefore,

in the present study these rules are further modified on the basis of fuzzy reasoning formulated by a group of fuzzy IF-THEN rules. Fuzzy logic mainly focuses upon different types of surveys and experiences from human thinking, so rather than knowledge it concentrates upon overall experiences.

Similarly, more rules can also be developed depending upon logic and observations of the conditions of currency notes. Here in the present study additional 12 rules are developed for further evaluation of security features. The modified 16 IF-THEN rules along with the presently developed 12 rules are given in Appendix in tabular form including their numbers.

3.3 The Surface Viewer

Once the Surface Viewer is opened, the mapping from the seven security features to the output result can be obtained from a three-dimensional curve. The Surface Viewer is prepared with drop-down menus having X (input), Y (input) and Z (output) that lets the user select any two inputs and any one output at a time for plotting the curve. There are grid lines present the number of which the user can specify in the two input fields, X grids and Y grids, respectively. For complex problems this option of facility permits the user to keep the time rea-

Table 1: Groupings of variations among different security features

Security feature	Group 1	Group 2	Group 3
Watermark	Security thread	Hologram, intaglio printing	Latent image, micro-lettering, see-through register
Security thread	Watermark	Hologram, intaglio printing	Latent image, micro-lettering, see-through register
Hologram	Watermark	Security thread, intaglio printing	Latent image, micro-lettering, see-through register
Intaglio printing	Watermark	Security thread, hologram	Latent image, micro-lettering, see-through register
Latent image	Watermark	Security thread, hologram, intaglio printing	Micro-lettering, see-through register
Micro-lettering	Watermark	Security thread, hologram, intaglio printing	Latent image, see-through register
See-through register	Watermark	Security thread, hologram, intaglio printing	Latent image, micro-lettering

sonable for any sort of calculation. When the selections of input or output variables are changed, by default, the surface plot, as well as the number of grid points, update automatically. Plot points help if the user wants to create a smoother plot in the input or output range where the field needs to be specified to the number of points on which the membership functions are evaluated. By default, this field is set to the minimum number of plot points which is 101. If the user wants to specify fewer plot points, then automatically the field value resets to 101 along with updating the output surface curve. Also, if the user wants to manipulate the surface to get the view from different angles, then by dragging the mouse and clicking on the plot axes the 3D curves can be seen. In some scenarios there are more inputs that are required by the system than the surface is mapping. In such situations the function Ref. Input is helpful as it allows the user to edit and explicitly set inputs that are not specified in the surface.

Suppose there is a five-input one-output system and the user would like to see the output surface. A three-dimensional output surface is generated by using the Surface Viewer where there is a variation between any two inputs, but the remaining three inputs must be assigned as constant since a computer monitor is unable to display a six-dimensional shape. When such case occurs, the input becomes a five-dimensional vector with undefined numeric data type Not a Number (NaN) being assigned to the place of the varying inputs while those input values that remain fixed are indicated with numerical values. Also, in the present study since it is a seven-input one-output system, the input is a seven-dimensional vector with NaNs holding the place of the varying inputs while the rest of the five numerical values indicate those inputs that remain fixed. The groupings of variations among different security features are stated in Table 1.

4. Results and discussions

The classification of the variations between different security features with one another is determined which generates different types of graphs as described in Table 2.

Table 2: Variations of individual security features under the different types of graphs

Type of graph	Variation of security features present under the graph
Type 1	Varies with watermark and security thread
Type 2	Varies with watermark, hologram and intaglio printing
Type 3	Varies with watermark, latent image, micro-lettering and see-through register
Type 4	Varies with security thread, watermark, hologram and intaglio printing
Type 5	Varies with security thread, hologram and intaglio printing
Type 6	Varies with security thread, hologram, intaglio printing, latent image, micro-lettering and see-through register
Type 7	Varies with latent image, watermark, micro-lettering and see-through register
Type 8	Varies with latent image, hologram, intaglio printing, security thread, micro-lettering and see-through register
Type 9	Varies with latent image, micro-lettering and see-through register

Among the seven security features, two features are taken simultaneously as input variables in the present study. Though this Table 2 depicts nine types of graphs but actually the variations among seven security features can generate forty-two numbers of graphs of

which some of the output surfaces for different input variables are similar in nature due to membership functions. Among these forty-two graphs only nine types of graphs are randomly selected for the purpose of analysis.

From the Surface Viewer, various graphs have been resulted with respect to the different security features. It is a 7-input 1-output system so to evaluate the security features, 2 inputs are taken at a time and its corresponding output is shown in a 3D curve. Since the output is generated based on IF-THEN rules as created from people’s feedback and experiences while handling banknotes, the fuzzy inference system gives the desired results.

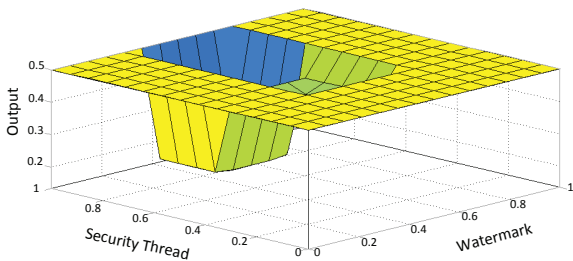


Figure 5: Type 1 graph

In Type 1 graph (Figure 5) it can be seen that the X input is assigned the variable watermark and the Y input is assigned the variable security thread, so the output curve is represented with a 3D curve. These two security features together can detect whether a note is counterfeit, worn or genuine. In this case variable watermark (x-axis) can only be varied with the variable security thread (y-axis) as output surfaces cannot be generated with other variables (shown in Table 2).

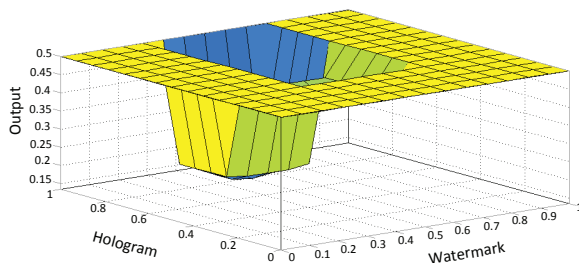


Figure 6: Type 2 graph

There comes a separate variation of graph in the Type 2 graph (Figure 6) in case of hologram and intaglio printing when varied with watermark. Thus, it can be predicted that watermark together with hologram and intaglio printing forms another unit for the detection of a fake note and also whether that particular fake note is worn or not.

In Type 3 graph (Figure 7) it can be seen that watermark varies with latent image of a banknote. Also, the same variation takes place in case of micro-lettering and see-through register when varied with watermark. So, it can be predicted that watermark together with latent image, micro-lettering and see-through register form another group for further detection in counterfeiting of currency notes.

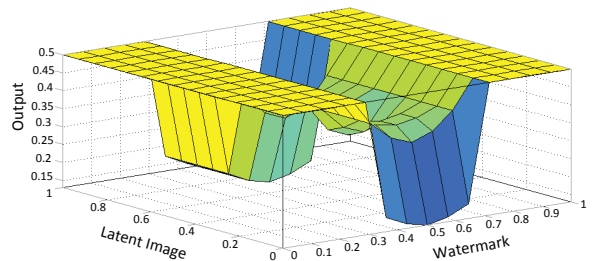


Figure 7: Type 3 graph

In Type 4 graph (Figure 8) it can be seen that the X input is assigned the variable security thread and the Y input is assigned the variable watermark, so the output curve is represented with a 3D curve. In this case it is seen that scaling in x-axis and z-axis is different as compared with Figure 5 (Type 1 graph) because two input variables are interchanged with x-axis and y-axis. These two security features together can detect whether a note is counterfeit, worn or genuine. Again, it can be analyzed that if watermark varies with security thread then the output is predicted to be a worn but genuine currency note since the output is shown by the value 0.5. While considering membership function 0.5 is taken under the category of worn, the output tends to be worn. So, the output is predicted to be a worn but genuine currency note. Moreover, if the variable security thread is varied with the variables hologram and intaglio printing (as given in Table 2), it is observed that same nature of 3D curves can be obtained.

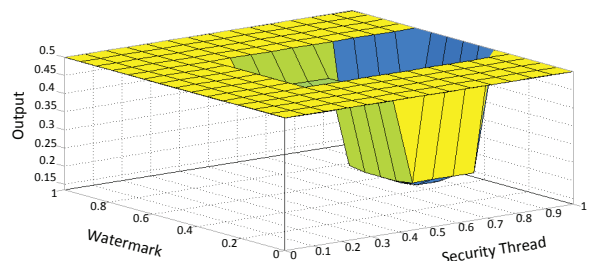


Figure 8: Type 4 graph

There comes a separate variation of graph in the Type 5 graph (Figure 9) in case of hologram and intaglio printing when varied with security thread. Thus, it can be predicted that security thread together with hologram

and intaglio printing form another unit for the detection of a fake note and also whether that particular fake note is worn or not.

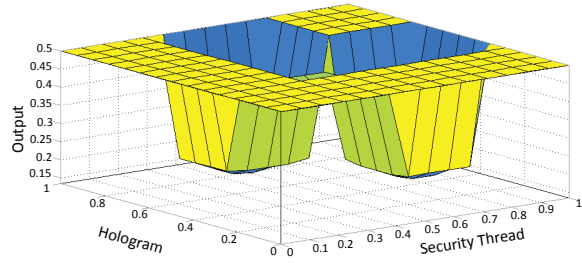


Figure 9: Type 5 graph

In Type 6 graph (Figure 10) it can be seen that security thread varies with latent image of a banknote. Also, the same variation takes place in case of micro-lettering and see-through register when varied with security thread. So, it can be predicted that security thread together with latent image, micro-lettering and see-through register form another group for further detection in counterfeiting of currency notes.

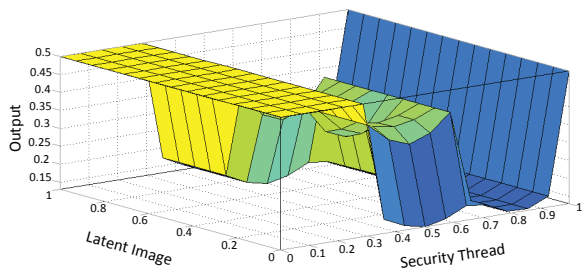


Figure 10: Type 6 graph

In Type 7 graph (Figure 11) it can be seen that the X input is assigned the variable latent image and the Y input is assigned the variable watermark, so the output curve is represented with the 3D curve.

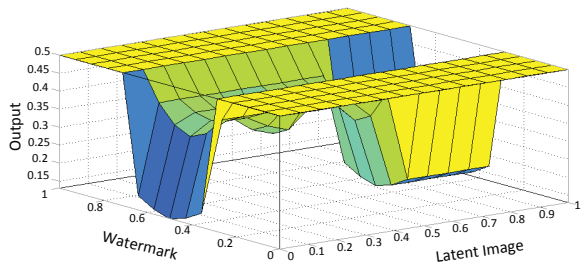


Figure 11: Type 7 graph

Here, the output surface is generated by interchanging the two input variables of Type 3 graph (Figure 7) in x- and y-axes. The same variation is observed in case of

micro-lettering and see-through register when varied with latent image. So, it can be postulated that latent image together with watermark, micro-lettering and see-through register together can detect whether a note is counterfeit, worn or genuine.

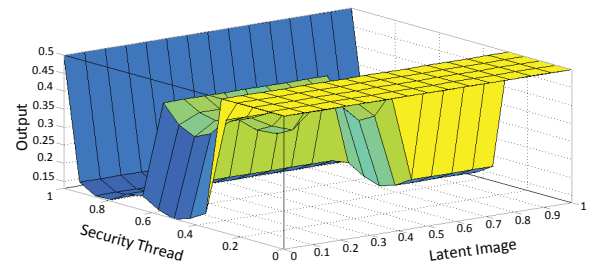


Figure 12: Type 8 graph

There comes a separate variation of graph in Type 8 graph (Figure 12) in case of security thread, hologram and intaglio printing when varied with latent image. Here, the output surface is generated by switching the two input variables of Type 6 graph (Figure 10) in x- and y-axes. The same variation is observed in case of micro-lettering and see-through register. Thus, it can be predicted that latent image together with security thread, hologram and intaglio printing forms another unit for the detection of a fake note and also whether that particular fake note is worn or not.

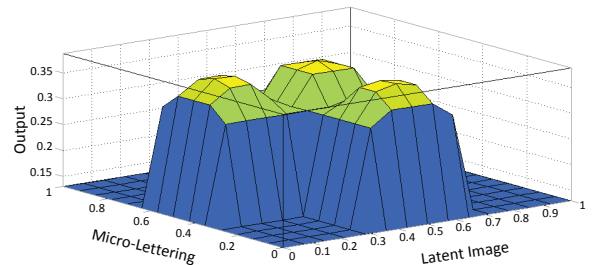


Figure 13: Type 9 graph

In Type 9 graph (Figure 13) it can be seen that latent image varies with micro-lettering of a banknote. It can be analyzed that if latent image varies with micro-lettering, then the output is predicted to be a counterfeit currency note since the output is shown by the value 0.3. While considering membership functions 0.3 is taken under the category of worn and counterfeit, the output is predicted to be a worn but counterfeit note. Also, the same variation takes place in case of see-through register when varied with latent image.

So, it can be predicted that latent image together with micro-lettering and see-through register form another group for further detection in counterfeiting of currency notes.

5. Conclusion

An integrated banknote detection system implementing a fuzzy-based security features classifier has been developed. The fuzzy inference system has been established which primarily consists of the membership functions that help to form linguistic variables that are applied at the input and output, fuzzy IF-THEN rules and fuzzy Surface Viewer. The security features such as watermark, security thread, hologram, intaglio printing, latent image, micro-lettering and see-through register present in the denominations used in this study as well as considering the important security features, which are accepted globally, to the input side with corresponding output gives the cluster of graphs that predicts the tendency of a currency note being counterfeit,

worn or genuine relying upon the conditions of its security features. The fuzzy IF-THEN rules are based upon logic, observation, people's feedback and experiences while dealing with currency notes. Finally, the Surface Viewer concentrates upon the decision making process and gives the outcome as a characteristic 3D curve by varying the input. Several graphs that have been generated by the Surface Viewer varying the security features with each other gives an evaluation approach to the existing security features for controlling banknote forgery. This research work may be expanded to a web-based design system to be implemented in the domain of evaluation of security features based on fuzzy logic. Moreover, increase in the number of security features may be considered to build an advanced fuzzy system for every type of currencies across the globe.

References

- Ali, S.E., Gogoi, M. and Mukherjee, S., 2014. Challenges in Indian currency denomination recognition & authentication. *International Journal of Research in Engineering and Technology*, 3(11), pp. 477–483. <https://doi.org/10.15623/ijret.2014.0311082>.
- Bae, R.E.T., Arboleda, E.R., Andilab, A. and Delloso, R.M., 2019. Implementation of template matching, fuzzy logic and K nearest neighbor classifier on Philippine banknote recognition system. *International Journal of Scientific & Technology Research*, 8(8), pp. 1451–1453.
- Chen, G. and Pham, T.T., 2000. *Introduction to fuzzy sets, fuzzy logic, and fuzzy control systems*. Boca Raton, FL: CRC Press.
- Darwish, N.R. and El Nour, A.M., 2018. A fuzzy logic framework for evaluating the security features of banknotes. *International Journal of Computer Applications*, 179(51), pp. 39–47. <https://doi.org/10.5120/ijca2018917338>.
- Iraji, M.S. and Moghadam, S.A., 2016. Fake banknotes classification using wavelet and Anfis topology based on vision. *International Journal of Computer Science and Information Security*, 14(8), pp. 126–134.
- Kwon, S.Y., Pham, T.D., Park, K.R., Jeong, D.S. and Yoon, S., 2016. Recognition of banknote fitness based on a fuzzy system using visible light reflection and near-infrared light transmission images. *Sensors*, 16(6): 863. <https://doi.org/10.3390/s16060863>.
- Mamdani, E.H. and Assilian, S., 1975. An experiment in linguistic synthesis with a fuzzy logic controller. *International Journal of Man-Machine Studies*, 7(1), pp. 1–13. [https://doi.org/10.1016/S0020-7373\(75\)80002-2](https://doi.org/10.1016/S0020-7373(75)80002-2).
- Mann, M., Shukla, S.K. and Gupta, S., 2015. A comparative study on security features of banknotes of various countries. *International Journal of Multidisciplinary Research and Development*, 2(6), pp. 83–91.
- Revati and Dhanyal, S., 2019. Image based approach for Indian fake note detection by dark channel prior. *International Research Journal of Engineering and Technology*, 6(7), pp. 2829–2832.
- Sanchez-Roger, M., Oliver-Alfonso, M.D. and Sanchís-Pedregosa, C., 2019. Fuzzy logic and its uses in finance: a systematic review exploring its potential to deal with banking crises. *Mathematics*, 7(11): 1091. <https://doi.org/10.3390/math7111091>.
- Sivanandam, S.N., Sumathi, S. and Deepa, S.N., 2007. *Introduction to fuzzy logic using MATLAB*. Berlin, Germany: Springer.
- Tsatiris, M. and Kitikidou, K., 2018. Sunflower for biodiesel production: a Mamdani-type fuzzy inference system using the fuzzy logic toolbox graphical user interface (GUI) tools. *Journal of Scientific and Engineering Research*, 5(5), pp. 162–169.

Appendix: IF-THEN rules

Rule No.	IF	THEN
1	(watermark is fair) and (security thread is fair) and (hologram is fair) and (intaglio printing is fair)	(output is Counterfeit)
2	(watermark is excellent) and (security thread is excellent) and (hologram is poor) and (intaglio printing is fair)	(output is Worn)
3	(watermark is fair) and (security thread is excellent) and (hologram is fair) and (intaglio printing is fair)	(output is Counterfeit)
4	(watermark is fair) and (security thread is fair) and (hologram is excellent) and (intaglio printing is fair)	(output is Counterfeit)
5	(watermark is fair) and (security thread is fair) and (hologram is fair) and (intaglio printing is excellent)	(output is Counterfeit)
6	(watermark is fair) and (security thread is fair) and (hologram is excellent) and (intaglio printing is excellent)	(output is Worn)
7	(watermark is fair) and (security thread is excellent) and (hologram is fair) and (intaglio printing is excellent)	(output is Worn)
8	(watermark is excellent) and (security thread is fair) and (hologram is excellent) and (intaglio printing is fair)	(output is Worn)
9	(watermark is excellent) and (security thread is excellent) and (hologram is fair) and (intaglio printing is fair)	(output is Worn)
10	(watermark is excellent) and (security thread is excellent) and (hologram is excellent) and (intaglio printing is fair)	(output is Genuine)
11	(watermark is excellent) and (security thread is excellent) and (hologram is poor) and (intaglio printing is excellent)	(output is Genuine)
12	(watermark is excellent) and (security thread is poor) and (hologram is excellent) and (intaglio printing is excellent)	(output is Genuine)
13	(watermark is fair) and (security thread is excellent) and (hologram is excellent) and (intaglio printing is excellent)	(output is Genuine)
14	(watermark is excellent) and (security thread is fair) and (hologram is excellent) and (intaglio printing is excellent)	(output is Genuine)
15	(watermark is excellent) and (security thread is excellent) and (hologram is fair) and (intaglio printing is excellent)	(output is Genuine)
16	(watermark is excellent) and (security thread is excellent) and (hologram is excellent) and (intaglio printing is excellent)	(output is Genuine)
17	(watermark is poor) and (security thread is poor) and (hologram is poor) and (intaglio printing is poor) and (latent image is poor) and (micro-lettering is poor) and (see-through register is poor)	(output is Counterfeit)
18	(watermark is fair) and (security thread is fair) and (hologram is fair) and (intaglio printing is fair) and (latent image is fair) and (micro-lettering is fair) and (see-through register is fair)	(output is Worn)
19	(watermark is excellent) and (security thread is excellent) and (hologram is excellent) and (intaglio printing is excellent) and (latent image is excellent) and (micro-lettering is excellent) and (see-through register is excellent)	(output is Genuine)
20	(watermark is poor) and (security thread is poor) and (hologram is poor) and (intaglio printing is poor) and (latent image is fair) and (micro-lettering is poor) and (see-through register is fair)	(output is Counterfeit)
21	(watermark is poor) and (security thread is poor) and (hologram is poor) and (intaglio printing is poor) and (latent image is poor) and (micro-lettering is fair) and (see-through register is fair)	(output is Counterfeit)
22	(watermark is poor) and (security thread is poor) and (hologram is poor) and (intaglio printing is poor) and (latent image is fair) and (micro-lettering is fair) and (see-through register is poor)	(output is Counterfeit)
23	(watermark is fair) and (security thread is fair) and (hologram is fair) and (intaglio printing is fair) and (latent image is fair) and (micro-lettering is fair) and (see-through register is poor)	(output is Worn)

Rule No.	IF	THEN
24	(watermark is fair) and (security thread is fair) and (hologram is fair) and (intaglio printing is fair) and (latent image is fair) and (micro-lettering is poor) and (see-through register is fair)	(output is Worn)
25	(watermark is fair) and (security thread is fair) and (hologram is fair) and (intaglio printing is fair) and (latent image is poor) and (micro-lettering is fair) and (see-through register is fair)	(output is Worn)
26	(watermark is excellent) and (security thread is excellent) and (hologram is excellent) and (intaglio printing is excellent) and (latent image is fair) and (micro-lettering is excellent) and (see-through register is excellent)	(output is Genuine)
27	(watermark is excellent) and (security thread is excellent) and (hologram is excellent) and (intaglio printing is excellent) and (latent image is excellent) and (micro-lettering is fair) and (see-through register is excellent)	(output is Genuine)
28	(watermark is excellent) and (security thread is excellent) and (hologram is excellent) and (intaglio printing is excellent) and (latent image is excellent) and (micro-lettering is excellent) and (see-through register is fair)	(output is Genuine)

JPMTR-2110
DOI 10.14622/JPMTR-2110
UDC 004.92:004.7|004.03

Research paper | 163
Received: 2021-08-15
Accepted: 2022-04-08

A comparison of current solutions for creating web animations on Apple hardware

Jaka Mušič and Helena Gabrijelčič Tomc

University of Ljubljana, Faculty of Natural Sciences and Engineering,
Department of Textiles, Graphic Arts and Design,
Chair of Information and Graphic Arts Technology

helena.gabrijelcic@ntf.uni-lj.si

Abstract

The content available online consists of titles, texts, images, and multimedia, including animations. Some animations are immediately noticeable, while others are less obvious, yet they play an important role in the interactivity of a website. When implemented correctly and working properly, animations can greatly enhance the user experience. In the theoretical part of this paper, the basic technologies of the web are introduced. These are Hypertext Markup Language, Cascading Style Sheets (CSS) and JavaScript. The history of web animations is presented as well as the perception of animations in terms of the qualities required by the human eye to perceive them as fluid. In the experimental part, methods for creating animations were selected for testing. These were CSS animations, Web Animations Application Programming Interface (WAAPI) and Lottie animations. For each of these methods, an identical animation was designed and implemented on a website. The animations were then tested with a different number of elements in two browsers on multiple devices and Apple hardware. During creation and testing, an analysis was made of how difficult it is to design and implement the animations on a website, and how powerful they are: the ability to display a high number of frames per second, how much memory they require on the graphics card, and how much data must be transferred from the server for them to play properly. The results were recorded and summarised. Some recommendations were made in the results, i.e. which method to use depending on the intended use case. The CSS and WAAPI animations and transitions were found to be more suitable for complex web animations, while Lottie was found to be useful for simpler animations.

Keywords: interactive website, cascading style sheets (CSS), web animations application programming interface (WAAPI), Lottie animations

1. Introduction

We are constantly surrounded by countless amounts of information, both in physical space and on the internet. It can thus become extremely exhausting to find the information we are looking for or to critically evaluate the value of the information we have. One of the tools we can use to enrich an online document with data and highlight the importance and value of certain information is animation. This can be in the form of micro-animations (for example, the transformation of the menu icon into a backspace icon) or animations that involve more intense movement (Pratt, et al., 2010). These are, for example, the animated graphic elements that accompany or guide us through the website. They make websites more attractive, but can also contribute to the user experience by speeding up the recognition

of graphic elements (Head, 2016). Animations have evolved since the beginning of web development, and every year a new solution for creating them appears. Moreover, the demand for animations is growing as websites and webpages change from static to dynamic. However, these solutions are not always of the same quality and complexity to use, and can also be costly in terms of hardware (Chinnathambi, 2017).

Web technologies have been evolving since 1989, when Tim Berners-Lee, then an employee of the European Council for Nuclear Research (CERN), had the idea for the World Wide Web and invented the Hypertext Transfer Protocol (HTTP) to properly display webpages, from servers to client devices, that is, in the browser of a computer or mobile device (Chrome, Safari, Firefox, etc.) (McCullough, 2018).

When we want to access a webpage, an HTTP request is made in this way, but not necessarily in this order, except for the first step: the browser requests the page, the server provides the Hypertext Markup Language (HTML) file, and if needed the browser requests the style file, the request is answered by returning the cascading style sheet (CSS) file, the browser requests images and additional files specified in the HTML file, the server provides images and additional files, the browser then also requests scripts and receives JavaScript (JS) files from the server (McCullough, 2018; Berners-Lee, 2021). We can now use the latest versions of CSS not only to design but also to animate content. For this purpose, two properties are available, namely animation and transition. In the first one, we can use keyframes to display the position and other properties for a particular frame. This animation can be called multiple times and can be given duration, delay and repeat properties. A transition, on the other hand, is more used for mouse movements, clicks, and mouse transformations (Weyl, 2016; W3Schools, 2021).

1.1 From early beginnings to modern animations

Animation is the perception of movement and the illusion of change using sequences of images that differ only slightly from one another (Ferreira, 2017). Simply put, animation is the movement of graphics or the visualisation of change over time, and while the basic ideas have remained the same, the methods of animation have changed over the years.

Dynamic elements on websites have been driven by Graphics Interchange Format (GIF) technology. The GIF format was introduced in 1987, and was the first technology to animate the previously static frames seen online. This format is now more than 30 years old and is still widely used. Due to its structure, it can represent 256 different colours (a JPEG can represent 16 million), and an advantage of this format is that a file can contain several consecutive frames. Today they are often used in reaction GIFs (a genre of meme), which can be used as a response instead of text in various online contexts. There are various online collections where users can find the perfect reaction GIF, such as Giphy (Shamms Mortier, 1997).

In the late 1990s, Adobe developed Flash technology, which was promoted as “a standard for delivering rich web content with powerful impact. Graphics, animations, and user interfaces can be rendered on all browsers and platforms” (Adobe, 2021). However, Flash has now fallen out of use and has not been supported since January 1, 2021, because it required considerable hardware resources that mobile devices were not able to provide at the time, and also had security vulnerabilities (Carrera, 2010).

1.2 SVG animations

Scalable Vector Graphics (SVG) animations are based on HTML elements, but add something unique, such as the path element. Their advantage is very good support in various browsers, except Internet Explorer. However, they are relatively expensive to use, and are becoming less common due to better alternatives being available (Drasner, 2017; Bellamy-Royds, Cagle and Storey, 2017).

1.3 CSS3 animation technology

Cascading Style Sheets version 3 (CSS3), was introduced, along with HTML5, to meet the needs of developers for better animation technology. Together these two new systems paved the way for interactive websites, creating a large number of interesting projects, although some issues still remained and thus many developers resorted to libraries written specifically for animation (Weyl, 2016; Chinnathambi, 2017).

1.4 Web Animations API

Web Animations Application Programming Interface (WA-API) is one of the newer technologies for creating web animations. It is built on top of JS and is based on two models, for timing and animation. The timing model is the basis for working with the Application Programming Interface (API). Each website and each document has its own timeline that extends from page loading to infinity, or to the point when the tab is closed. The animations are distributed along the timeline in an order specified by the `startTime` parameter. An animation model is a sequence of images arranged according to a time model. This model thus ensures that animations or changes to elements are executed in the order specified by the time model (MDN Web Docs, 2021).

1.5 Libraries

There are many libraries on the internet that help us create or add animations to elements. One of them is `animate.css`, which provides us with preset CSS animations that we can easily attach to elements using classes, identifiers, or element names. However, the most advanced option is the GreenSock Animation Platform (GSAP) library, which allows users to create their own animations, is based on JS, and also supports various plug-ins (GreenSock, 2020).

1.6 Lottie animations

Lottie animations are JavaScript Object Notation (JSON) animation files that make it possible to publish and display animations similar to static files (images). The files are small and of the vector type, so there are no size limitations due to resolution. Lottie is also a

library for Android, iOS, React, and the web, which converts animations created in Adobe After Effects (which must be exported as a JSON file using the Bodymovin plug-in) and then rendered natively by Lottie on the device (Bassett, 2015).

1.7 User aspects and objectives of the research

For the user of a website or mobile app, the technical side or implementation of a system is not as important as its usability, usefulness, learnability, and so on. For animations, this means they need to load quickly and run smoothly. The latter aspect is particularly important, as it greatly affects the user experience (Head, 2016; Pierce, 2016; Brundrett, 2016).

The human eye has a light-sensitive tissue called the retina, located at the back, opposite the lens. Its photoreceptors are responsible for converting an image into an electrical signal and sending it to the brain.

When an object moves through our field of vision, the photoreceptors are stimulated. However, the brain cannot track objects that move faster than sixteen times a second, and this is why most videos and movies are shot and played at 24 frames per second. Since this is more than we can perceive, we see the separate images as a single movement rather than a sequence of shots.

The eye also has a limit to the amount of motion it can detect. Although change is a continuous flow of information and is not perceived by the eye in individual frames, for most people this limit is 60 Hz or less (or about 60 frames per second). Recent research suggests that we might see up to 75 Hz, or that the lower limit of the speed at which we can perceive change is as low as 13 milliseconds, but such measurements are very difficult to make, so there is no definitive answer (Potter, et al., 2014). Most digital displays have a refresh rate of 60 Hz, which seems to be sufficient at the present (Merleau-Ponty, 2013). For the purposes of this study, the lower limit was more important because it determines how the animation is perceived: whether it is smooth or choppy.

This research was planned with the aim of uncovering the best balance among simplicity, usability, and complexity of web animations for designers, developers, users and devices. The main goal of the research was to find a solution for web animation design. We examined the design method, the complexity of implementation in the web environment, and the impact on hardware resources: how many frames per second the browser can display, how much memory is used on the graphics card, and how much data must be transferred from the server to the device for the animation to work.

The objectives of the research were to review some recent solutions for creating web animations (CSS3 animations, WAAP, and Lottie animations), to test and compare these, and to analyse and select the most suitable solution in terms of the relationship between operational efficiency and ease of production.

Before conducting the research, we hypothesised the following:

- Lottie animations offer the best balance between simplicity and performance,
- WAAP animations will consume more hardware resources than CSS animations,
- Safari will play animations at more frames per second than other browsers.

2. Experimental

In the experimental part, the animations were created, analysed, and tested in three different technologies: CSS3 animations, WAAP, and Lottie animations.

The visual appearance of the animations was the same, the differences were only in the design, development and rendering process. The animations were tested on a simple website created for this purpose, with different technologies to choose from. The tool also displayed the number of frames per second that the animation could show.

2.1 The development of the tool

There are several ways to test the quality of animations. We could test how much space they take up on the graphics card RAM, how much processing power they require, or how much data is transferred from the server, but the most important is the rate of frames per second at which they can be displayed, since this is the only aspect that visitors perceive. Therefore, this is the most important metric we used to test the quality of our animations.

At the time of writing, none of the popular browsers had developer tools that provided a detailed overview of the information we needed to test the technologies. Therefore, we developed a tool that displays and measures the performance of animations. This also opened up the possibility of testing animations on mobile devices. Figure 1 shows the entire implementation of the functional part of the frame per second (fps) rate measurement.

In Figure 1 FPSMeter evaluates the framerate of an animation embedded in a web page using CSS transitions. We used fpsmeter from Corvoysier (2014). The principle uses CSS itself and three steps to evaluate the

```

<script type='text/javascript'>
  start();

  function start() {
    const vrednosti = document.getElementById("vrednosti");

    if(!window.FPSMeter) {
      alert("Meter se ni pravilno inicializiral!");
    }

    document.addEventListener('fps', function(e) {
      vrednosti.innerHTML = vrednosti.innerHTML + e.fps + " ";
    }, false);

    FPSMeter.run();
  }

  function end() {
    FPSMeter.stop();
  }
</script>

```

Figure 1: Script that takes care of calling and manipulating the frame rate measurement script

actual rendering frame rate of a page. The steps are the insertion of the CSS animated item in a page, calculation of the computed position of the CSS animated item at regular intervals and, finally, for every elapsed second there is a counting of the number of different positions occupied by the item (Corvoysier, 2011).

2.2 The making of animations

The canvas size was 1920 pixels wide and 1080 high. For the animation, we designed eight graphic elements with different shapes (four circles and four rectangles), sizes and colours. In the initial state, the graphic elements were placed randomly on the canvas without covering each other (Figure 2).

The animation consists of six keyframes (Figure 2), with the first and last keyframes being identical, allowing for an infinite loop. At each keyframe, we specify

the position, rotation, size, and colour of the elements. Between the keyframes, we let the technologies compute the transition paths. This template was then made for Lottie in Adobe After Effects and exported with the help of a free plug-in Bodymovin into the required JSON file and developed in CSS and WAAPI. All three types of animation were then implemented in the tool for testing.

Tables A1 and A2 in Appendix show the changes in the circular (Table A1) and rectangular (Table A2) graphic elements during six levels of testing.

The animation is 2500 ms (or two and a half seconds) long, and the keyframe comes every 500 ms. We chose this length so that the timing would be as fast as possible, that the animations is as demanding as possible for the browser, and at the same time slow enough for pleasant viewing.

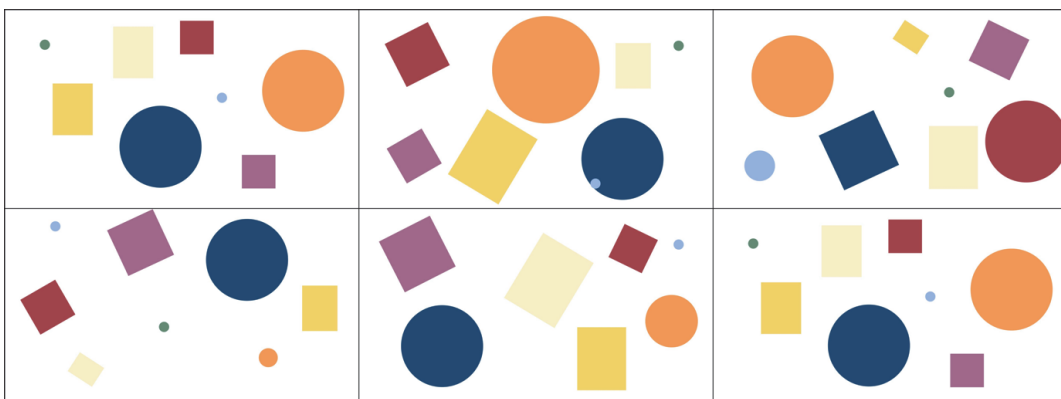


Figure 2: Keyframes of the animation used in the experiment

2.2.1 CSS animations code

While the Lottie animations have less programming, the CSS animations have everything written in code. For CSS animations, we used the method of keyframes in CSS, where we set six key levels that were tied to the percentage of elapsed time rather than time. We started the process again by creating eight graphic elements and setting the basic parameters. We had to determine the position from the left and top, and for those values to be valid we also had to determine the absolute positioning and the position correction by half in both directions. At the same time, we had to set the size, colour, and radius of the frame (50 %) in the case of a circle. Animation information (name, length and loop) was also required for the animation to work.

To improve responsiveness, we added information to the browser about which property will change (will-change property). The complete syntax for one graphic element is shown in Figure 3.

Keyframes were defined to allow the browser to track changes in graphic elements. We had some main keyframes in our animation, so we split the frames into CSS keyframes in segments of 20 % each to cover all the main frames, since the first and last frames had to be identical to allow a seamless loop. We also used the CSS transform property for movement instead of the traditional positioning property, as this ensured that the browser used GPU acceleration for rendering instead of the slower browser rendering engine. The key to this property was not to enter the offset value,

```
.krog-1 {
  animation: krog 2.5s infinite;
  background-color: #558564;
  height: 54px;
  left: 217px;
  top: 190px;
  width: 54px;

  /* Lastnosti skupne vsem elementom */
  border-radius: 50%;
  position: absolute;
  transform: translate(-50%, -50%);
  will-change: transform;
}
```

Figure 3: CSS code for the circular graphic element in the animation

```
@keyframes krog1 {
  0% {
    transform: translate(-50%, -50%) scale(1);
    background-color: #0D3B66;
  }
  20% {
    transform: translate(calc(-50% + 584px), calc(-50% + 66px)) scale(1);
    background-color: #0D3B66;
  }
  40% {
    transform: translate(calc(-50% + 853px), calc(-50% - 28px)) scale(1);
    background-color: #AD3A42;
  }
  60% {
    transform: translate(calc(-50% + 469px), calc(-50% - 465px)) scale(1);
    background-color: #0D3B66;
  }
  80% {
    transform: translate(calc(-50% - 396px), calc(-50% + 3px)) scale(1);
    background-color: #0D3B66;
  }
  100% {
    transform: translate(-50%, -50%) scale(1);
    background-color: #0D3B66;
  }
}
```

Figure 4: Example of CSS animation properties for one circular graphic element

but to change the (delta) position. Due to the correction of the centre alignment, the position change was calculated as 50 % of the size and the offset was subtracted from or added to that. The complete syntax for the animation is shown in Figure 4.

This procedure was repeated for all eight graphic elements, and elements were prepared in the HTML file to be animated.

2.2.2 Web Animations API code

This method is also based on writing the code, but some part of it is common to that of the CSS set. The HTML elements are the same, as is the basic CSS (Figure 5).

We have redefined the basic properties (size, position, colours ...) of the elements, only this time we have left out the animation property. This was written in JS. The animation part (in JS) consists of two parts of animation data: i) keyframes and ii) animation time and style.

The animation data is unique for each element we want to move independently. The animation data can be global (as in our case, since we animate all elements

at the same time and for the same amount of time) or unique for each element. We have defined six levels that match those of the CSS method, only the syntax was slightly different. This time, the percentages were written as a value between 0 and 1, for example, 0.6 instead of 60 %. The properties of the animation are shown in Figure 6.

In addition to the class, a unique identifier was added so that HTML elements could be animated. The IDs in JS were called and assigned to the animation properties, or the predefined variables were called. With that, the animation was determined.

2.2.3 Lottie animation code

Lottie animations are JSON files that we export from Adobe After Effects using the Bodymovin plug-in.

In After Effects, we created eight graphic elements and assigned them colours and start positions. In the timeline, we set keyframes, layers, position changes, and other properties for each element. After completing the animation in After Effects, we exported it to the JSON format using the Bodymovin plug-in. For the pur-

```
.krog-1 {
  background-color: #558564;
  height: 54px;
  left: 217px;
  top: 190px;
  width: 54px;

  /* Lastnosti skupne vsem elementom */
  border-radius: 50%;
  position: absolute;
  transform: translate(-50%, -50%);
  will-change: transform;
}
```

Figure 5: Example of CSS code for animation with WAAPI

```
const krog1podatki = [
  { transform: 'translate(-50%, -50%) scale(1) rotate(0deg)' },
  { transform: 'translate(calc(-50% + 1516px), calc(-50% + 6px)) scale(1)', offset: 0.2},
  { transform: 'translate(calc(-50% + 1063px), calc(-50% + 259px)) scale(1)', offset: 0.4},
  { transform: 'translate(calc(-50% + 647px), calc(-50% + 453px)) scale(1)', offset: 0.6},
  { transform: 'translate(calc(-50% + 79px), calc(-50% + 514px)) scale(1)', offset: 0.8},
  { transform: 'translate(-50%, -50%) scale(1) rotate(0deg)' },
]

const animacijaPodatki = {
  duration: 2500,
  iterations: Infinity
}
```

Figure 6: Example of the JavaScript code configuration part for WAAPI animation


```

const animacija = bodymovin.loadAnimation({
  container: document.getElementById('lottie-animacija'),
  path: 'animacija.json',
  renderer: 'svg/canvas/html',
  loop: true,
  autoplay: true
})
    
```

Figure 7: JavaScript code with the Lottie animation settings

poses of this study, we chose a JSON file as the result of the rendering. To animate the JSON file on the website, a bit more code was required. We first imported a JS library that takes care of the execution of the animations and can convert the JSON file into SVG elements. We created an object that the animation binds to. We gave the library information about which element the animation should appear in, the path to the JSON file, the rendering mode, and other optional parameters such as loops and autoplay (Figure 7). The library also allows buttons to be associated with actions such as starting and stopping playback. These can be used in a playback environment for a better user experience but are not critical to the operation of the animations and do not change the display of the animations. With this code, the implementation of the Lottie animations was complete and ready for display in the browser.

2.3 Performance testing

After all the animations were implemented, the web pages with the animations were transferred to the server in a structure that allowed easy testing by type of animation and number of graphic elements. We created four identical animations for each of the technologies, with a different number of elements, stacked on top of each other.

When testing performance, we were inspecting three aspects: how many frames per second are displayed, how much graphics card RAM is used, and how much data is transferred from the server (Figure 8).

The base animation features eight shapes, with different parameters. As we wanted to better compare the different solutions, we increased the number of shapes by multiplying them and stacking them on top of each other in groups of eight. We created additional animations with 176, 368, and 560 elements. Those animations became complex enough for devices and browsers to not be able to display them optimally anymore. We looped each animation four times (each would play for 10 seconds) and repeated measurements three times for each browser and device.

The tests were performed in the following browsers: Microsoft Edge version 89.0.774.76 and Safari version 14.0.3 on a laptop MacBook Pro 15 (2018 – 2,2 GHz 6-Core Intel Core i7) with the operating system macOS 11.2.3 (Big Sur); on an iPad Pro 11 (2018) in Safari and Microsoft Edge (46.3.7); on a mobile phone iPhone 12 Pro with iOS 14.4.2 in Safari and Microsoft Edge (46.3.7); and on a low-budget phone Nokia 7.1 with Android 10 in Microsoft Edge (46.03.4).

The Nokia 7.1. device was tested to have a reference for a low-end device operating under the same stress of the animations.

Microsoft Edge was chosen because it is based on Chromium, has a modern rendering engine, and is widely available on many devices. The Chrome browser was not tested, as at the time of the research Microsoft Edge included better reporting of resource usage (more data in the report) compared to Chrome.

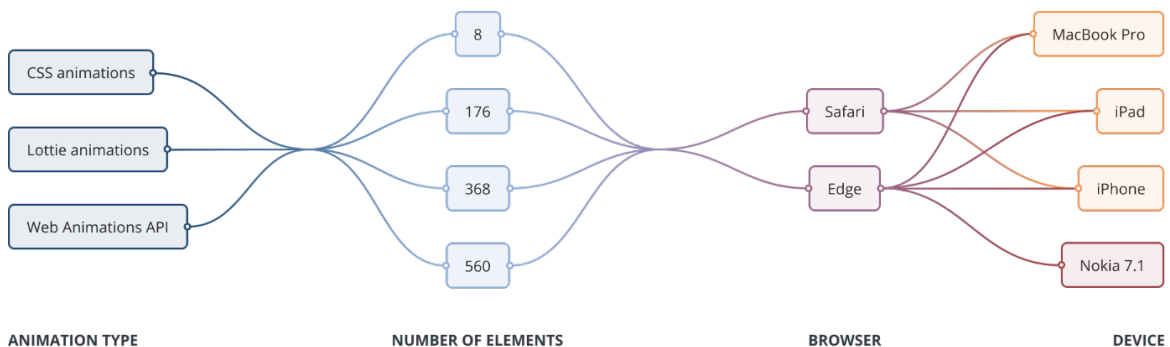


Figure 8: Parameters examined in the experiment

Safari was included in order to make comparisons with a browser that was already built into the system, and could theoretically perform better because of the deep integration of software with hardware.

3. Results and discussion

3.1 Performance

The frames displayed per second depending on play time are presented in Figure 9 as the average values for different devices in 560-element CSS, WAAPI and Lottie animations and in the Edge browser, and this is followed by explanations for the different devices used.

This was also the limit of what our devices could output. As expected, due to the lower end of the specifications with not very capable hardware, the Nokia phone displayed the smallest number of frames on average. For the largest number of elements, the iPhone displays the most graphic elements on average, followed by the iPad and MacBook. The minimum number of frames displayed per second was 9.7 and the maximum was 58.0. At 560 elements, the Nokia phone scored the worst with an average of 12.2 frames per second.

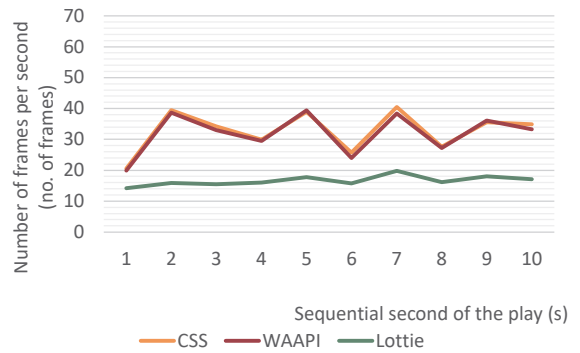


Figure 9: Average frames displayed on the devices per second depending on the play time with 560-element animations in the Edge browser

However, this device was very consistent in its display when compared with other devices. With the other devices, the variations are greater, averaging about 35 frames per second.

At 560 elements, the laptop (MacBook) plays the animation without major problems, only the frame rate is quite low. It ranges from 21.3 to 34.3 per second, but that is still enough for what appears to be smooth

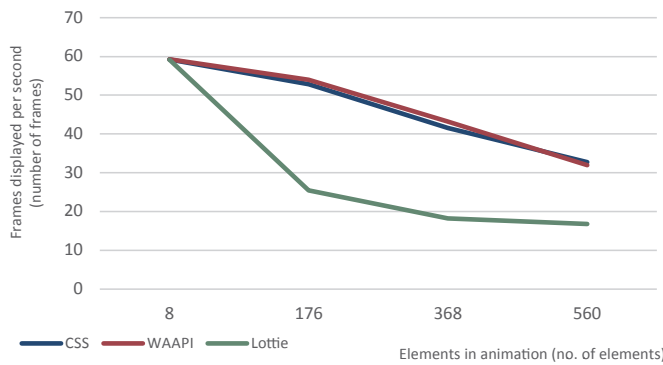


Figure 10: The average number of frames displayed per second depending on the number of elements in the animation for different types of animations in the Edge browser

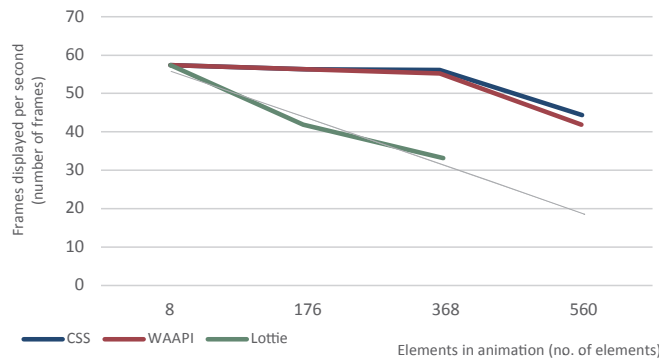


Figure 11: The average number of frames displayed per second depending on the number of elements in the animation for different types of animations in the Safari browser with added grey projection line

Table 1: An overview of the resource consumption of all animations

No. of graphic elements	Memory usage (MB)			Amount of transferred data (kB)		
	CSS	WAAPI	Lottie	CSS	WAAPI	Lottie
8	15.9	15.3	28.7	11.9	12.7	20.8
176	75.9	78.5	346.4	19.0	19.8	450.0
368	150.6	150.6	536.9	27.0	27.8	941.0
560	222.7	222.7	536.9	35.0	35.8	1400.0

motion. When animating on a Nokia phone, however, the slow operation is very noticeable, as the elements do not move and only random inserts from the animation are displayed. The frame rate averages around five per second. On the iPad, trying to replay the animation caused the webpage to crash. On the iPhone, it did not work much better, managing to display the first four seconds at between 12 and 16 frames per second, then the page crashed.

In Figures 10 (Edge browser) and 11 (Safari browser), we can track the trend of decreasing quality by adding the number of graphic elements presented in the animation. A comparison of the results in Figures 10 and 11 shows that the decrease in the quality or the number of frames per second displayed is more severe in the Edge browser. This is particularly noticeable for CSS and WAAPI animations, where the number did not change or changed imperceptibly in the first three stages in Safari. The quality decreased slower for Lottie animations as well in Safari, compared to Edge, although the animation completely broke at 560 elements, whereas in Edge it could still render and play, even if at a low frame rate. For a better overview, we have added a projection line to the Safari graph (Figure 11), so we can predict how many frames per second the browser would be able to render.

Based on the results, we can also assume that the quality of the technologies themselves, based on the frames per second, declined. For a low number of elements, all the solutions chosen for creating the animations are appropriate, as they achieved similar results across the tested devices and two browsers. This was not the case with the increase in the number of elements displayed in an animation. As is evident in Figures 10 and 11, Lottie animations saw a dramatic fall in frames per second with the increase in the number of elements, so they are less suitable for complex animations. The CSS animations and WAAPI produced similar results throughout the experiment, so they are both viable choices.

When testing, we also monitored how demanding the technologies are for the hardware, measuring the amount of graphics card memory required for the ren-

dering of the animations, as well as how much data was transferred from the servers as the page loaded. For the measurements of the amount of graphic card memory the report by the browser on a per-tab basis (GPU memory usage) was used.

Table 1 presents an overview of the resource consumption of all tested animation technologies. In this table showing memory usage and data transfer we can see that both CSS and WAAPI animations used very similar amounts of memory and data downloaded. In the Lottie animations we notice that with eight elements the situation is similar to that with the other two animation technologies, while for 176, 368 and 560 elements there is a clear rise of memory usage. With only 368 elements Lottie had no more memory available. With regard to data transfer, Lottie also took the lead. Where CSS and WAAPI animations downloaded about 35 kilobytes of data for 560 elements, Lottie transferred some 40 times more – 1400 kilobytes (1.4 megabytes).

3.2 Ease of build

All three methods have their advantages and disadvantages. One aspect that can be used to determine the usefulness of the solutions is their learning curve.

All three solutions use the three core technologies of the web – HTML, CSS, and JS. None of the animation technologies require advanced knowledge of the core languages, although WAAPI requires a little more knowledge of JS since it is based on that.

Lottie animations are the easiest to create from a design perspective, because the editor (After Effects) is visually oriented. This means that apart from a few clicks when saving keyframes, we can do all the designing by moving the shapes around, move around the timeline, change the properties of the shapes, and save the changes. The slightly harder part is implementing the animation in the website. However, this only requires a few lines of code. Lottie is therefore the first choice for animators and anyone who does not know much about coding. It is also the fastest method and allows for more complex animations that would take much more time to develop in CSS or WAAPI.

The other two methods rely entirely on programming, and the animator must be at least somewhat familiar with web technologies (HTML, CSS, and JS – the latter only in the case of using WAAPI). For beginners, CSS may be the better choice, as they only need to use two languages.

The CSS animations require some basic knowledge of inserting elements into Document Object Model (DOM) and using classes in CSS with `@keyframe`. The CSS animations and WAAPI animations work in a similar way, using keyframes depending on 100 % of the available time. We also need to set the playback time and the type of transformations separately. JavaScript opens up a vast number of additional possibilities for website development. Therefore, WAAPI is perhaps more suitable for advanced developers or complex websites, as it allows many manipulations with animations. The creation of an animation is much more time-consuming than simply drawing the changes, since every change has to be written in the code, while in After Effects we just move the element, and the program does the rest.

3.3 Compatibility

Lottie animations are based on the use of SVG elements and JS code, so they have very good compatibility with browsers. Only browsers older than Internet Explorer (IE) 8 cannot display them, but the market share of these browsers is less than 0.04 % at the time of writing. The CSS3 animations are also supported in all major browsers newer than IE 9.

Web Animations API is a newer technology and already supported by all modern and updatable browsers. Older versions of Chrome, Firefox, Edge and Safari cannot display them, however, nor can any version of Internet Explorer.

4. Conclusions

The results show that we can reject the first hypothesis, i.e. Lottie animations have the best balance between simplicity and performance, since we found that the balance between the simplicity and performance of Lottie animations is not the best among all the tested methods for creating animations, although their creation is extremely simple.

We can also reject the second hypothesis, i.e. WAAPI animations will consume more hardware resources than CSS animations. This is because CSS and WAAPI animations work very similarly, and thus their use of hardware resources is comparable. We can, however, confirm the third hypothesis. Safari, due to its integration with the hardware that is possible on Apple devices, can better maintain the quality of animations when they become more complex.

Based on the results, we can make some recommendations, and the overview of the creation and operation of the animations presented in this work can be used as a guide when choosing the right method for displaying animations online, although not all the available methods were tested in this study. We recommend Lottie animations as the most appropriate method for simple animations (e.g., turning the menu icon into a back arrow) because they are easy to create and implement in a visual environment.

Complex animations are the easiest to design in Adobe After Effects, as the tool is visually based. The created animation is easily exported into a JSON file needed for Lottie to work, and then implemented in a website. This ease of creation comes with some drawbacks, though. Many elements make high demands on device resources, so the fps might drop if we have too many, which can lead to a few dropped frames, creating a bad user experience. For more complex work CSS animations are best, because the quality is maintained as the number of elements grows. Production is more difficult as it relies solely on programming, but this method is valuable because smooth operation is paramount to the user experience. Although the operation is similar to WAAPI, we suggest choosing CSS as it is a general recommendation not to burden browsers with executing JavaScript code when an activity can be created in CSS with similar effort.

The research presented in this work provides a good insight into comparing the performance of different online animations and can serve as an example for further research in this area. The investigation could be extended to other common methods and libraries for creating animations, such as SVG animations, animations with the canvas element, WebGL and others, as this could give a more complete picture of the state of online technologies, while the recommendations would have a wider scope.

References

- Adobe, 2021. *Adobe Flash Player*. [online] Available at: <<https://get.adobe.com/flashplayer/about/>> [Accessed August 2021].
- Bassett, L., 2015. *Introduction to JavaScript object notation: a to-the-point guide to JSON*. Sebastopol, CA: O'Reilly Media.
- Bellamy-Royds, A., Cagle, K. and Storey, D., 2017. *Using SVG with CSS3 and HTML5: vector graphics for web design*. Sebastopol, CA: O'Reilly Media, pp. 41–70.
- Berners-Lee, T., 2021. *Tim Berners-Lee*. [online] Available at: <<https://www.w3.org/People/Berners-Lee/>> [Accessed August 2021].
- Brundrett, A., 2016. Motion design: an intro to UX choreography. *User Experience Magazine*, 16(4). [online] Available at: <<https://uxpamagazine.org/motion-design/>> [Accessed August 2021].
- Carrera, P., 2010. *Adobe Flash® animation: creative storytelling for web and TV*. Sudbury, MA: Jones & Bartlett Learning, pp. 85–113.
- Chinnathambi, K., 2017. *Creating web animations: bringing your UIs to life*. Sebastopol, CA: O'Reilly Media, pp. 11–72.
- Corvoysier, D., 2011. *Effectively measuring browser framerate using CSS*. [online] Available at: <<http://www.kaizou.org/2011/06/effectively-measuring-browser-framerate-using-css.html>> [Accessed August 2021].
- Corvoysier, D., 2014. *fpsmeter*. [computer program] GitHub, inc. Available at: <<https://github.com/kaizouman/fpsmeter>> [Accessed August 2021].
- Drasner, S., 2017. *SVG animations: from common UX implementations to complex responsive animation*. Sebastopol, CA: O'Reilly Media., pp. 15–66, pp. 77–86.
- Ferreira, M., 2017. *The history of web animation*. [online] Medium. Available at: <<https://medium.com/@milberferreira/the-history-of-web-animation-63b106c97fd>> [Accessed August 2021].
- GreenSock, 2020. *The standard for modern web animation*. [online] Available at: <<https://greensock.com>> [Accessed August 2021].
- Head, V., 2016. *Designing interface animation: improving the user experience through animation*. New York, NY: Rosenfeld Media.
- McCullough, B., 2018. *How the internet happened: from Netscape to the iPhone*. New York, NY: Liveright.
- MDN Web Docs, 2021. *Web animations API*. [online] Available at: <https://developer.mozilla.org/en-US/docs/Web/API/Web_Animations_API> [Accessed August 2021].
- Merleau-Ponty, M., 2013. *Phenomenology of perception*. Translated from French by D.A. Landes. New York, NY: Routledge, pp. 270–311.
- Pierce, P., 2016. *UI animation – an ideal tool for immersive UX*. [online] UX magazine. Available at: <<https://uxmag.com/articles/ui-animation-an-ideal-tool-for-immersive-ux>> [Accessed August 2021].
- Potter, M.C., Wyble, B., Hagamann, C.E. and McCourt, E.S., 2014. Detecting meaning in RSVP at 13 ms per picture. *Attention, Perception & Psychophysics*, 76(2), pp. 270–279. <https://doi.org/10.3758/s13414-013-0605-z>.
- Pratt, J., Radulescu, V.P., Guo Mu, R. and Abrams, R.A., (2010). It's alive! Animate motion captures visual attention. *Psychological Science*, 21(11), pp. 1724–1730. <https://doi.org/10.1177/0956797610387440>.
- Shamms Mortier, R., 1997. *Gif animation web magic*. Indianapolis, IN: Hayden Books.
- Weyl, E., 2016. *Transitions and animations in CSS: adding motion with CSS*. Sebastopol, CA: O'Reilly Media, pp. 7–50, pp. 55–106.
- W3Schools, 2021. *HTML attribute reference*. [online] Available at: <https://www.w3schools.com/tags/ref_attributes.asp> [Accessed August 2021].

Appendix

Table A1: Changes (in six levels) of the parameters of the circles: colour, distance from the left of the screen (dis. left), distance from the top of the screen (dis. top) and size

Level	Green	Orange	Dark blue	Light blue
1. Dis. left (px)	218	1 618	844	1 180
Dis. top (px)	190	440	744	478
Size (%)	100	100	100	100
2. Dis. left (px)	1 733	1 013	1 428	1 282
Dis. top (px)	196	326	810	944
Size (%)	100	131	100	100
3. Dis. left (px)	1 280	431	1 697	253
Dis. top (px)	449	361	716	848
Size (%)	100	100	100	300
4. Dis. left (px)	864	1 428	1 313	275
Dis. top (px)	643	810	279	97
Size (%)	100	23	100	100
5. Dis. left (px)	296	1 695	450	1 733
Dis. top (px)	704	612	747	196
Size (%)	100	64	100	100
6. Dis. left (px)	218	1 618	844	1 180
Dis. top (px)	190	440	744	478
Size (%)	100	100	100	100

Table A2: Changes (in six levels) of the parameters of the rectangles: colour, distance from the left of the screen (dis. left), distance from the top of the screen (dis. top), rotation and size

Level	Yellow	Red	Violet	Sandy
1. Dis. left (px)	368	1 040	1 374	696
Dis. top (px)	541	151	879	232
Rotation (°)	0	0	0	0
Size (%)	100	100	100	232
2. Dis. left (px)	725	316	300	1 486
Dis. top (px)	798	243	797	304
Rotation (°)	31	63	240	360
Size (%)	147	144	120	88
3. Dis. left (px)	1 072	790	1 548	1 302
Dis. top (px)	149	763	217	803
Rotation (°)	-57	155	386	540
Size (%)	56	180	135	122
4. Dis. left (px)	1 708	233	739	440
Dis. top (px)	542	536	184	874
Rotation (°)	360	240	155	-57
Size (%)	88	120	150	56
5. Dis. left (px)	1 316	1 486	316	1 029
Dis. top (px)	816	217	243	390
Rotation (°)	540	386	63	31
Size (%)	122	110	170	147
6. Dis. left (px)	368	1 040	1 374	696
Dis. top (px)	541	151	879	232
Rotation (°)	0	0	0	0
Size (%)	100	100	100	100

TOPICALITIES

Edited by Markéta Držková

CONTENTS

News & more	143
Bookshelf	145
Events	151

News & more

Recently ending EU-funded Horizon 2020 projects

Among the projects supported under Horizon 2020 programmes and closed during past months belong, for example, the innovation actions FiberEUse that contributed to a circular economy through the reuse of end-of-life composites reinforced by glass or carbon fibres, e.g., in UV-assisted 3D printing or using 3D-printed moulds, and M3DLoC that was focused towards the pilot line producing 3D microfluidic detection devices using multi-material printing technologies, which also involved the development of biodegradable thermoplastic materials with suitable thermal and thermomechanical properties and solving the rheological issues of carbon-based inks, the research and innovation action REFREAM (re-thinking of fashion in research and artist collaborating development for urban manufacturing), which employed 3D printing on textiles and resulted, among other outcomes, in new printer concepts, PRINT-CHEMO, funded through an individual fellowship, which aimed to develop 3D-bioprinted osteoinductive constructs for localised delivery of drugs for osteosarcoma, and much more. Details of the selected projects are given in the following sections.

MATERIALIZABLE – Intelligent fabrication-oriented computational design and modeling

This project, combining data-driven and physically-based modelling to provide both the required speed and accuracy, received the ERC Starting Grant and resulted in two dissertations and over twenty articles dealing, for example, with the computational design of nanostructural colour, geometry-aware scattering compensation, and measurement of volume transport parameters in solid photopolymer materials for 3D printing.

WEARPLEX – Wearable multiplexed biomedical electrodes

The publications resulting from this research and innovation action present the environmentally friendly conductive inks, high-performance screen-printed electrodes, monolithic integration of display driver circuits and displays manufactured by screen printing, design and fabrication of printed human skin model equivalent circuit, and more.

GREENSENSE – Sustainable, wireless, autonomous nanocellulose-based quantitative DoA biosensing platform

The scientific outcomes of this research and innovation action toward the Drug-of-Abuse analysis platform include the use of nanocellulose in printable ionogels for supercapacitors, water-based conductive inks with Ag nanoparticles for printed electronics and carbon ink for electrochromic displays and supercapacitors, as well as the studies assessing the environmental risk of nanocellulose and the knowledge of its human hazard potential.

Mag-ID – Magnetic identification

This innovation action aimed to develop a cost-effective and reliable system for high-volume tracking and tracing as an alternative to radio-frequency

Additive manufacturing using high-performance polymers for industrial applications

The technology was developed and patented by Cubicure, a company founded in 2015 as a spin-off of the TU Wien. The technology is named Hot Lithography and comprises stereolithography-based 3D printing at elevated temperatures. A special heating and coating mechanism allows the use of highly viscous, high-performance photopolymers enabling to achieve unique material properties of the manufactured components. The 3D-printing system is available in the compact version for processing prototypes or small series and the large-scale one for industrial series printing. The range of photopolymers offered by Cubicure includes materials for high-resolution components, flame-retardant or flame-resistant components, as well as highly flexible, elastic components.

In cooperation with the German company Hachtel, Hot Lithography was integrated into a complete procurement solution, from the digitalisation of the original part to optimisation and additive manufacturing of high-quality parts, up to the part qualification by industrial computer tomography. The project that aimed to bring to market the cost-efficient solution for additive manufacturing of components with material quality fulfilling industrial requirements was EU-funded through the SME Instrument. The related scientific publications describe the cationic ring-opening photopolymerisation of 2-oxazolines for direct UV-induced curing, the development of an ivory-like 3D printable material based on a dimethacrylic resin filled with calcium phosphate particles, and the synthesis of a new hybrid oligomer based on poly(propylene oxide) and its implementation as a migration-inhibited toughening agent and reactive diluent for viscous resins.

The Intergraf publications released during the past year

An updated version of the Intergraf recommendations



on CO₂ emissions calculation in the printing industry (2.1) is available from September 2021. It identifies thirteen sources that are normally responsible for most CO₂ emissions and thus should be included in any calculation, no matter whether for a printing site or a printed product.

These comprise the production of purchased inputs, namely substrates, energy, image carriers, such as plates and cylinders, inks, varnishes, toners and cartridges, packaging materials, isopropyl alcohol or similar additives and cleaning agents, combustion of fuels on-site and in company vehicles, transport of finished product and raw materials, employees commuting, production and transportation of fuels for on-site combustion, transportation and purchased energy production, including transmission losses.

Within the EU-funded project Print Your Future: Attracting a New Skilled Workforce for Quality Jobs in the European Graphic Industry, the publication How to Find, Attract and Keep the Next Generation: Best Practice Toolkit for the European Graphical Sector was released in November in eight languages. In spring, Intergraf published its annual activity and economic reports. The 2022 Intergraf Economic Report again provides the statistics relevant for the graphics industry in Europe and a collection of country reports on current trends. As each year, the list is a bit different. Besides the regularly contributing member federations from Bulgaria, Denmark, Germany, Italy, The Netherlands, Norway, and Portugal, the data for this edition were provided by Estonia, Latvia and the United Kingdom. Newly, it reviews the current paper supply disruptions, covering the paper industry profile, production and consumption of paper, price developments, graphic paper capacity, and the European reliance on paper, pulp and wood from Russia. Also, it includes the European print market review for 2021–2026 contributed by Smithers.

identification. The solution for product identification and verification of its authenticity utilises the sensing technology based on the tunnel magnetoresistance effect. The project results include optimised magnetic barcodes, new sensors with sensitivity higher than that of the existing magnetic ink sensors, the swipe reader and the one-shot reader, along with the firmware and communication interfaces. Another outcome is the report assessing the digital printers as well as physical characteristics and magnetic components of inks concerning their suitability for the production of printed magnetic barcodes.

DecoChrom – Decorative applications for self-organized molecular electrochromic systems

This innovation action demonstrated various applications of printed electrochromic components, such as the electrochromic running shoe, weather or dishwasher status display, a Qi wireless charger with an integrated power bank, interactive work board, modular wall panels, and ambient display with controllable shadow projection.

EnABLES – European infrastructure powering the Internet of Things

This research and innovation action joined several European research institutes and knowledge hubs of excellence to advance energy harvesting, storage and micropower management solutions for the integrated design and deployment of miniaturised autonomous sensors. The dozens of related publications cover, among other topics, screen-printable flexible textile-based ultra-broadband millimetre-wave DC-blocking transmission lines and fully printed components – inverters and electrolyte-gated oxide transistors.

IMPETUS – Pilot line for paper based electrochemical test strips dedicated to quantitative biosensing in liquids

The pilot line for the inline production of various sensors and actuators within this research and innovation action was equipped with the units for screen printing, flexographic printing, inkjet printing, chip placement and three drying options. Also, the project involved the design and development of all necessary materials and components.

WASP – Wearable applications enabled by electronic systems on paper

The publications resulting from this research and innovation action present, for example, the battery-free wireless photosensor with screen-printed graphene antenna and inkjet-printed WS₂ photodetector, printed solar cells, energy storage devices and field-effect transistors, and characterisation of Hall mobility and low-frequency noise of inkjet-printed graphene.

SELFSENS – Printed self-power platform for gas sensing monitoring

The scope of this project supported through a fellowship was broader than its title suggests, as illustrated by the resulting publications that describe the over-stretching tolerant conductors from silver nanoparticles deposited on rubber films by inkjet printing, printed and flexible microheaters based on carbon nanotubes, carbon dots as sensing layer for printed humidity and temperature sensors, the chipless wireless temperature sensor and the security button for radio frequency identification tags produced by screen printing, recent advances in printed capacitive sensors, and more.

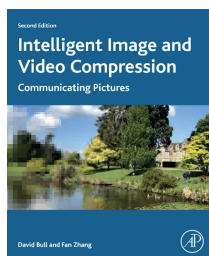
Bookshelf

Intelligent Image and Video Compression Communicating Pictures

The scope of this book is much broader than the intelligent compression methods for visual information themselves. In an accessible style, the authors give a comprehensive account of the development in this area as well as many related concepts and put the described techniques in the context of recent trends, current requirements and expected future outlook. This edition reflects the progress made since the original book published in 2014, *Communicating Pictures* by D. Bull. It includes, in particular, the video compression requirements associated with more immersive applications and the corresponding format extensions, new approaches to perceptual quality assessment and measuring engagement, recently available databases with more comprehensive datasets, the importance of machine learning algorithms and resulting recent innovations, new techniques and standards supporting dynamic adaptive streaming, and the key attributes of the recently emerged video coding standards.

After the introduction explaining the need for compression and the basics, the book describes the human visual system and perception, provides the fundamentals of signal processing and information theory, and outlines digital picture formats and representations, including the concepts of gamma correction, colour spaces and quality metrics. The next three chapters deal with image and video coding transforms, filter-banks and wavelet compression, and lossless compression methods. Their content covers, among others, the basic principles and transforms, optimal transforms, the discrete cosine transform, the short-time Fourier transform and the Gabor transform, multi-rate filtering, bit allocation, hierarchical coding, symbol formation and encoding, Huffman, Golomb and arithmetic coding, as well as the JPEG and JPEG2000 standards, and provides performance comparisons. The eighth chapter discusses motion prediction for coding moving pictures; it explains temporal correlation and presents motion models, motion estimation methods and motion vector coding. The ninth chapter details the block-based hybrid video codec, which employs intraframe prediction, subpixel and multiple-reference frame motion estimation, variable-sized transforms and in-loop deblocking operations. The following chapter is dedicated to measuring and managing picture quality. Then, one chapter presents considerations for delivery across networks together with the available solutions, including robust coding strategies, error concealment and congestion management, and another one brings an overview of video coding standards and formats. In the last chapter, the authors reflect on the future challenges and outlook, with new formats and compression approaches.

The text is complemented by illustrations, algorithms, glossary, tutorial problems and additional resources, including tutorial solutions and interactive demonstration software, available online.



Authors: David R. Bull, Fan Zhang

Publisher: Academic Press
2nd ed., April 2021
ISBN: 978-0-12-820353-8
608 pages
Softcover
Available also as an eBook



Vector Analysis for Computer Graphics

Author: John Vince

Publisher: Springer
2nd ed., June 2021
ISBN: 978-1447175049
259 pages, 141 images
Hardcover
Also as an eBook



Although this new edition has eleven chapters as the first one, its content is restructured to a large extent; several topics are elaborated on in more detail, some were left out, while some are new. After an outline of the vector analysis history, the book presents linear equations, vector algebra, products of vectors, vector-valued functions, vector differential operators, and computation of tangent and normal vectors. Then, two chapters introduce equations for straight lines and the plane, followed by the chapter dealing with intersections. The last chapter is dedicated to three ways of rotating vectors, including the use of Hamilton's quaternions (see this section in JPMTR Vol. 11, No. 1).

Media and Management

Authors: Rutvica Andrijasevic,
Julie Y. Chen, Melissa Gregg,
Marc Steinberg

Publisher: University of
Minnesota Press
1st ed., July 2021
ISBN: 978-1517912246
124 pages, 7 images
Softcover



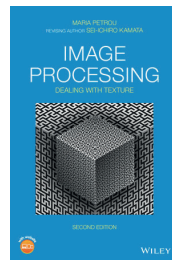
The open-access digital edition of this publication is available from the Meson Press as a part of the In Search of Media series, which is a collaboration between the two publishers. This book explores the mutual relationship between media and management, with management innovations learned through media and media formats producing management opportunities.

The introduction examines the management and its mediation. Also, it presents the just-in-time

Image Processing Dealing with Texture

The first edition, written by M. Petrou and P. García Sevilla with both novice and more advanced readers in mind and presenting the texture as a major part of image processing, comprises a comprehensive guidebook to texture analysis techniques. This new edition revised by S. Kamata reflects the development in this area since the original publication in 2006. The companion website now provides MATLAB codes instead of executable programs.

The content remained organised into three main chapters dealing with the binary textures, stationary grey texture images, and non-stationary grey texture images. The first of them introduces shape grammars used to describe the regular binary textures as well as Boolean models and mathematical morphology for the irregular ones. Almost 300 pages of the following chapter present image binarisation, greyscale mathematical morphology, extended coverage of fractals and multifractals, the updated content on image statistics, texture features based on the Fourier transform, Markov random fields, Gibbs distributions, and the newly added section on texture repair. The last chapter with over 400 pages is dedicated to grey images that contain more than one type of texture. It covers implications of the uncertainty principle in signal and image processing, Gabor functions, prolate spheroidal sequence functions, local phase features in a new section, wavelets, including the dual-tree complex wavelet transform, ridgelets and curvelets in two new sections, pattern recognition, Laws' masks, local binary patterns, the Wigner distribution, and the new content dealing with convolutional neural networks used for deep texture features extraction.



Authors: Maria M. P. Petrou, Sei-ichiro Kamata

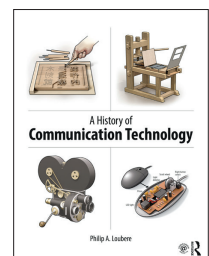
Publisher: Wiley
2nd ed., March 2021
ISBN: 978-1-119-61855-3
816 pages
Hardcover
Available also as an eBook

A History of Communication Technology

This new textbook intends to show a clear timeline of the significant inventions that brought about new means of communication and covers also the related concepts relevant for understanding the presented technologies. Besides explaining the working principle and providing the facts about their inventors, devices and machines used, etc., it also discusses the effects that each technology had on society and culture.

Author: Philip A. Loubere

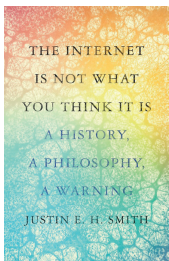
Publisher: Routledge
1st ed., April 2021
ISBN: 978-0-367-21149-3
310 pages
Hardcover
Available also as an eBook



After introducing the theme of the book and its aims, one chapter provides a brief overview of the milestones in human history and significant communication technologies that emerged sequentially in East Asia, Europe, and the United States. The following chapter reviews the period from prehistory to early history. Four chapters then track the development of writing, paper and printing, their improvements and the emergence of entirely new media during the industrial revolution and the Modern Era. Next, three chapters deal with industrial printing (not in its present meaning, but in terms of devices, machines, presses and other technologies used in the printing industry), photography and film, and electronic communication. The last chapter before the conclusion presents the core tools and concepts of the current digital age.

The Internet Is Not What You Think It Is A History, a Philosophy, a Warning

The content of this new publication dealing with the internet is clearly outlined in its title. Building on his scholarly work, the author presents a novel interpretation of the internet origins, showing connections with nature and ideas formulated deep in history, and discusses many current and future aspects of the internet with thoughtful scepticism.



Author: Justin E. H. Smith

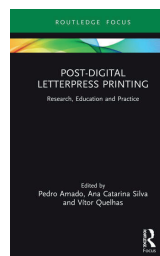
Publisher: Princeton University Press
1st ed., March 2022
ISBN: 978-0-691-21232-6
208 pages, 6 images
Hardcover
Available also as an eBook

Post-Digital Letterpress Printing Research, Education and Practice

While the commercial potential of letterpress printing greatly diminished, the technology is again of interest in search for innovative approaches across different fields ranging from historical research to applications in education and design. This book collects the contributions of almost twenty authors who present the research on letterpress and the contemporary digital practices inspired by this traditional technology. The content is divided into three parts, each beginning with an introduction and containing the selected highlight, followed by three to four chapters presenting the case studies and projects exploring the contribution of letterpress to the fields of arts and design research, the relationship between letterpress practice and design education, and the current letterpress practices.

Editors: Pedro Amado, Ana C. Silva, Vítor Quelhas

Publisher: Routledge
1st ed., November 2021
ISBN: 978-1-03-200180-7
152 pages, 11 images
Hardcover
Available also as an eBook



approach and the platform as managerial concepts. Three main chapters elaborate on the mediation of management, demonstrated using the Toyota Production System example and reflected in Agile software development as well as the lean start-up movement, time-based management in on-demand electronics manufacturing, and the intersections of management and mediation of labour in the so-called platform economy. The concluding passage pays attention to the challenges and changes that arose due to COVID-19 and the geopolitical issues.

The History of Graphic Design 40th Ed.

Author: Jens Müller

Editor: Julius Wiedemann

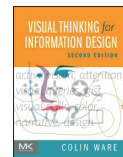


Publisher: Taschen
March 2022
Multilingual Edition:
English, French, German
ISBN: 978-3836588065
512 pages, Hardcover

This compact edition of a highly praised work tracing 13 decades of graphic design is a part of the series published by Taschen on the occasion of its 40th anniversary. The original two-volume edition in a large format is still available as well.

Visual Thinking for Information Design

Author: Colin Ware



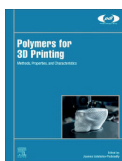
Publisher:
Morgan Kaufmann
2nd ed., March 2021
ISBN: 978-0128235676
224 pages, Softcover
Also as an eBook

This new edition is revised based on new findings, especially the theory of predictive cognition, which provides the framework for the new chapter discussing visualizations as a means for building mental models. For C. Ware's more extensive book on perception for design see this section in JPMTR Vol. 9, No. 3.

Polymers for 3D Printing Methods, Properties, and Characteristics

Editor: *Joanna Izdebska-Podsiadły*

Publisher:
William Andrew
1st ed., June 2022
ISBN: 978-0128183113
408 pages, Hardcover
Also as an eBook



Two parts of this book provide at first a general introduction to 3D printing and then more details of vat photopolymerisation, material extrusion and jetting, powder bed fusion, binder jetting, sheet lamination, and direct energy deposition 3D-printing methods. The third part presents the properties and attributes of polymers used in 3D printing – photopolymers, polymers in printing filaments, polymer powders, plastic pellets, films for sheet lamination, and polymers for 3D bioprinting. The book concludes with two chapters dealing with the global market structure and the trends and perspectives in 3D printing.

Novel Materials for Dye-containing Wastewater Treatment

Editors: *Subramanian S. Muthu,
Ali Khadir*

Publisher: Springer
1st ed., July 2021
ISBN: 978-9811628917
236 pages, 80 images
Hardcover
Also as an eBook



Focused on the topic important for many industries, including textile, food, paper, leather, rubber, cosmetics as well as printing, this book presents novel materials for the treatment of wastewater containing dyes together with other compounds, both inorganic and organic. Various biomaterials and nanocomposites, such as chitosan, luffa fibres, nanocellulose-based membranes and TiO₂-based composites, are among the materials considered promising to reduce health and environmental hazards.

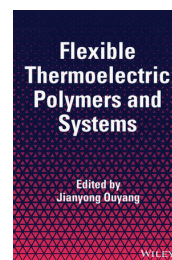
Flexible Thermoelectric Polymers and Systems

After providing readers with the background on thermoelectric materials and their use, this book covers the recent developments in flexible thermoelectric polymeric and composite materials, their applications and novel designs helping to overcome the drawbacks concerning flexibility and cost of thermoelectric devices.

The first chapter describes the effects taking place in thermoelectric materials, their properties and applications in thermoelectric generators, Peltier coolers and thermoelectric sensors. The second one introduces the main types of conductive polymers, their mechanism, synthesis and doping, as well as their utilisation in flexible thermoelectric systems together with the processing techniques used for their production, which include screen printing and inkjet printing. The third chapter is focused on flexible thermoelectrics based on poly(3,4-ethylenedioxythiophene), produced e.g. by the stencil-printing technique, and the next chapter describes the flexible thermoelectric plastic fabricated by electrochemical deposition. The following two deal with the thermoelectric properties of conducting polymers with ionic conductors and composites of carbon nanomaterials in polymers. The last chapter is dedicated to low-dimensional thermoelectric materials.

Editor: *Jianyong Ouyang*

Publisher: Wiley
1st ed., February 2022
ISBN: 978-1-119-55070-9
272 pages
Hardcover
Available also as an eBook

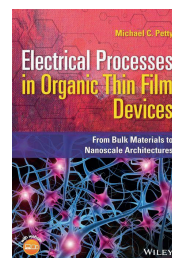


Electrical Processes in Organic Thin Film Devices From Bulk Materials to Nanoscale Architectures

This book, which is intended primarily for advanced readers, first discusses electronic and vibrational states in organic solids and the limited applicability of the band theory. Then, it presents the fundamental principles of electrical conductivity, defects and nanoscale phenomena, ohmic and rectifying electrical contacts, the field effect in metal/insulator/semiconductor devices, DC and AC conductivity, as well as polarisation. Finally, it deals with organic field-effect transistors, electronic memory, light-emitting devices, photoconductive and photovoltaic devices, and also the emerging devices and systems, such as molecular logic circuits and various nature-inspired approaches, including organic neuromorphic devices, microtubule electronics, fault tolerance and self-repair, biochemical sensors, and more.

Author: *Michael C. Petty*

Publisher: Wiley
1st ed., January 2022
ISBN: 978-1-119-63127-9
480 pages
Hardcover
Available also as an eBook



Bookshelf

Academic dissertations

Development of Printed Computer Generated Holograms Reconstructing System

The focus of this thesis was on holography, which can be seen as a specific area of graphic technology. It provides a means of visualisation and communication of information combined with a very high level of product protection. In particular, the work dealt with the computer-generated holograms that can be manufactured in the required quality using the standard, commercially available graphic equipment to make the holographic technology more feasible and accessible, thus opening new applications. The approach was based on proper consideration of the technical capabilities of the selected printing technique, the correlation between digital and physical quantities, as well as possible negative effects when manipulating digital values. The corresponding input parameters were taken into account during the calculations, and the effects of both physical and digital parameters of fabrication on the quality of optical reconstruction were determined.

The dissertation explains the phenomena employed in hologram recording and reconstruction, i.e. the optical field, interference and diffraction, brings an overview of the classification and types of holograms, and presents the digital holography processes for computer generation and numerical reconstruction of holograms. It also describes the holographic security elements, including those utilising computer-generated holograms. The methods presented in the experimental part include the process of making a 3D point cloud model, the development of the mathematical model for hologram generation together with its implementation in a computer programme optimised for calculation speed, prepress setup for printing computer-generated holograms and a laboratory prototype for their reconstruction and authentication. The results are discussed in terms of the quality of optical reconstruction concerning print resolution, edge sharpness, optical density, raster tone value, positions of reference source and 3D model, sizes of the model and printed hologram, and the resulting security features.

Development of a Robotic Cell for the Printing of Electronic Circuits on Free Form Surfaces and Industrial Applications

This thesis contributed to the development of systems for printing electronics onto the existing 3D objects. Although the demand in this area is growing and individual technologies, tools and materials are available, there is a lack of ready-made solutions suitable for prototyping and small-scale manufacturing. The work aimed to provide a versatile, easy-to-implement and cost-effective system for automated functionalisation of 3D objects by depositing electronic components on their surface. To accomplish this, a six-axis multi-tool industrial robot was equipped with the tools enabling scanning of the object to be functionalised and direct writing following a resulting trajectory, which is determined and transformed into the control programme using the dedicated, custom-made software. It was necessary to consider the sources of inaccuracy in the process, such as the representation of the object geometry and its position, select and integrate appropriate deposition techniques, and develop a protocol for controlling the robotic arm movements

Doctoral thesis – Summary

Author:

Vladimir Cviljušac

Speciality field:

Computer Graphics

Supervisor:

Nikola Mrvac

Defended:

3 September 2020, University of Zagreb, Faculty of Graphic Arts Zagreb, Croatia

Language:

Croatian

Original title:

Razvoj sustava rekonstrukcije tiskanih računalno generiranih holograma

Contact:

vladimir.cviljusac@grf.unizg.hr

Further reading:

<http://eprints.grf.unizg.hr/id/eprint/3167>

Doctoral thesis – Summary

Author:

Gioia Furia

Speciality field:

Engineering Sciences

Supervisors:

Davide Beneventi

Didier Chaussy

Defended:

29 January 2021, LGP2, Grenoble INP Grenoble, France

Contact:

gioia.furia@cea.fr

during the patterning of conductive tracks. The other aspects taken into account included the speed optimisation and the ease of use for non-expert users. In addition, a method to predict the circuit morphology was proposed.

The dissertation is organised into three main chapters. The first one provides the background on the robotic arm and measuring equipment, relevant printing and annealing processes, and properties of inks and substrates. Further, it describes the moulded interconnect devices, additive manufacturing of 2D and 3D functional components, and using robotics in research and industrial applications. The second chapter details the development of the robotic cell and the software. It discusses the robot language, simulation and off-line programming tools, object data collection, mesh generation and optimisation, projecting and printing of electronic circuits, the complete setup of the printing robotic cell and the user interface. Finally, the third chapter presents the application of the cell in two projects. The study of printing on 3D objects included characterising printed lines, creating and validating a predictive model, and optimising the trajectory. In the second study, the system was used for the manufacturing of encapsulated microfluidic devices.

Further reading:

<https://tel.archives-ouvertes.fr/tel-03228497>

Doctoral thesis – Summary

Author:

Edgar Ricardo Nandayapa Bermudez

Speciality field:

Applied Physics

Supervisor:

Emil J. W. List-Kratochvil

Defended:

*8 April 2021, Humboldt-Universität
zu Berlin, Mathematisch-
Naturwissenschaftliche Fakultät
Berlin, Germany*

Contact:

edgar.nandayapa@helmholtz-berlin.de

Further reading:

DOI: 10.18452/23121

Metal Halide Perovskites: Photophysics and Inkjet Printing of Solar Cells

The research within this thesis dealt with metal halide perovskites, which are considered promising materials for the economic production of photovoltaic devices. While they show several advantageous properties and are comparable to silicon-based solar cells at a laboratory scale, some limitations impede their large-scale production for practical use and adoption into the consumer market. In particular, this work investigated the mechanisms that hinder the stability of perovskites in atmospheric conditions and explored the crystallisation process of metal halide perovskites deposited by inkjet printing in areas larger than one square inch.

First, the dissertation outlines fundamentals concerning the crystal structure of metal halide perovskites as well as their physical and chemical characteristics, the basic functioning of solar cells, their types, and the key features affecting their performance. It also describes the characterisation methods used for the investigations, focusing mainly on photoluminescence lifetime and quantum yield. Additionally, it examines the principles of inkjet printing and the requirements needed for depositing perovskite materials using this technique. One of the chapters focuses on the stability of perovskites in atmospheric conditions. Using photoluminescence spectroscopy, the charge transfer processes leading to a fast degradation and reduction of power conversion efficiency were studied by applying the Stern-Volmer model. Perovskite films were exposed to increasing concentrations of particular atmospheric gases, leading to a signature change of photoluminescence that can be used to elucidate how degradation is happening. These findings can help develop and apply specific passivation techniques to increase the stability of the solar cells. Another chapter is dedicated to the large-area deposition of metal halide perovskites by inkjet printing. It discusses typical defects encountered when printing perovskites, and how to mitigate them. Then, it presents the study using three different techniques to promote the crystal quality after printing. It was found that a single-step deposition of perovskite materials leads to a higher quality crystal. Furthermore, using a combination of vacuum conditions and a stream of nitrogen at low pressures resulted into the smoothest layers, a requirement for highly efficient solar cells.

Events

NANOTECHNOLOGY 2022

nano Thessaloniki, Greece
technology 2–9 July 2022

For the third time, this event is held in a hybrid format. The 16th International Summer Schools on Nanosciences & Nanotechnologies, Organic Electronics and Nanomedicine are offered on the weekend days that precede and follow the conference programme and the exhibition. Besides attending the common lectures and parallel sessions of the three summer schools, the participants can present their current research in a special ISSON22 Poster Session that this year features over 30 contributions. The four days of the 15th International Symposium on Flexible Organic Electronics offer over 50 invited lectures and eight keynotes, for example ‘Organic electronics for a net zero carbon future sustainable society’ by Ravi Silva, ‘Non-radiative recombination in organic photovoltaics’ by Koen Vandewal, ‘Virtual screening for organic solar cells and light emitting diodes’ by Denis Andrienko, ‘Organic semiconductors: new opportunities in visible light communication’ by Ifor Samuel, and ‘Nanomanufacturing of sustainable circular electronics’ by Thomas Anthopoulos. The plenary session features Paul Blom on ‘Device operation of organic light-emitting diodes based on thermally activated delayed fluorescence’, Lorenzo Moroni on ‘Biofabrication in regenerative medicine: from textile scaffolds to bioprinting’ and Jenny Nelson on ‘Optimising solar energy conversion in molecular electronic materials’. The sessions of the 19th International Conference on Nanosciences & Nanotechnologies also span four days, while the 5th International Conference on 3D Printing & Bioprinting, AI, Digital & Additive Manufacturing, co-organised in the scope of six EU-funded Horizon 2020 projects, comprises three sessions in two days.

FLEPS 2022


4th IEEE International Conference on Flexible, Printable Sensors and Systems

Vienna, Austria
10–13 July 2022



This in-person event offers tutorials on the first day and three days of lectures in sessions dedicated to emerging materials, advanced manufacturing, physical sensors and smart systems, biosensors for advanced diagnostic applications, energy harvesting and storage, green and low-power electronics, hybrid integration and packaging, reliability, simulation and modelling, smart tags and communication devices, emerging applications, point-of-care diagnostics, brain-inspired computing, e-textile sensor systems, technology computer-aided design for micro/nanosystems, e-waste and sustainable electronics. The announced keynotes are ‘Organic Semiconductors in Opto-electronic Devices’ by Thuc-Quyen Nguyen, ‘Ultra flexible elastic integrated circuit system for comprehensively monitoring brain activity’ by Tsuyoshi Sekitani and ‘Unconventional materials and platforms for stretchable transistor- and resistor-based sensors’ by Antonio Facchetti.

8th Colour Management Symposium

 Munich, Germany
6–7 July 2022

The slogan of this edition, which newly offers the option to join the event online via live stream, is ‘Matching colour – Matching people’. On the first day, the schedule includes the topics of managing customer expectations in reality, modern colour workflows, including the case of using spot colour tone value for FOGRA51 stochastic printing, implementations of the expanded colour gamut in the printing of calendars and labels, and colour management for different applications of the high-speed inkjet printing. The keynote by Dimitris Mylonas, scheduled during the social event, deals with colour perception and colour naming in various languages, showing how to facilitate colour communication within and between cultures. The morning sessions of the second day focus on colour proofing and communication in packaging and textile printing. The last session discusses the future of colour management.

London Imaging Meeting 2022

London, UK
6–8 July 2022



In its third year, this event, held by the Society for Imaging Sciences and Technology with the Institute of Physics, takes place in person for the first time, with the option to attend online technical sessions. Four courses of the Summer School on Display Science are offered on 6 July. The keynote speakers are Steven M. LaValle presenting ‘Foundations of perception engineering’ and Robert Pepperell with the lecture ‘The display of perception and the perception of displays’.

21st International Coating Science and Technology Symposium

Minneapolis, Minnesota, USA
11–14 September 2022


In 2022, the schedule of this biennial event includes parallel sessions dedicated to coating applications, design and manufacturing of flexible electronics, coating, drying and curing fundamentals, wetting, solidification and microstructure development.

XVII Color Conference

Florence, Italy
12–13 September 2022

The current edition of this conference held by the Italian Color Association is announced in a hybrid format. In the same venue, the 2nd edition of the Colour Photography and Film event takes place on 15–16 September.

ERA Annual Conference and the Packaging & Decorative Conference 2022

Baveno, Italy 
21–23 September 2022

The programme for this year includes the study of the ecological impact and sustainability of the gravure process, the comparison of water-based and solvent-based inks, future alternative cylinder solutions, and other topics.

Other events in brief

Over two years after the outbreak of the COVID-19 pandemic, the organisers still face uncertainty. The 6th International Conference on Computer Graphics and Digital Image Processing had to be changed into a virtual event held on 9 July 2022, while The Print Show, postponed from 2020, is announced to take place in Birmingham, UK (20–22 September). Whereas High-Performance Graphics 2022 continues as a virtual conference (11–14 July), SIGGRAPH takes place virtually and in Vancouver, Canada (8–11 August 2022).

FLEX 2022



San Francisco, California, USA
11–14 July 2022

This edition of FLEX entitled ‘Electronics in Motion’ is co-located with SEMICON West, covering the advances across the microelectronics supply chain. The events are held in a hybrid format, with virtual access available until 13 August 2022. The FLEX opens with the keynotes ‘Electrophoretic display technology will change the look of automobiles, transportation and beyond’ by Michael D. McCreary, ‘IARPA’s SMART ePANTS program – weaving electronics into textiles’ by Dawson Cagle and ‘Multilayer flexible electronic devices for IoT and RF applications’ by John D. Williams. Then, the FLEXTalks focus on custom, rapid manufacturing of batteries, gravure offset versatility, transparent antennas and heaters with copper micro-wire, and scalable 3D-printed electronics. The technical sessions cover flexible hybrid electronics market outlook, various applications, materials, printing, processing and integration, reliability and inspection, sustainability, and more.

SPIE Optics & Photonics 2022



San Diego, California, USA
21–25 August 2022

This multidisciplinary event is this year held again in person. The rich programme presents, among other topics, the research involving printing, dealing with the flexible transistor based on carbon nanotubes, high-density temperature sensor array, flexible and large-scale Bragg mirrors, sensors for toxic, flammable, and atmospheric gases, and other applications.

Textile Printing & Sustainability Conference 2022



Düsseldorf-Neuss, Germany
8–9 September 2022

This new ESMA event covers the textile printing technology from materials, systems and their components to different aspects of workflow automation, applications in various sectors from home textiles to workwear, up to smart textiles, as well as the topics related to sustainability, such as water and energy consumption, circular economy and successful business models.

48th iarigai and 53rd International Circle Conferences



Greenville, South Carolina, USA
19–21 September 2022

After being successfully held in Europe, the joint conference of the International Association of Research Organizations for the Information, Media and Graphic Arts Industries and the International Circle of Educational Institutes of Graphic-Media Technology and Management is this year hosted by the Clemson University with the theme ‘Print Travels’. The participants can attend the lectures of both events, the 48th International research conference of iarigai, Advances in Printing and Media Technology, and the 53rd Conference of the IC, Graphic Communication Education – Future Orientations.

Call for papers

The Journal of Print and Media Technology Research is a peer-reviewed periodical, published quarterly by **iarigai**, the International Association of Research Organizations for the Information, Media and Graphic Arts Industries.

JPMTR is listed in Emerging Sources Citation Index, Scopus, DOAJ – Directory of Open Access Journals, Index Copernicus International, NSD – Norwegian Register for Scientific Journals, Series and Publishers.

Authors are invited to prepare and submit complete, previously unpublished and original works, which are not under review in any other journals and/or conferences.

The journal will consider for publication papers on fundamental and applied aspects of at least, but not limited to, the following topics:

- ⊕ **Printing technology and related processes**
Conventional and special printing; Packaging; Fuel cells, batteries, sensors and other printed functionality; Printing on biomaterials; Textile and fabric printing; Printed decorations; 3D printing; Material science; Process control
- ⊕ **Premedia technology and processes**
Colour reproduction and colour management; Image and reproduction quality; Image carriers (physical and virtual); Workflow and management
- ⊕ **Emerging media and future trends**
Media industry developments; Developing media communications value systems; Online and mobile media development; Cross-media publishing
- ⊕ **Social impact**
Environmental issues and sustainability; Consumer perception and media use; Social trends and their impact on media

Submissions for the journal are accepted at any time. If meeting the general criteria and ethic standards of scientific publishing, they will be rapidly forwarded to peer-review by experts of relevant scientific competence, carefully evaluated, selected and edited. Once accepted and edited, the papers will be published as soon as possible.

There is no entry or publishing fee for authors. Authors of accepted contributions will be asked to sign a Licensing agreement (CC-BY-NC 4.0).

Authors are asked to strictly follow the guidelines for preparation of a paper (see the abbreviated version on inside back cover of the journal).

Complete guidelines can be downloaded from: <http://iarigai.com/publications/journals/guidelines-for-authors/>
Papers not complying with the guidelines will be returned to authors for revision.

Submissions and queries should be directed to: journal@iarigai.org



Vol. 11, 2022

Prices and subscriptions

Since 2016, the journal is published in digital form; current and archive issues are available at:
<<https://iarigai.com/publications/journals/>>.

Since 2020, the journal is published as “open access” publication, available free of charge for **iarigai** members, subscribers, authors, contributors and all other interested public users.

A print version is available on-demand. Please, find below the prices charged for the printed Journal, for four issues per year as well as for a single issue

Regular prices

Four issues, print JPMTR (on-demand)	400 EUR
Single issue, print JPMTR (on-demand)	100 EUR

Subscription prices

Annual subscription, four issues, print JPMTR (on-demand)	400 EUR
---	---------

Prices for **iarigai** members

Four issues, print JPMTR (on-demand)	400 EUR
Single issue, print JPMTR (on-demand)	100 EUR

Place your order online at: <<http://www.iarigai.org/publications/subscriptions-orders/>>

Or send an e-mail order to: office@iarigai.org

Guidelines for authors

Authors are encouraged to submit complete, original and previously unpublished scientific or technical research works, which are not under reviews in any other journals and/or conferences. Significantly expanded and updated versions of conference presentations may also be considered for publication. In addition, the Journal will publish reviews as well as opinions and reflections in a special section.

Submissions for the journal are accepted at any time. If meeting the general criteria and ethical standards of the scientific publication, they will be rapidly forwarded to peer-review by experts of high scientific competence, carefully evaluated, and considered for selection. Once accepted by the Editorial Board, the papers will be edited and published as soon as possible.

When preparing a manuscript for JPMTR, please strictly comply with the journal guidelines. The Editorial Board retains the right to reject without comment or explanation manuscripts that are not prepared in accordance with these guidelines and/or if the appropriate level required for scientific publishing cannot be attained.

A – General

The text should be cohesive, logically organized, and thus easy to follow by someone with common knowledge in the field. Do not include information that is not relevant to your research question(s) stated in the introduction.

Only contributions submitted in English will be considered for publication. If English is not your native language, please arrange for the text to be reviewed by a technical editor with skills in English and scientific communications. Maintain a consistent style with regard to spelling (either UK or US English, but never both), punctuation, nomenclature, symbols etc. Make sure that you are using proper English scientific terms. Literal translations are often wrong. Terms that do not have a commonly known English translation should be explicitly defined in the manuscript. Acronyms and abbreviations used must also be explicitly defined. Generally, sentences should not be very long and their structure should be relatively simple, with the subject located close to its verb. Do not overuse passive constructions.

Do not copy substantial parts of your previous publications and do not submit the same manuscript to more than one journal at a time. Clearly distinguish your original results and ideas from those of other authors and from your earlier publications – provide citations whenever relevant.

For more details on ethics in scientific publication consult Guidelines, published by the Committee on Publication Ethics (COPE): <https://publicationethics.org/resources/guidelines>

If it is necessary to use an illustration, diagram, etc. from an earlier publication, it is the author's responsibility to ensure that permission to reproduce such an illustration, diagram, etc. is obtained from the copy-right holder. If a figure is copied, adapted or redrawn, the original source must be acknowledged.

Submitting the contribution to the Journal, the author(s) confirm that it has not been published previously, that it is not under consideration for publication elsewhere and – once accepted and published – it will be disseminated and made available to the public in accordance to the Creative Commons Attribution-NonCommercial 4.0 International Public License (CC-BY-NC 4.0), in English or in any other language. The publisher retains the right to publish the paper online and in print form, and to distribute and market the Journal containing the respective paper without any limitations.

B – Structure of the manuscript Preliminary

Title: Should be concise and unambiguous, and must reflect the contents of the article. Information given in the title does not need to be repeated in the abstract (as they are always published jointly), although some overlap is unavoidable.

List of authors: I.e. all persons who contributed substantially to study planning, experimental work, data collection or interpretation of results and wrote or critically revised the manuscript and approved its final version. Enter full names (first and last), followed by the present address, as well as the E-mail addresses. Separately enter complete details of the corresponding author – full mailing address, telephone number, and E-mail. Editors will communicate only with the corresponding author.

Abstract: Should not exceed 500 words. Briefly explain why you conducted the research (background), what question(s) you answer (objectives), how you performed the research (methods), what you found (results: major data, relationships), and your interpretation and main consequences of your findings (discussion, conclusions). The abstract must reflect the content of the article, including all keywords, as for most readers it will be the major source of information about your research. Make sure that all the information given in the abstract also appears in the main body of the article.

Keywords: Include three to five relevant scientific terms that are not mentioned in the title. Keep the keywords specific. Avoid more general and/or descriptive terms, unless your research has strong interdisciplinary significance.

Scientific content

Introduction and background: Explain why it was necessary to carry out the research and the specific research question(s) you will answer. Start from more general issues and gradually focus on your research question(s). Describe relevant earlier research in the area and how your work is related to this.

Methods: Describe in detail how the research was carried out (e.g. study area, data collection, criteria, origin of analyzed material, sample size, number of measurements, equipment, data analysis, statistical methods and software used). All factors that could have affected the results need to be considered. Make sure that you comply with the ethical standards, with respect to the environmental protection, other authors and their published works, etc.

Results: Present the new results of your research (previously published data should not be included in this section). All tables and figures must be mentioned in the main body of the article, in the order in which they appear. Make sure that the statistical analysis is appropriate. Do not fabricate or distort any data, and do not exclude any important data; similarly, do not manipulate images to make a false impression on readers.

Discussion: Answer your research questions (stated at the end of the introduction) and compare your new results with published data, as objectively as possible. Discuss their limitations and highlight your main findings. At the end of Discussion or in a separate section, emphasize your major conclusions, pointing out scientific contribution and the practical significance of your study.

Conclusions: The main conclusions emerging from the study should be briefly presented or listed in this section, with the reference to the aims of the research and/or questions mentioned in the Introduction and elaborated in the Discussion.

Note: Some papers might require different structure of the scientific content. In such cases, however, it is necessary to clearly name and mark the appropriate sections, or to consult the editors. Sections from Introduction until the end of Conclusions must be numbered. Number the section titles consecutively as 1., 2., 3., ... while subsections should be hierarchically numbered as 2.1, 2.3, 3.4 etc. Only Arabic numerals will be accepted.

Acknowledgments: Place any acknowledgements at the end of your manuscript, after conclusions and before the list of literature references.

References: The list of sources referred to in the text should be collected in alphabetical order on at the end of the paper. Make sure that you have provided sources for all important information extracted from other publications. References should be given only to documents which any reader can reasonably be expected to be able to find in the open literature or on the web, and the reference should be complete, so that it is possible for the reader to locate the source without difficulty. The number of cited works should not be excessive – do not give many similar examples.

Responsibility for the accuracy of bibliographic citations lies entirely with the authors. Please use exclusively the Harvard Referencing System. For more information consult the fifth edition of the Guide to Referencing in the Harvard Style, used with consent of Anglia Ruskin University, released by ARU University Library, available at: <https://library.aru.ac.uk/referencing/harvard.htm>

C – Technical requirements for text processing

For technical requirement related to your submission, i.e. page layout, formatting of the text, as well of graphic objects (images, charts, tables etc.) please see detailed instructions at:

<http://iarigai.com/publications/journals/guidelines-for-authors/>

D – Submission of the paper and further procedure

Before sending your paper, check once again that it corresponds to the requirements explicated above, with special regard to the ethical issues, structure of the paper as well as formatting.

Once completed, send your paper as an attachment to: journal@iarigai.org

If necessary, compress the file before sending it. You will be acknowledged on the receipt within 48 hours, along with the code under which your submission will be processed.

The editors will check the manuscript and inform you whether it has to be updated regarding the structure and formatting. The corrected manuscript is expected within 15 days.

Your paper will be forwarded for anonymous evaluation by two experts of international reputation in your specific field. Their comments and remarks will be in due time disclosed to the author(s), with the request for changes, explanations or corrections (if any) as demanded by the referees.

After the updated version is approved by the reviewers, the Editorial Board will decide on the publishing of the paper. However, the Board retains the right to ask for a third independent opinion, or to definitely reject the contribution.

Printing and publishing of papers, once accepted by the Editorial Board, will be carried out at the earliest possible convenience.

2-2022

Journal of Print and Media Technology Research

A PEER-REVIEWED QUARTERLY

The journal is publishing contributions
in the following fields of research

- ⊕ Printing technology and related processes
- ⊕ Premedia technology and processes
- ⊕ Emerging media and future trends
- ⊕ Social impacts

For details see the Mission statement inside

JPMTR is listed in

- ⊕ Emerging Sources Citation Index
- ⊕ Scopus
- ⊕ DOAJ – Directory of Open Access Journals
- ⊕ Index Copernicus International
- ⊕ NSD – Norwegian Register for Scientific Journals, Series and Publishers

Submissions and inquiries

journal@iarigai.org

Subscriptions

office@iarigai.org

More information at

www.iarigai.org/publications/journal



Publisher

The International Association of Research Organizations
for the Information, Media and Graphic Arts Industries
Magdalenenstrasse 2
D-64288 Darmstadt
Germany

